2024

Spinal Control of Sexual Excitation and Copulatory Behaviour

Evidence For A Group Of Galanin-Positive Cells In The Lumbar Spinal Cord Controlling Sexual Behaviour In Male Mice

Ana Rita Pimentel Mendes

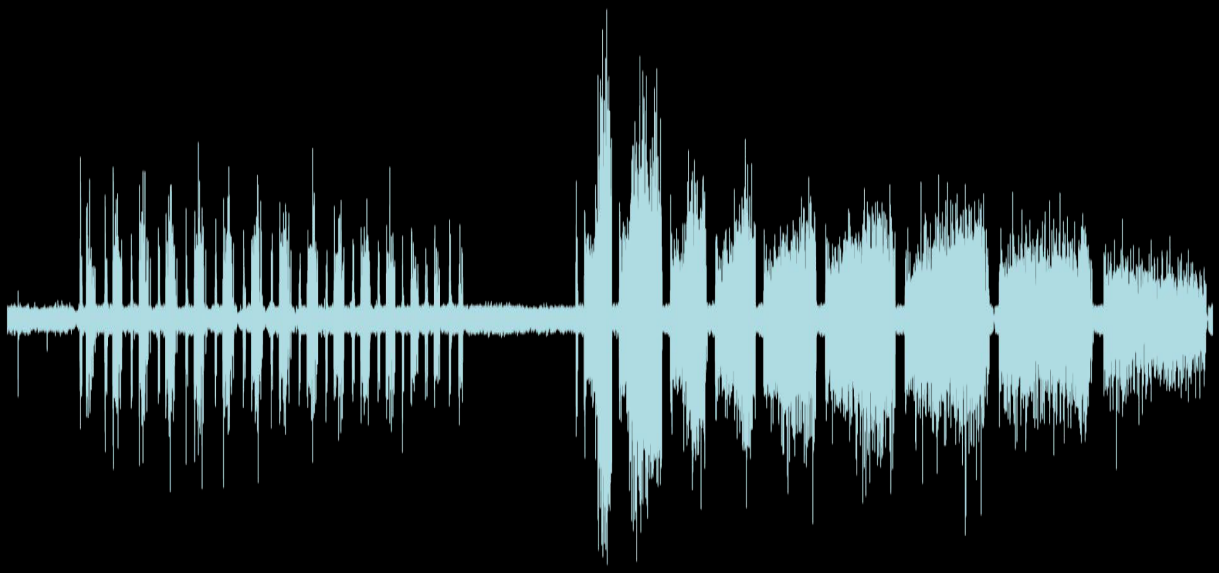

Dissertation presented to obtain the **Ph.D degree in Neurosciences**

International Neurosciences Doctoral Programme

Oeiras, September, 2024

INSTITUTO DE TECNOLOGIA QUÍMICA E BIOLÓGICA ANTÓNIO XAVIER | UNIVERSIDADE NOVA DE LISBOA

SPINAL CONTROL OF SEXUAL EXCITATION AND COPULATORY BEHAVIOR

EVIDENCE FOR A GROUP OF GALANIN-POSITIVE CELLS IN THE LUMBAR SPINAL CORD CONTROLLING SEXUAL BEHAVIOUR IN MALE MICE

Ana Rita Mendes

A Dissertation

Presented to the Universidade Nova de Lisboa

in Candidacy for the Degree

of Doctor of Philosophy in Neuroscience

Supervised by: Dr. Susana Q. Lima

International Neuroscience Doctoral Programme

Champalimaud Research

Lisbon, Portugal

2024

“So it turns out it’s quite hard to come up with something original to say about love, but I’ve had a go. Love is awful. It’s painful. Frightening. It makes you doubt yourself, judge yourself, distance yourself from the other people in your life. Makes you selfish, makes you creepy, makes you obsessed with your hair. Makes you cruel. Makes you say and do things you never thought you would do. It’s all any of us want and it’s hell when we get there. So it’s no wonder it’s something we don’t want to do on our own.”

— The Priest in the TV Show Fleabag, written by Phoebe Waller Bridge

Acknowledgements

I am writing this text on the day that I turn 30 years old, and it's the most amazing feeling to think back on all the good things that this PhD brought me in the last almost 7 years.

I want to start by thanking my supervisor, Susana Lima. She believed in me from the very beginning, when I came to do a lab rotation and ended up staying for my MSc thesis. She's been a support in this process and without her valuable emotional, scientific and technical support this project wouldn't have come to life.

Secondly, I need to thank Constanze Lenschow. We started as the postdoc and the PhD student that wanted to study the ejaculatory circuits in mice and little did we know that we would end up becoming close friends. I thank her for all the scientific knowledge transfer, for pushing me to be better everyday and for making me believe in my scientific capacities. But mainly I thank her for the family she was during these years and for allowing me to be part of hers (thank you Laurent, Paulinha and Marta for also allowing me to love you). There will always be a house for all of you in Portugal.

I would also like to thank the Lima Lab. They have been the safe harbour through the journey that a PhD always is. To Nico for listening to me complain about my ephys experiments not working but always being there ready to help. Thank you for reading this thesis and for helping with all the analysis, without you this work would be way worse. To Banas and Luís that welcomed me from the start and made me feel part of the lab despite my youthful naivety. You two are some of the best people I know and constantly prove that the north of Portugal definitely makes the best type of people! To António, that strikes you as a distant type of guy but when

you get to know him you realise that he's just a sweetie. Thank you for helping me with all the stupid technical questions, for discussing movies, TV Shows and books with me and most importantly for bringing Diana into my life (she's definitely the best part of you!). To Basma and Baylor for being the kindest people I know and for bringing my mood up every time I need it. To Margarida and Liliana for carrying this lab and making sure that everything works. Without you this lab would have collapsed. To Bertand and Oihane for all the discussions on data analysis and for bringing the nicest vibes to the lab. To Jonathan for all the project discussions and help with the technical problems. To all the alumni of the Lima Lab that shaped the lab and me to be the person I am today. And finally to Inês, forever my lab friend that started this madness a few months after me and has been through this rollercoaster of emotions with me. Coming to the lab was definitely easier knowing you would be there to support me, thank you from the bottom of my heart. May we continue to discuss the tiniest to the biggest problems of life together but always come out laughing.

I also want to thank my Thesis Committee Members, Megan Carey and Joe Paton. Besides the helpful scientific discussions, what I valued most was your faith in the project and in me throughout this process. Thank you for always having a positive attitude and kind words in my TCMs.

To Hugo Marques for all the help with the setup, Bonsai and data analysis. And for being one of the most helpful and kindest people on CCU, making our lives much better.

I definitely also need to thank all the people that worked in the Graduate Studies Office during the time I was a PhD student. More specifically though, I would like to thank Teresa Dias for being extremely caring and supportive with all of us and for making sure that all the documents were

delivered. Without all of you, I would still be stuck in bureaucracy with ITQB.

To my INDP year, INDP 2017 or 2018 or whatever they want to call us, I really need to say that we were the best year this institute ever had! You made this journey easier and to be part of the scientific but also social parts of this journey with you made it much more special. You have a special place in my heart and I will never forget that we survived the journal club mania together. Special thanks to Margarida, Filipe, Mafalda and Lucas for hearing me complain a bit more than the others!

To the Champalimaud Foundation community I owe you the best of times in these last years. To everyone that organises retreats, scientific and social activities, to all the platforms that help us every day to achieve our goals, to the To All emails that help someone, I really am thankful to be part of this community. This is where I met some of my best friends and people that I will take with me forever. Margarida Pexirra, Jeroen and Beatriz thank you for having been there in the beginning of this journey, and for continuing to be there until now.

To the PSC friends, Sofia, Bea, Rita, Juan, Miguel and Catarina. To have shared the struggles of representing the PhD students with you in the last 2 years was one of the most rewarding and annoying experiences of my life. Thank you for helping me through all the times I wanted to scream at people and couldn’t (and on the times I did!).

To the Students Retreat 2019 Committee and the CR Retreat 2023 Committee, thank you for all the good times organising such incredible events. It made me realise that I was good at something else besides science and it really was a pleasure to exchange crazy ideas with you.

This said, thank you to the CEO team! You all welcomed me with open arms in these last months and it has been the best experience of my life. It is a pleasure to be part of such a diverse and incredible group of people. Thank you António for seeing my potential and believing I could do this job, I am eternally grateful. Thank you Catarina and Teresa for giving me this opportunity and letting me flourish. Thank you Diana and João for being the best office mates and making me laugh everyday. And thank you Emilie for sharing my slightly crazy vibe and being the kindest person.

Another thing that this PhD brought was experiences abroad to which I am extremely grateful to have been part of. To the people in Bordeaux, namely Sandrine, Jean-Rene, Theo and Camille for helping us with experiments and showing us the cool side of ex vivo ephys. The Neural Systems and Behaviour course and everyone from Woods Hole, I don't even have the words to thank you. Those 2 months will forever be one of the greatest experiences of my life. From meeting extremely talented and caring PIs (special thanks to Michael, Ann and the wind whiskers crew) to making friendships that felt like years long even though we know each other for only a couple of weeks. Sol, Mati and Niko, thank you for all the nice conversations and for being some of the greatest scientists and people I met in the last years. I miss you dearly.

To the sports of CCU, namely the football and the basketball people. When Nuno and André pushed me to start going to the games I never thought I would be here thanking everyone for all the relaxing and funny moments I lived there. Special thanks to the Basketball Friends that became real life friends and that pushed me to improve both in my pick and rolls but also as a person. Special thanks to Masha, Dennis, Mert and Martim, for all the movie nights and weekend plans, you made my life in Lisbon so much better and I love you for that. Also to Nuno, Diego, Diogo

and Rosária for all the Monday dinners after the game, I will cherish those moments forever.

But finally the best thing that the CCU brought me was the group of friends with the best name ever, the Pacohs! To all of you I am eternally grateful for choosing me to be your friend and accepting me with all my good and bad parts. To André and Nuno for being my first friends at CCU and for continuing to be there for me after all this time. To Mert and Merit for being such good listeners and always having kind words to say to me. To Malpica, Raquel and Raquel, for all the dinners and game nights. And to Rasteiro and Inês for all the shared rides, for listening to me complain about my life and always being kind to me. I love you all for simply being there and for screaming Pacooooh back in the CCU corridors.

To Rita and Manel, thank you for being the best roommates Lisbon could have given me. All the hours we spent together in Ajuda, all the phone calls and dinners will forever be in my most cherished memories. Thank you also for adding me to your friend group and allowing me to meet Telmo, Samuel and Rita. I will never forget our weekends together in Lisbon and how you showed me that living here was actually fun!

To the friends that Coimbra gave me, thank you for your support on the weekends that I would visit and through phone calls and texts. It has now been more than 10 years since we met and I still love and miss all of you. Thank you Bea for being the best friend one can have, I wish I was physically closer to you, but the weekends together with Maria Inês and Ana are compensating. Similarly, thank you Joana for always welcoming me in Madrid and for all the patience with me in the last years, I miss you dearly. To Carolina, the best ‘afilhada de praxe’ one could ask for, thank you for all the talks and for always being there for me. I wish you could come back to sleep on my floor so that we could talk forever! (I’m kidding,

please go and be the successful scientist I'm so proud of). To José, thank you for all the lanches in CCU and for putting up with my weekly dramas. I love that we can talk about cute guys and politics in the span of a lunch break and I hope that never changes!

To André, Mela, DD and Filipe, thank you for all the video calls during covid, to all the quiz and game nights and simply for being there. You made this journey so much better. Ana Tomé, thank you for becoming the best friend one could ask for. All the movies, talks about life, dinners and emotional support really helped me become a better person. I love you and hope we can continue to gossip in the car forever, thank you for always being here.

To my friends in Condeixa, Tiago, Nando, JP, Vicente and Inês, thank you for making my weekends happier and full of joyful moments. This powered me through the rougher weeks of this journey and I'm forever grateful. Special thanks to Sara, for being one of the best people I know, for always being there even when I couldn't be for her and for helping me finish this thesis. You really are a special one, love you!

Finalmente, à minha família, por todo o apoio que me deram ao longo dos anos. Ao meu avô Manel por ter estado sempre lá, nunca ter duvidado de mim e me ter permitido ser uma criança criativa, acredita que isso me tornou uma cientista melhor. À minha avó Lucinda, por todo o mimo incondicional e todas as marmitas preparadas com carinho aos domingos. À minha avó Maria, pela atitude sempre positiva perante a vida e os obstáculos que ela nos põe à frente. Ao meu tio por toda a boa disposição e ajuda ao longo dos anos. À Didi por todo o carinho e por nunca se esquecer de nós. À Francisca por ser a melhor prima que uma pessoa pode pedir. Cresceste mais ou menos ao mesmo tempo deste doutoramento e é um orgulho ver-te tornar uma criança tão incrível e

amorosa. Ao Tiago e à Matilde por serem a família alargada que eu sempre desejei e por cuidarem tão bem das pessoas mais preciosas da minha vida. Obrigada do fundo do meu coração.

Ao meu pai, por todo o apoio ao longo destes anos, desde as mudanças de casa às inundações do carro, estava sempre lá assim que possível. Obrigada por teres acreditado que eu conseguia fazer este doutoramento.

À minha mãe, por todo o amor que me deu e por todas as conversas quando precisava de conselhos e de uma palavra carinhosa. Obrigada por me teres apoiado quando considerei mudar-me para Lisboa e por não teres duvidado de mim. Infelizmente acho que não te consigo dar o Nobel como gostavas, mas acho que este doutoramento não correu muito mal.

Também não podia deixar de agradecer ao Fleabag, o melhor gatinho do mundo e que tornou estes anos de doutoramento menos solitários.

E finalmente aos meus irmãos. Estes últimos anos trouxeram desafios e vocês foram sempre um porto de abrigo. João Pedro, obrigada por todos os momentos felizes e por estares sempre pronto a ajudar. És o melhor irmão mais velho e sei que vais estar sempre lá para nos proteger. Maria Inês, obrigada por seres a melhor gémea que uma pessoa pode pedir. Quando éramos pequenas sinto que eras tu que precisavas mais de mim para florescer, mas acredita que nestes últimos anos, foste tu a âncora desta família e por isso estou para sempre grata. És a minha inspiração. Obrigada aos dois por todo o apoio durante este doutoramento e por, mesmo à distância, protegerem-me o melhor que podiam.

Título

Controlo através da medula espinhal da excitação sexual e comportamento copulatório: Evidência sobre um grupo de células positivas para galanina na medula espinhal lombar que controlam o comportamento sexual em murganhos machos

Sumário

Durante o comportamento sexual, a excitação masculina aumenta até atingir o ponto em que a ejaculação está prestes a acontecer, permitindo que a informação sensorial da zona pélvica desencadeie uma ejaculação. Embora se acredite que a cópula e a excitação sexual sejam reguladas diretamente pelo cérebro, a ejaculação é considerada um reflexo controlado por um circuito localizado na medula espinhal. Sendo assim, presume-se que a medula espinhal esteja a ser fortemente inibida por circuitos descendentes vindos do cérebro até ao momento em que a ejaculação acontece, não desempenhando nenhum papel na regulação do comportamento sexual. No entanto, esta hipótese ainda não foi testada. Aqui, mapeamos o circuito espinhal que controla o músculo bulboesponjoso, o principal músculo envolvido na expulsão de esperma em murganho. O nosso projeto revela que os neurónios motores do músculo bulboesponjoso recebem informações de neurónios da medula espinhal que expressam galanina. Esta população positiva para galanina recebe estímulos genitais e, embora a sua estimulação conduza à ativação do músculo bulboesponjoso, essa ativação depende das projeções inibitórias do cérebro serem cortadas, do estado interno do animal e diminuem com a estimulação repetida das células positivas para galanina. Além disso, a eliminação dos neurónios positivos para galanina afeta a latência para ejacular e altera o padrão copulatório. Estes

resultados sugerem um papel inesperado dos circuitos espinhais no controle da cópula e da excitação sexual, além do seu papel estabelecido na ejaculação.

Palavras-chave

Medula espinhal, ejaculação, comportamento sexual, músculo bulboesponjoso, eletrofisiologia, optogenética, mapeamento de circuitos

Title

Spinal control of sexual excitation and copulatory behaviour: evidence for a group of galanin-positive cells in the lumbar spinal cord controlling sexual behaviour in male mice

Abstract

During sexual behaviour, male arousal increases to reach the ejaculatory threshold, allowing genital sensory information to trigger ejaculation. While copulation and sexual arousal are thought to be centrally regulated by the brain, ejaculation is considered a reflex controlled by a spinal circuit. In this framework, the spinal cord is assumed to be strongly inhibited by descending input from the brain until the ejaculatory threshold, playing no role in the regulation of copulatory behaviour. However, this remains untested. Here, we mapped the spinal circuit controlling the bulbospongiosus muscle, the main muscle involved in sperm expulsion in mice. Our findings reveal that the bulbospongiosus muscle-motor neurons receive input from galanin-expressing neurons. This galanin-positive population receives genital input and, while its stimulation leads to bulbospongiosus muscle activity, the evoked muscle-potentials are dependent on spinalization, the male's internal state and decrease with repeated stimulation. Moreover, ablation of galanin-positive neurons affected the latency to ejaculate and altered the copulatory pattern. These results suggest an unexpected role of the spinal circuits in the control of copulation and arousal, in addition to its established role in ejaculation.

Keywords

Spinal cord, ejaculation, sexual behaviour, bulbospongiosus muscle, electrophysiology, optogenetics, circuit mapping

Author Contributions

Ana Rita Mendes (A.R.M.), Constanze Lenschow (C.L.) and Susana Quelhas Lima (S.Q.L.) conceptualised the experiments and project ideas. A.R.M. and C.L. conducted all the experiments, part of the histology and most of the data analysis. Liliana Ferreira helped with histological analysis. Bertrand Lacoste helped with data analysis, namely regarding the behavioural experiments. C.L. with the help of Camille Quilgars and Sandrine Bertrand conducted in vitro electrophysiological experiments at the INCIA. A.R.M. performed the electromyogram experiments in behaving animals and, together with Hugo Marques and Nicolas Gutierrez-Castellanos, their analysis. A.R.M. wrote this thesis supervised by S.Q.L.

Financial Support

This work described in this monograph was performed under the International Neuroscience Doctoral Programme (INDP 2018), funded by the Fundação para a Ciência e Tecnologia (FCT) with a doctoral fellowship (PD/BD141576/2018 and COVID/BD/152654/2022) and was developed with the support from the Champalimaud Foundation, the Institut de Neurosciences Cognitives et Intégratives d'Aquitaine (INCIA), a Human Frontier Science Program Postdoctoral Fellowship (LT000353/2018-L4) (Constanze Lenschow (C.L.)), a H2020 Marie Skłodowska-Curie Actions Individual Fellowship (799973) (C.L.), the research infrastructure Congento, co-financed by the Lisboa Regional Operational Programme (Lisboa2020), under the PORTUGAL 2020 Partnership Agreement, through the European Regional Development Fund (ERDF), FCT under the project LISBOA-01-0145-FEDER-022170, an InterEmerging Actions 2020 (301137) (Susana Quelhas Lima (S.Q.L.)) and an European Research Council (ERC) Consolidator Grant (772827) (S.Q.L.).

Overview

This monograph is composed of five Chapters. Chapter 1 consists of a general introduction, where the relevant literature for this project is discussed. We start by generally describing sexual behaviour importance in several areas and then evolve to describing copulation in mammals and rodents. We highlight the differences in the copulatory sequence between rats and mice and why these differences may readout in distinct neuronal pathways. We describe said neuronal circuits, spanning from the brain control of sexual behaviour to the spinal control of ejaculation and the seminal papers in the rat describing a spinal ejaculation generator composed by a group of Gal+ cells that control the BSM-MNs. We end by depicting the peripheral nervous system role in the control of the pelvic organs and how it impinges on the spinal circuit responsible for controlling ejaculation and sexual behaviour.

From Chapter 2 to Chapter 4 we present the results of this project. In Chapter 2 we anatomically and functionally describe the BSM-MNs and the Gal+ cells that are upstream of these neurons. Using various tracing techniques (viral and non-viral) we describe the location of both BSM-MNs and the Gal+ cells in the spinal cord and the nature of their monosynaptic connection. We also depict the physiological properties of the BSM-MNs using optogenetic stimulation. Finally, we described a sensory connection from the pelvic area to both the BSM-MNs and the Gal+ cells.

In Chapter 3 we further characterised the Gal+ population and their functional role in ejaculation. Using electric and optogenetic stimulation of the spinal cord, we described the properties of the BSM activity after Gal+ cells activation. We also analyse the muscle activity in vivo using BSM EMG recordings in behaving animals during copulation. Finally, we observed that the Gal+ cells and consequent BSM activity was dependent

on the internal state of the animal, namely if the male mouse had any sexual encounter moments before the electrical stimulation experiments.

Chapter 4 wraps up this circuit description by evaluating the role of the Gal+ cells in behaving animals. Using cFos, a proxy for neuronal activity, we observed that the Gal+ cells are progressively active with different phases of copulation, with a higher number of cells being active after ejaculation takes place. Finally, using a chemogenetic approach based on Diphtheria Toxin, we ablated the Gal+ cells and evaluated the effect on mice sexual behaviour. This manipulation led to a proportion of animals not being able to ejaculate, even though they performed other copulatory behaviours, and to several other changes in the copulatory sequence and its components.

Chapter 5 consists of a general discussion where we summarise and further discuss our findings. We also analyse the limitations of the techniques used in our work and how they might influence the interpretation of the results presented in this monograph.

Table of Content

List of Figures

List of Abbreviations

AAV	Adeno-associated Virus
AH	Anterior hypothalamus
BNST	Bed Nucleus of the Stria Terminalis
BSM	Bulbospongiosus Muscle
CAN	Central Autonomic Nucleus
ChAT	Choline Acetyltransferase
ChR2	Channelrhodopsin
CPG	Central pattern generators
DLN	Dorsolateral Nucleus
DPN	Dorsal penile nerve
DT	Diphtheria Toxin
DTR	Diphtheria Toxin Receptor
EMG	Electromyography
EMG	Electromyography
EPSCs	Excitatory Postsynaptic Currents
FG	Fluorogold
Gal-ChR2	Gal-cre Mouse Line Crossed with a ChR2 Mouse Line
Gal+	Galanin-positive

GFP Green Fluorescent Protein

Gi Gigantocellular Reticular Nucleus

GRP Gastrin Releasing Peptide

IML Intermediolateral Nucleus

ITI Inter-thrust Interval

L Lumbar Spinal Segments (L1-L6)

LFP Local Field Potentials

LS Lateral septum

MeA Medial Amygdala

MI Mount with Intromission

MNs Motor Neurons

MOE Main Olfactory System

MP Mount with Probing

MPOA Medial preoptic area

mSPFp Medial portion of the SPFp

PAG Periaqueductal grey

PEI Post Ejaculation Period

PFA Paraformaldehyde solution

PRV Pseudorabies virus

PVN	Paraventricular nucleus
rAAV	Retrograde Travelling Adeno-associated Virus
S	Sacral Spinal Segments (S1-S4)
S1	Primary Somatosensory cortex
SBN	Social Brain Network
SEG	Spinal Ejaculation Generator
SN	Sexually Naive
SPFp	Parvocellular Subparafascicular thalamic nucleus
SPN	Sacral Parasympathetic Nucleus
TA	Tibialis Anterior
TA	Tibialis Anterior
VGLUT1	Vesicular Glutamate Transporter 1
VGLUT1	Vesicular Glutamate Transporter 1
VMH	Ventromedial hypothalamus
VMHvl	VMH ventrolateral part
VNO	Vomeronasal organ
VTA	Ventral Tegmental Area

1 General Introduction

1.1 Introduction

When studying animal behaviour, most studies have focused on rather negative aspects, such as pain processing or how animals cope with stress or distress. This focus is often due to the higher survival value associated with identifying and managing these responses. However, the study of pleasure, an equally important component of an animal's wellbeing, has received far less attention (Balcombe, 2009). In recent years, some laboratories have begun to explore pleasurable behaviours, such as play (Reinhold et al., 2019), responses to tickling (Ishiyama et al., 2019), or even social touch and genital stimulation (Lenschow & Brecht, 2015; Qi et al., 2024; Sigl-Glöckner et al., 2019), but these remain a small fraction of overall behavioural research. These pleasurable behaviours are just as important for an animal's well-being as negative ones, and should be equally considered (Balcombe, 2009).

Sexual behaviour is another understudied aspect of pleasure in animals, often examined primarily for its role in reproduction and species evolution. However, animals engage in sexual activities beyond reproduction, such as same-sex copulation or masturbation (Adkins-Regan, 1999), which are pleasurable and rewarding behaviours observed across species; these behaviours contribute to the animals' well-being and should be recognized as such (Adkins-Regan, 1999). Besides, sex plays a vital role in pair bonding, which is not only important for the individual's success but also for the success of the pair and their progeny (Blumenthal & Young, 2023).

From a neuroscience perspective, sexual behaviour follows a pleasure cycle that includes motivation, consummation, and satiety (Georgiadis et al., 2012). In humans, sex has been shown to have additional effects on well-being, such as improved cognitive function (Maunder et al., 2017) and disease prevention (Leitzmann et al., 2004). On the other hand,

sexual dysfunction can lead to significant distress for individuals and their sexual partners, negatively impacting mental health (Althof, 2006; Carson & Gunn, 2006). Focusing on behavioural therapies that increase pleasure, arousal and satisfaction, may enhance the effectiveness of pharmacological treatments for sexual dysfunction (Althof, 2006), further underscoring the importance of considering sex a positive experience.

Yet, despite the ubiquity of sex, its importance to well-being and its fundamental role in reproduction, the mechanisms controlling sexual behaviour remain poorly understood.

1.2 Structure of sexual behaviour in mammals

As noted, sexual behaviour has distinct roles in an animals' well-being, but ultimately, its main biological function is to facilitate sperm deposition into an egg, ultimately leading to its fertilisation. To ensure reproductive success, mammals have evolved specific copulatory sequences designed to maximise the chances of fertilisation and species survival (Dewsbury, 1972).

In seminal work, Dewsbury categorised various copulatory behaviours from the male's perspective, identifying distinct patterns across species based on these behavioural traits. He analysed behaviours such as the number of intromissions, the presence or absence of thrusting, the duration of copulation, and the refractory period following copulation. His work revealed that even closely related species use different mating strategies to achieve sperm deposition (Dewsbury, 1972).

Broadly speaking, sexual behaviour can be divided into three main phases:

1. Pre-copulatory behaviours - These are actions used to build up arousal and assess the fitness of the mating partner.

2. Copulatory behaviours - The actual motor behaviours that lead up to ejaculation and sperm deposition.

3. Ejaculation and the refractory period - once ejaculation takes place, most animals enter in an inhibitory phase during which they temporarily disengage from sexual activity.

It is important to study and understand these components, as they all play a role in ensuring a successful sexual encounter.

1.2.1 Rodent sexual behaviour

In rodents, even among closely related but diverse species, there are significant differences in copulatory strategies (Figure 1.1). Dewsbury documented a wide range of copulatory behaviours, noting differences in the number of intromissions, ejaculation patterns, and the timing of copulation. These differences highlight the unique reproductive strategies evolved within the rodent family, with specific copulatory behaviours serving as adaptations to particular ecological and social environments (Dewsbury, 1975).

Nowadays, most research on rodent sexual behaviour focuses on rats and mice. Therefore, it is important to discuss the differences in the copulatory strategies used by these two rodents. In this thesis I will discuss the copulatory sequence of these two species, from a male-centred perspective, while acknowledging that the female perspective is also crucial and deserves the same attention in the broader scope of sexual behaviour research.

Before examining the sequential and temporal organisation of the copulatory sequence, it is important to define some terms:

1. Mounts - This occurs when the male places both front paws on the female's rear, specifically above her flanks, inducing lordosis if she is receptive. The mount ends when the male removes the paws from the female's back.
2. Probing - At the beginning of a mount, the male performs shallow pelvic thrusting movements to locate the entrance of the female's vagina, trying to obtain penile intromission.
3. Intromission - In a successful mount, the male is able to insert his penis in the female's vagina.
4. Pelvic thrusts - Following penile intromission, the male performs repeated pelvic movements, without the penis exiting the female's vagina, each of which is referred to as a thrust.

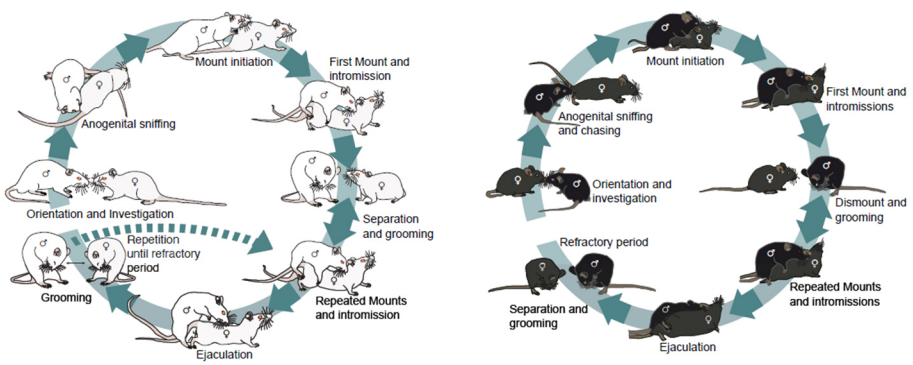

Figure 1.1 Sequence of a sexual encounter in rats and mice. On the left panel, there is a scheme with the details of copulation in rats, whereas on the right panel we show the copulatory sequence for mice. Adapted from (Lenschow & Lima, 2020).

1.2.1.1 Pre-copulatory behaviours

Pre-copulatory behaviours are essential to the success of a sexual encounter. These behaviours include the investigation of the mating pair, which is critical for their fitness assessment and to increase sexual arousal and motivation to start the copulatory/consummatory phase (Georgiadis et al., 2012).

Rat

In male rats, pre-copulatory behaviours occur in response to the female's behaviour. Females display ear-wiggling, darting (short runs that end with the female showing her posterior to the male) and hopping (similar to darting, but the female is jumping around) (Agmo, 1997). The male rat will begin investigating the face and anogenital area of the female, to better access volatile and non-volatile olfactory cues, and they both emit 50 kHz ultrasonic vocalisations that are thought to increase the arousal. Afterwards the male will try mounting the female and perform several rapid shallow thrusts with his pelvis, to find the female's vagina. Once the male successfully inserts is penis, this marks the beginning of the copulatory phase (Hull & Dominguez, 2007).

Sexual experience in rats can lead to some differences in the timing of the behavioural epochs but does not significantly alter the copulatory behaviour. However, one of the changes is the latency to start mounting, which assumes a shorter and more efficient pre-copulatory phase, which suggests that sexual experience helps males recognize and respond to cues from the female more effectively (Dewsbury, 1969).

Mice

The pre-copulatory behaviours of male mice are similar to those of male rats. As in rats, male mice will engage in anogenital and facial exploration to have access to tactile and non-volatile olfactory information (Hull &

Dominguez, 2007; Lenschow & Lima, 2020). Furthermore, male mice emit ultrasonic vocalisations that seem to promote female approach behaviour (Asaba et al., 2017) and the female mice emit a courtship song that may signal increased receptivity (Neunuebel et al., 2015).

Eventually, the male will display mount attempts, and if the female is receptive, she will show lordosis behaviour (arching of the back to facilitate access to the vagina) in response to the male touching her flanks (Lenschow & Lima, 2020). The male will likely perform mounts with probing until he successfully intromits, marking the change to the copulatory behaviour phase (McGill, 1962).

1.2.1.2 Copulatory behaviours

Once the animals conclude assessing the suitability of their partner, the male initiates the copulatory behaviours, by performing successful mounts with intromissions and thrusts. This phase is very different in form and in timing from species to species and usually ends when the male achieves ejaculation and enters the refractory period (Dewsbury, 1975).

Rat

In rats, the copulatory sequence is composed of several mount bouts, where the male performs mounts that can or not have intromissions and are not interrupted by other behaviours not female oriented. Mount bouts are therefore separated by longer periods where the male is not interacting with the female (Huijgens et al., 2021; Sachs & Barfield, 1970). These mount bouts are not dependent on the male being able to intromit, since rats that are only able to mount still organise their copulatory

behaviour in mount bouts. Therefore, some authors consider the mount bouts the basic unit of rat copulation (Sachs & Barfield, 1970).

The time between the mount bouts, usually called time outs, is one of the components that set the copulatory pace. The copulatory pace, together with the sensory integration (number of intromissions), is an important part of the male copulatory behaviour since it determines the latency to ejaculation (Huijgens et al., 2021).

Mice

For mice, like rats, the copulatory behaviours start once the male mice successfully does a mount with intromission. However, the mount dynamics is strikingly different from the rat. One mount starts with the male mouse doing probing until he finds the vaginal opening and can intromit (McGill, 1962). Afterwards, the male will do a variable number of deep pelvic thrusts, contrary to the rat, that does only one intromission and one thrust. The mount ends after a series of thrusts and the male dismounts the female. These mounts with intromission and thrusts will be repeated several times until ejaculation is reached (Lenschow & Lima, 2020; McGill, 1962).

1.2.1.3 Ejaculation and the refractory period

The final step in a rodent sexual encounter is ejaculation. Some species will perform several ejaculations in one encounter whereas others will achieve only one (Dewsbury, 1972). Independently, after a certain number of ejaculations, the male will enter the post ejaculatory refractory period which marks the end of the sexual interaction with the male no longer engaging in copulatory behaviours (Valente et al., 2021).

Rat

As explained above, male rat copulation is organised in mount bouts, that can be composed of mounts or mounts with intromission. After a variable amount of mount bouts the male will have an ejaculation, characterised by a deeper and longer intromission (Hull & Dominguez, 2007). He will then enter the post ejaculation period (PEI), that consists of several minutes in which the male will not interact with the female, finishing the first series of the sexual encounter (Huijgens et al., 2021). However, after some time the male rat will resume the copulatory behaviours (entering the second series), namely by restarting the mount bouts, and eventually ejaculate a second time and enter a new PEI (Huijgens et al., 2021; Hull & Dominguez, 2007). It is not surprising that PEI is also an important component in the regulation of the copulatory pace in male rats (Huijgens et al., 2021). The PEI duration increases with the number of ejaculations (Karen & Barfield, 1975) and can be manipulated by the availability of the female (Bermant, 1964).

This sequence of behaviours is repeated several times, with male rats being able to reach 7 or 8 ejaculations in a single sexual encounter. Eventually the male will reach sexual satiety and will not copulate for several days (Hull & Dominguez, 2007).

Mice

Very differently from rats, but similar to humans, male mice usually only ejaculate once per sexual encounter. After a variable number of mounts with intromission and thrusting, male mice will do a final mount where the rate of the thrusting increases and finally the male will quiver strongly (shuddering), strongly hold the female and fall to the side (Lenschow & Lima, 2020; McGill, 1962). This posture is maintained for several seconds

in order for ejaculation to happen but also to deposit a plug in the female's vagina to avoid copulation from another male (McGill & Coughlin, 1970; Sutter & Lindholm, 2016).

Afterwards, the male will enter the post ejaculatory refractory period that can last several days depending on the strain, and where the male is no longer interested in copulation with that female (Valente et al., 2021). If presented with a novel receptive female, some males can resume sexual behaviour after 2-3 hours, but most will take at least 24 hours to be able to gain sexual interest again. Interestingly, males that resume sexual behaviour in hours, will take less intromissions and thrusts to ejaculate (McGill, 1962).

Ejaculation marks a clear shift in male mice behaviour towards a female. They drastically change from being extremely engaged with a receptive female into a state where they do not interact or even avoid the female. Therefore, understanding the physiological and neuronal processes behind this process is of extreme importance.

Details of the ejaculatory process: emission and expulsion of sperm

The ejaculatory process is composed of several steps that ultimately lead to the production and accumulation of sperm and its consequent ejection from the penis. Therefore, this process can be divided into two major steps, emission and expulsion (Sheu et al., 2014). The emission phase is the physiological process responsible for the accumulation of the sperm (spermatozoa and seminal fluids) in the prostatic urethra. The expulsion phase, as the name suggests, controls the expulsion of the sperm by the rhythmic contraction of the perineal muscles (Clement & Giuliano, 2016; Sheu et al., 2014).

In mice, the emission phase depends on the coordinated action of the testis, the epididymis, efferent ducts, and vas deferens, together with the accessory sex glands, the seminal vesicles, coagulating glands, prostate gland, bulbourethral glands, ampullary glands, preputial glands, and finally the urethra and penis (Knoblaugh & True, 2012). These organs are responsible for testosterone production, spermatogenesis, and sperm maturation, storage, and discharge (Huang et al., 2022).

On the other hand, the expulsion phase needs the coordinated action of the external urethral sphincter and the rhythmical contraction of the perineal striated muscles, which include the bulbospongiosus muscle (BSM), ischiocavernosus and levator ani muscles, being the BSM the main responsible for the ejection of sperm (Clement & Giuliano, 2016; Sheu et al., 2014).

In mice, information regarding the specific role of the pelvic muscles and consequently the BSM is virtually lacking. Elmore et al. (1988) observed that in the house mouse, excision of the BSM caused a significant increase in the number of interruptions during a mount with thrusts. This suggests that the BSM is also involved in maintaining erection in mice (Elmore & Sachs, 1988).

Several studies in rats however point to the role of the BSM in sperm expulsion. Induction of the urogenital reflex in anaesthetised rats leads to a fictive ejaculation that is preceded with strong BSM contractions measured with electromyogram (EMG) (Carro-Juárez & Rodríguez-Manzo, 2000; Holmes & Sachs, 1991; Tanahashi et al., 2012).

BSM in vivo EMG recordings in sexually behaving male rat further confirms the role of this muscle in copulation (Holmes et al., 1991). The authors observed BSM activation during mounts, intromission and

ejaculation, being the latter the strongest signal registered (Holmes et al., 1991). To my knowledge, there is no data on in vivo recordings of the BSM activity in sexually behaving male mice.

1.3 Neuronal circuits for ejaculation

As stated above, ejaculation marks a shift in the internal state of males. Animals that initially were extremely interested in females and engaged in copulatory behaviours, switch into a sexual satiety state where they are uninterested in the female upon ejaculation. This satiety state is present in both rats and mice despite the strategies used to reach ejaculation being very different, as highlighted in the previous sections (Dewsbury, 1975).

So far, most studies on the neuronal circuits controlling the ejaculatory process were performed in rats. However, in this thesis I will elaborate on why mice represent a valuable animal model to study this circuitry. First, behaviourally, mice are more similar to humans in terms of sexual behaviour structure, presenting one ejaculation with a longer refractory period, contrary to rats that can have up to 6 ejaculations in a very short time period. Secondly, the genetic and viral tools available in the mouse allow for a much deeper dissection of the circuitry and therefore a higher potential to understand how the spinal cord and the brain are controlling this behaviour.

In the next sections I will be reviewing the knowledge of the central and peripheral nervous system control of copulation and the ejaculatory process and speculate on the possible sharing of circuits between these two rodent species and why it is important to study this circuit in mice.

While it is widely accepted that pre-copulatory and copulatory processes and the arousal increase that accompanies them is mainly centrally regulated by the brain with the involvement of the autonomic and sensory-somatic nervous systems (Allard et al., 2005; Corona et al., 2012; Giuliano & Clement, 2005), ejaculation is hypothesised to be triggered by genital input (Carro-Juárez & Rodríguez-Manzo, 2005) and controlled by autonomic and somatic circuits located within the spinal cord, being considered a reflex that is under brain inhibition (Veening & Coolen, 2014). Emission of sperm would mainly be controlled by the autonomic system (H. F. Newman et al., 1982; Sheu et al., 2014) whereas expulsion would be a somatic reflex caused by the activation of spinal motor neurons (MNs) that lead to the contraction of the BSM (Peikert et al., 2015; Sachs, 1982; Tang et al., 1999). Yet, how copulatory sequences and arousal increase are coordinated, how the ejaculatory reflex is inhibited until the arousal threshold and, importantly, how the arrival to the arousal threshold is communicated to the spinal cord allowing the reflex to be triggered, remains unresolved. More importantly, even the spinal circuit responsible for triggering the ejaculatory reflex is not fully uncovered.

1.3.1 Brain control of copulation and ejaculation

In the pre-copulatory phase of the behaviour, volatile and contact-dependent pheromones play the biggest role in mate choice and sex initiation (Dulac & Wagner, 2006). In mice, volatile cues are primarily sensed by neurons of the main olfactory epithelium (MOE) which relay information onto the main olfactory system, whereas contact-dependent cues are primarily sensed by neurons of the vomeronasal organ (VNO) and the accessory olfactory system (Dulac & Wagner, 2006; Matsuo et al., 2015). Main and accessory olfactory signals are then conveyed into

higher brain areas (such as the amygdala and olfactory cortex) in order to evaluate multiple features of their conspecifics, namely their reproductive, health and social status as well as their sexual identity (Hurst, 2009).

Another important sensory modality used by rodents in the pre-copulatory phase is touch. Facial and genital touch are initially processed in the primary somatosensory cortex (S1), and they drive socio-sexual specific activity (Lenschow & Brecht, 2015; Sigl-Glöckner et al., 2019).

The chemosensory information together with other external and internal cues is integrated in higher brain areas that belong to the so-called Social Brain Network (SBN). The SBN is a complex network composed of hypothalamic and extra-hypothalamic areas and is involved in the control of distinct social behaviours from mating to aggression or maternal care (Chen & Hong, 2018; S. W. Newman, 1999). The main areas that form the SBN are the lateral septum (LS), the medial extended amygdala (Bed Nucleus of the Stria Terminalis, BNST), the medial preoptic area (MPOA), the anterior hypothalamus (AH), the ventromedial hypothalamus (VMH) and the periaqueductal grey (PAG), which are all heavily and reciprocally interconnected (S. W. Newman, 1999). The coordinated activation of these brain regions leads to specific social behaviours, namely copulation.

With respect to male sexual behaviour, the MPOA has been one of the most studied nuclei. It projects to brain areas related to sensory processing, such as those related to social olfactory cues like the Media Amygdala (MeA) and the BNST, which may facilitate its role in male sexual behaviour (Láng et al., 2024; Simerly & Swanson, 1986). Besides, it sends projections to brain nuclei that control autonomic and motor responses associated with copulation (Simerly & Swanson, 1988). The MPOA is capable of driving mounting behaviour (Wei et al., 2018) and sexual experience induces plasticity in this brain area (Jean et al., 2017) in mice, correlating with long-lasting mating behaviour improvements.

Another brain area with a relevant role in male sexual behaviour is the VMH, especially its ventrolateral part (VMHvl). This nucleus is also involved in socio-sexual behaviours, namely mating and fighting (Hashikawa et al., 2016). Ablation of specific neuronal subpopulations leads to a reduction in mating and aggression in male mice (Yang et al., 2013), whereas optogenetic stimulation leads to an increase in mounting, similarly to the MPOA (Lee et al., 2014).

More specific to ejaculation, lesions to the hypothalamic paraventricular nucleus (PVN), impair male rat sexual behaviour (Liu et al., 1997), whereas, its activation promoted the ejaculatory response, by decreasing intromissions latency and facilitating ejaculation (Xia et al., 2017). Furthermore, Xia and colleagues observed that the PVN activation caused an increase in the lumbar sympathetic response, thus representing a candidate mechanism by which the PVN promotes ejaculation (Xia et al., 2017). The PVN has direct projections to the lumbar segments 5 and 6, specifically to the dorsomedial and dorsolateral areas, which is where the MNs responsible for the innervation of the pelvic muscles are present.

Another brain structure potentially relaying copulation related information from the hypothalamus to the brainstem and spinal circuits controlling potential ejaculatory motor outputs is the PAG. While the involvement of the PAG in mating behaviour has been repeatedly established, conflicting results are present in the literature on whether the PAG promotes or inhibits mating behaviour. On one hand, a study reported increased cFos activity in PAG cells after mating (Gréco et al., 1996), whereas on the other hand lesioning of this nuclei accelerated mounting behaviours, contrary to the expected suppression (Brackett et al., 1986). Independently, the MPOA cells that are active during copulation project to

the PAG, which clearly indicates a role of this nuclei in relaying copulatory signals to the spinal cord (Struthers, 2001)

Also involved in the control of ejaculation is the parvocellular subparafascicular thalamic nucleus (SPFp). Previous work has shown that a galanin-positive neuronal population present at the medial portion of the SPFp (mSPFp) is active upon ejaculation but not other phases of male sexual behaviour (Coolen, Veening, Petersen, et al., 2003). The projections of the mSPFp are not fully characterised, which prevent the total understanding of its role in the ejaculatory process. However, it is known that the SPFp projects to several ejaculation-related nuclei like the raphe nuclei and the PAG (Marini et al., 1999). Furthermore, this nucleus receives direct input from the spinal nuclei involved in the ejaculatory reflex (see below) and from several brain areas described before to be involved in male sexual behaviour like the brainstem (namely the paragigantocellular reticular nucleus and the ventral tegmental area (VTA)) the hypothalamus (like the PVN and MPOA) and the amygdala (anterior medial and basomedial amygdala) (Coolen, Veening, Wells, et al., 2003), placing it in a privileged position to relay sensory information from the pelvic area and integrate the external and internal state of the animal during copulation.

Finally, the brainstem is the last relay for the regulation of copulation and ejaculation in rodents, before information is sent to the spinal cord. Injections of fluorogold (a classical retrograde tracer) in the spinal motor nucleus that innervates the BSM, revealed a direct projection from the Gigantocellular Reticular Nucleus (Gi), to the lumbar segments of the spinal cord that control the pelvic muscles (Facchinetti et al., 2014; Shen et al., 1990). Other brainstem structures were also identified as lumbar spinal cord projecting, namely the caudal Raphe Nuclei like the Raphe

Magnus and the Raphe Pallidus, which may have a role in promoting ejaculation (Facchinetti et al., 2014; Shen et al., 1990).

1.3.2 Spinal control of copulation and ejaculation

The brain is the main orchestrator of copulation by integrating the animal's internal cues and the external signals it receives from the environment. However, when it comes to ejaculation, the spinal cord has been seen as the main responsible for the so-called 'ejaculatory reflex'. Besides, it has the important role of coordinating the brain outputs to drive sexual behaviour and produce the correct motor responses.

Classical work, hypothesised that the spinal cord control of ejaculation could work identically to the rhythmic control of central pattern generators (CPG) like the one for locomotion (Zhong et al., 2012), which are capable of producing rhythmic motor patterns in the absence of sensory or descending inputs that carry specific timing information (Marder & Bucher, 2001). In the context of ejaculation, a CPG was defined in rats and named Spinal Ejaculation Generator (SEG) (Truitt & Coolen, 2002). However, the true properties associated with CPGs are still to be fully described for the SEG, especially since it seems to be activated by sensory stimulation of the pelvic area (Carro-Juárez & Rodríguez-Manzo, 2005), which goes against the classical definition of a CPG.

The rat SEG is composed of a group of interneurons expressing galanin (Gal+), but also neurokinin-1 receptor, enkephalin, cholecystokinin, gastrin releasing peptide and substance P (Coolen, Veening, Wells, et al., 2003; Kozyrev et al., 2012; Nicholas et al., 1999; Truitt & Coolen, 2002). These Gal+ cells are located in the lumbar spinal cord, more specifically, in the case of the rat, in the segments L3 and L4, around the central canal

in lamina X and VII (Truitt & Coolen, 2002). Studies in rats manipulating the location of the SEG showed impairments in ejaculation. Namely, while electrical stimulation at the location of the putative SEG evoked ejaculation in anaesthetised rats (Borgdorff et al., 2008), its ablation resulted in complete disruption of the ejaculatory reflex, with no effect on copulatory behaviour (Truitt & Coolen, 2002). Therefore, SEG Gal+ cells represent a putative key player in the spinal control of ejaculation in rats.

Connectivity wise, SEG Gal+ cells have been shown to send a direct projection to the thalamus, more specifically to the SPFp (Coolen, Veening, Wells, et al., 2003). For this reason, these cells have also been called lumbar spinothalamic cells in the past. Because of the existence of this connection, it has been hypothesised that this pathway relays pelvic sensory information to the brain and communicates that ejaculation should take place in order for the ejaculatory reflex to be triggered. This would happen by inducing the releasing of the inhibitory projections that these Gal+ cells are putatively receiving from the brainstem, namely from the Gi and the Raphe Nuclei (Facchinetti et al., 2014; Shen et al., 1990).

Besides their connection to the brain, the main role of SEG Gal+ cells seems to be to locally orchestrate ejaculation. They are connected within the spinal cord to the main centres that control the peripheral nervous system response to induce an ejaculatory response. Namely, the rat SEG receives direct projections from the pelvic sensory innervation. The main input comes from the dorsal penile nerve (DPN), part of the sensory branch of the pudendal nerve (Carro-Juárez & Rodríguez-Manzo, 2005; Larsson & Sodersten, 1973; Núñez et al., 1986). Stimulation of the DPN leads to the initiation of the ejaculatory reflex in rats, namely, electrostimulation of the DPN led to expulsion-like responses in the BSM and bilateral transection of the sensory branch of the pudendal nerve ablated this response (Allard & Edmunds, 2008).

Furthermore, the rat SEG is connected to the MNs that control the pelvic muscles, namely through the pudendal nerve, which will promote the expulsion of sperm that is controlled by the BSM and its MNs located in the segments L5 and L6, more exactly in the Onuf's nucleus (Juárez & Cruz, 2014; Tang et al., 1999).

Finally, the rat SEG has been described as connected to the autonomic nervous system in order to coordinate the emission of sperm. Namely, to the sympathetic centre, which sends information through the hypogastric and the intermesenteric nerves, and the parasympathetic centre which projects through the pelvic nerve to the pelvic organs in order to promote the emission of sperm (Allard et al., 2005). This would put the SEG in the perfect position to coordinate all the steps of the ejaculatory process (Figure 1.2).

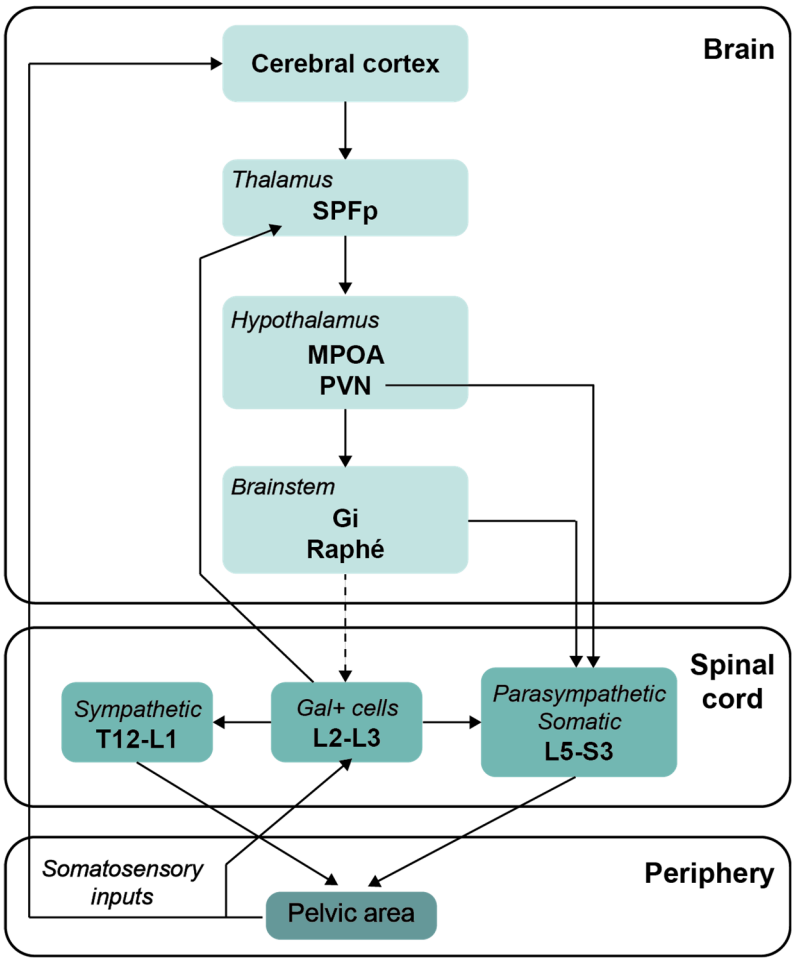

Figure 1.2 Main brain and spinal cord areas involved in the control of male sexual behaviour and ejaculation.

Most of the studies performed in the past support the idea that the SEG has no role in the organisation of copulation, as its ablation did not impair sexual performance (Truitt & Coolen, 2002). However, this working model remains incomplete, and in some cases controversial, in part because most studies were performed either in humans, where causal

manipulations remain challenging, or in rats, with methods that have poor anatomical and cellular specificity, and/or low temporal resolution.

In this thesis, we took advantage of the mouse as a model. Besides all the genetic and molecular tools now available for mice, they also have a copulatory pattern that closely resembles human sexual dynamics, with respect to repeated vaginal thrusting preceding ejaculation, in contrast to rat sexual behaviour, as discussed above (Dewsbury, 1972; Lenschow & Lima, 2020; Valente et al., 2021). However, very little is known about the spinal control of ejaculation in mice.

To our knowledge we are the first to describe in detail a spinal circuit for ejaculation in mice. Therefore, we believe that this thesis is an important contribution to the field as it is the first to address this circuit in mice and bring to the light the role of the Gal+ cells not only in the control of the ejaculatory process but also in the control of male mice sexual behaviour. We will describe said circuits in the next chapters.

2 Anatomical description of the spinal circuit controlling the bulbospongiosus muscle

Sexual behaviour is essential for evolution and species continuation, with ejaculation being the main outcome of the copulatory sequence from the male's perspective. In mice, the BSM is the main responsible for the expulsion of sperm when ejaculation takes place. However, the spinal circuit controlling this muscle remains largely unknown. Here we describe the location and properties of the MNs controlling the BSM, as well as the neurons upstream of this spinal circuit responsible for ejaculation. Using viral and non-viral tracers we identified the location of the BSM-MNs in the lower lumbar and upper sacral spinal segments and observed that they can robustly drive BSM activity when optogenetically stimulated. Furthermore, we characterise a group of Gal+ cells that are

monosynaptically connected to the BSM-MNs, with both the BSM-MNs and the Gal+ cells receiving sensory information from the penis. Together, these results describe for the first time the spinal circuit controlling the BSM, and consequently sperm expulsion, in mice.

2.1 Introduction

Sexual behaviour can be divided into two phases with presumably different neuronal control systems: (1) arousal increase and copulation, and (2) the ejaculatory process itself. Copulation and arousal increase are thought to be centrally regulated, involving the autonomic and sensory-somatic nervous systems (Allard et al., 2005; Corona et al., 2012; Giuliano & Clement, 2005). Ejaculation, in contrast, is a two-step reflex triggered by genital input and controlled by autonomic and somatic circuits located within the spinal cord. During the first step, called emission, sperm and seminal fluids are released and accumulated in the prostatic urethra (Newman et al., 1982; Sheu et al., 2014). The second step, expulsion, is a somatic reflex caused by the activation of spinal MNs and the associated contraction of the BSM, a large, striated muscle surrounding the base of the penis (Peikert et al., 2015; Sachs, 1982; Tang et al., 1999).

How copulatory sequences and arousal increase are coordinated, how the ejaculatory reflex is inhibited until the arousal threshold and, importantly, how the arrival to the arousal threshold is communicated to the spinal cord allowing the reflex to be triggered, remains unresolved.

Important clues come from experiments in anaesthetised male rats, where stimulation of the penis (via electrical stimulation of the dorsal penile nerve) was shown to elicit ejaculation in spinalized animals, but not in intact ones (Marson & McKenna, 1990; Pescatori et al., 1993). While this result suggests that genital stimulation can trigger the ejaculatory reflex per se, descending inhibitory signals to the spinal cord must modulate the impact of such incoming sensory input to prevent the inadvertent activation of the ejaculatory reflex (Carro-Juárez & Rodríguez-Manzo, 2008; Coolen et al., 2004), contributing to a view of the brain as a “spinal-reflex inhibitor“, in addition to a central organiser of sexual behaviour

(Marson & McKenna, 1992, 1996; Normandin & Murphy, 2011; Pescatori et al., 1993). However, an integral question remains unanswered - what spinal circuit does the descending input modulate?

A key finding in the field stemmed from studies in humans (Chéhensse et al., 2017; Coolen et al., 2004) and rats (Dobberfuhl et al., 2014; Truitt et al., 2003; Truitt & Coolen, 2002): the identification of a group of galanin-expressing (Gal+) interneurons in the lumbar spinal cord that contact and drive the activity of BSM-MNs, the “spinal ejaculation generator” (SEG). Several lines of evidence support the decision to label the Gal+ population as a SEG. While electrical stimulation at the location of the putative SEG evokes ejaculation in anaesthetised rats (Borgdorff et al., 2008), its ablation results in complete disruption of the ejaculatory reflex, with no effect on copulatory behaviour (Truitt & Coolen, 2002). Furthermore, the SEG seems to be anatomically connected to the sensory branch of the pudendal nerve, indicating that genital information might reach this population (Carro-Juárez & Rodríguez-Manzo, 2005; Larsson & Sodersten, 1973). Thus, in this model, reaching ejaculatory threshold may be communicated to the spinal circuitry by a transient interruption of the descending inhibitory input, allowing genital stimulation to activate the SEG and the ejaculatory reflex (Allard et al., 2005). However, this working model remains incomplete, and in some cases controversial, in part because most studies were performed either in humans, where manipulations are limited, or in rats, with methods that have poor anatomical and cellular specificity, and/or low temporal resolution.

With this in mind, we decided to use the mouse as a working model to study this spinal circuitry controlling sperm expulsion. The genetic toolkit available in the mouse, that allows cell specific labelling, viral tracing and neural manipulations with state-of-the-art techniques such as optogenetics, in combination with standard techniques such as non viral

tracers and electrophysiology, gives the mouse an enormous advantage when performing anatomical descriptions of a neuronal circuit. Therefore, in this chapter we traced the MNs controlling the BSM and the location of their presynaptic partners, the Gal+ cells. We also electrophysiologically described the BSM-MNs patterns of activity and how they impinge in the BSM. Finally, we described the sensory input arriving from the pelvic area to the BSM-MNs and the Gal+ cells.

2.2 Results

2.2.1 Anatomical and functional characterization of the bulbospongiosus muscle motor neurons (BSM-MNs)

To visualise the MNs involved in sperm expulsion, we targeted the BSM to identify the corresponding BSM-MNs in the spinal cord. Fluorogold (FG), a well-established retrograde tracer (Köbbert et al., 2000), was injected into the BSM of adult mice (N = 12, Figure 2.1 A, B). Serial rostrocaudal reconstruction of the spinal cords revealed a consistent distribution of FG-positive (FG+) BSM-MNs in the dorsomedial part of the ventral horn, near the dorsal grey commissure (Figure 2.1B). FG+ somas were observed across several spinal segments, spanning from the lumbar 3 (L3) to the sacral 2 (S2) segments (Figure 2.2), with the majority of cells located between lumbar 6 (L6) and sacral 1 (S1) segments (Figure 2.1 C).

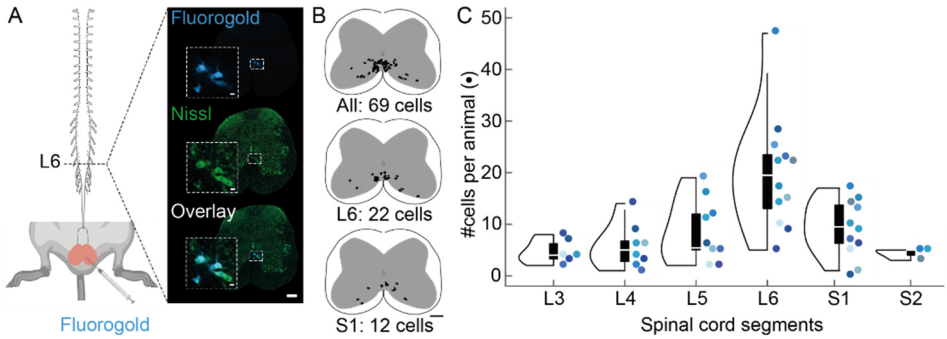

Figure 2.1 Anatomical tracing of the BSM-MNs in the spinal cord of male mice shows a cluster of MNs around the L6/S1 spinal segments. (A) Left panel: Flurogold (FG) was injected into the BSM of adult mice (N=12), leading to labelling across the rostrocaudal lumbosacral spinal cord. Right panel: FG-positive cells (blue) within the lumbar spinal segment 6. Nissl stain (green) was used to identify the spinal cord segment based on the atlas80. (B) Serial reconstruction of all labelled FG-positive cells between lumbar segment 3 and sacral segment 2 revealed their distribution at the dorsomedial ventral spinal cord, close to the grey commissure. Upper panel: distribution of all labelled FG-positive cells for one animal; middle panel: cell distribution within lumbar segment 6 (L6); lower panel: cell distribution within sacral segment 1 (S1). (C) Total FG-positive cell numbers along the lumbosacral spinal cord. Different coloured dots represent different animals. The majority of cells were found at L6 and S1 spinal segments (violin plots elements: see Methods).

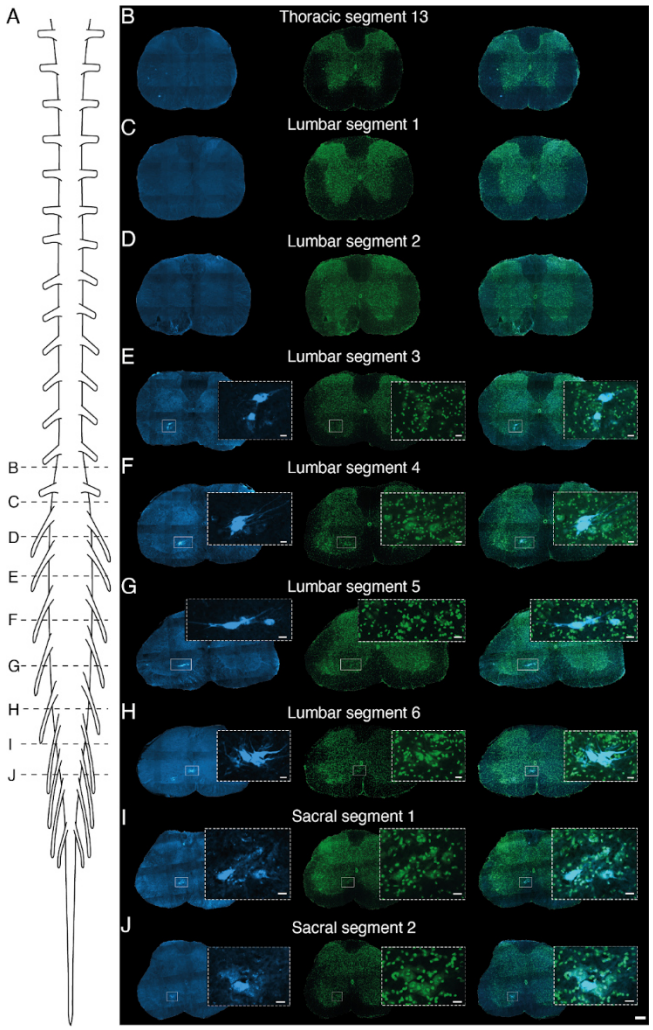

Figure 2.2 Anatomical distribution of the BSM-MNs along the rostrocaudal axis of the spinal cord. (A) Spinal cord scheme illustrating segments that are shown in B-J. (B - J) Left panels: Blue channel revealing FG labelled BSM-MNs (E -J). Middle panel: Green channel illustrating the Nissl stain in order to identify the spinal cord segments. Right panel: Overlap of both channels. Scale bar 200 µm. Inset scare bar: 50 µm.

Immunohistochemical characterization of the FG+ somas revealed that BSM-MNs are classic alpha MNs, expressing choline acetyltransferase (ChAT) and osteopontin, which are alpha MN markers (Misawa et al.,

2012) (Figure 2.3 A). These neurons also receive sensory afferent input, as indicated by the presence of Vesicular Glutamate Transporter 1 (VGLUT1) positive boutons (Figure 2.3 A). Nearly all FG+ BSM-MNs expressed ChAT (75 out of 76 FG+ cells quantified) and VGLUT1 (76 out of 76 FG+ cells) and 80% were osteopontin positive (61 out of 76 FG+ cells quantified; Figure 2.3 B). The soma size of FG+ MNs was similar to that classically reported for alpha MNs (Friese et al., 2009) (Figure 2.3 C).

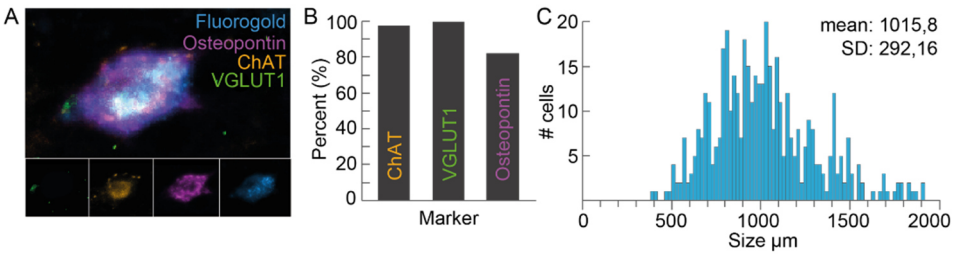

Figure 2.3 Immunohistochemical and size characterization of the BSM-MNs classifies them as alpha MNs. (A) Post-hoc immunohistochemical staining for the alpha MN markers osteopontin (purple), choline acetyltransferase (ChAT, orange) and the sensory input marker Vesicular Glutamate Transporter 1 (VGLUT1, green) revealed that all three markers are expressed by FG-positive cells (blue). (B) Percentages of FG-positive cells expressing ChAT (97.7 ± 2.2 %), VGLUT1 (100%) and osteopontin (81.95 ± 2.2 %). (C) Cell size distribution of FG-positive cells along the rostrocaudal lumbar spinal cord. Frequency histogram depicting number of MNs in each size bin and size of the MNs (binned in 20 μm^2 steps).

To establish a causal relationship between the activity of BSM-MNs and muscle activity, we employed optogenetic methods to selectively activate these MNs (Boyden et al., 2005) while simultaneously monitoring BSM activity with electromyography (EMG). We injected a retrograde travelling adeno-associated virus (rAAV), carrying the gene for the light activated

channel channelrhodopsin-2 (ChR2; rAAV-CAG- -ChR2tdTomato, Addgene (Mao et al., 2011)), into the BSM of postnatal day 3-6 (P3-P6) mouse pups (Figure 2.4 A), as the efficiency of viral particles to infect motor endplates is known to drastically drop at later postnatal days (Stepien et al., 2010), and animals were raised until sexual maturity (2-3 months of age). To activate the ChR2-expressing somas, a laminectomy was performed to allow blue light illumination of several BSM-MNs-containing spinal segments. To assess the specificity of the light stimulation, activity was recorded from both the BSM and a locomotor hindlimb muscle, the Tibialis Anterior (TA) (N = 10, Figure 2.4 A). BSM EMG potentials were tightly locked to laser stimulation (Figure 2.4 B, BSM trace, Figure 2.5). The largest amplitudes (Figure 2.4 C), lowest light intensities to induce activity (Figure 2.4 D), and shorter latencies (Figure 2.4 E), were obtained with illumination above the L6 and S1 segments, in agreement with the BSM-MN rostrocaudal density (Figure 2.5). No activity was observed in the TA (Figure 2.4 B, TA trace, Figure 2.5) nor in animals with minimal or no viral expression in BSM-MNs (data not shown), confirming the specificity of the obtained results.

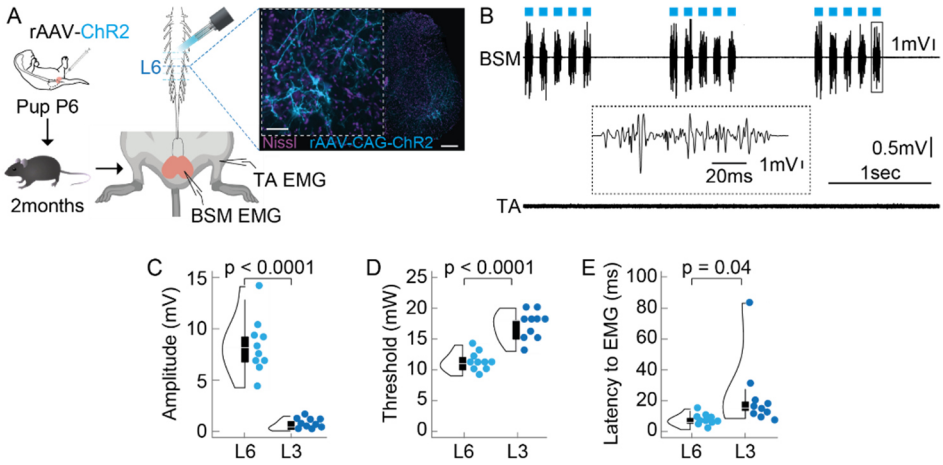

Figure 2.4 Optogenetic activation of the BSM-MNs leads to BSM specific time locked responses. (A) Left panel, experimental setup: For functional characterization, a rAAV-CAG-ChR2 was injected into the BSM of pups (P3-P6), later used for optogenetic stimulation when reaching adulthood. For optogenetic stimulation, a fibre was moved on top and along the rostral caudal lumbar spinal cord while monitoring muscle activity in the BSM and a leg muscle (Tibialis anterior, TA) using electromyogram (EMG). Right panel: rAAV-CAG-ChR2 expression (light blue) in L6 spinal segment (Nissl stain, purple). (B) Example BSM and TA EMG trace recorded while optogenetically stimulating above the L6 spinal segment. (C) Higher BSM EMG amplitudes were triggered when illuminating above the L6 spinal segment (mean amplitude 8.37 ± 1.15 mV), compared to illuminating above the L3 segment (mean amplitude 0.57 ± 0.2). Student's t-test $p < 0.0001$ (violin plots elements: see Methods). (D) The laser power necessary to elicit BSM potentials was lower above the L6 spinal segment (mean threshold 11.2 ± 0.64 mW), compared to stimulating above the L3 segment (mean threshold 17 ± 0.97 mW). Student's t-test $p < 0.0001$ (violin plots elements: see Methods). (E) The onset of BSM activity was shorter with illumination above the L6 spinal segment (mean latency to EMG 7.16 ± 1.58 ms) when compared to the L3 segment (mean latency to EMG 23.48 ± 9.43 ms). Student's t-test $p = 0.04$ (violin plots elements: see Methods).

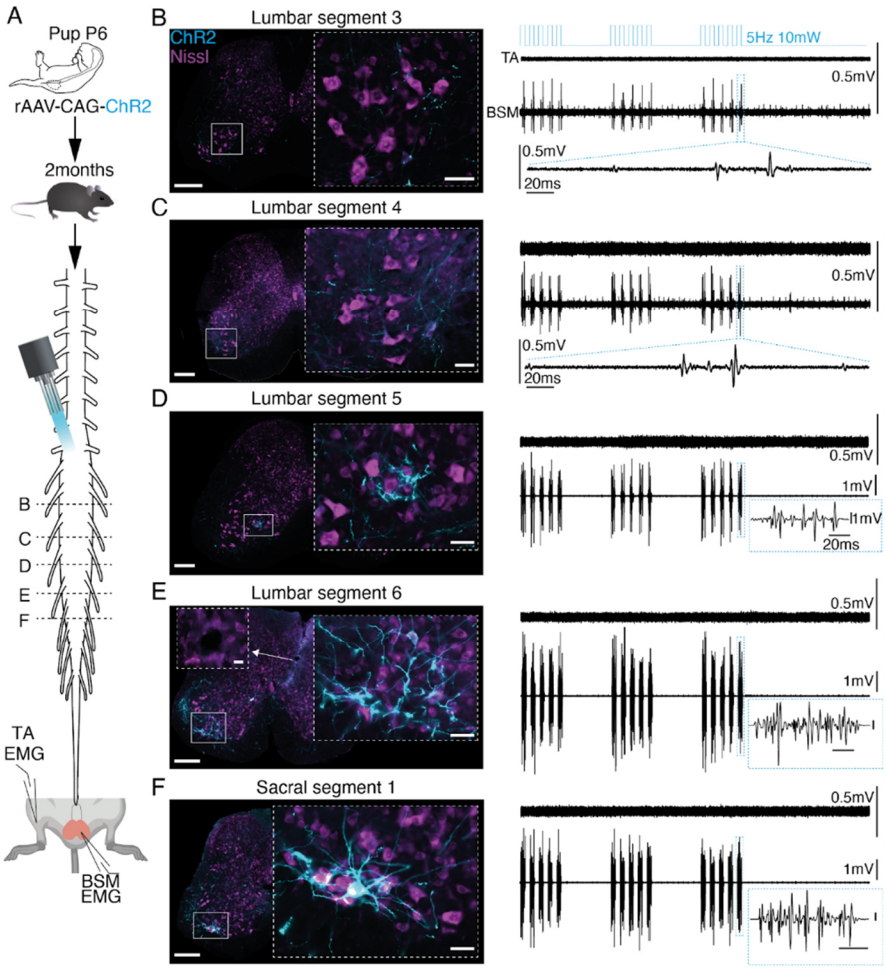

Figure 2.5 Optogenetic stimulation of the BSM-MNs along the rostrocaudal axis of the spinal cord. (A) Experimental setup. Left panel: BL6 mice pups (aged postnatal day 3-6) received an injection of a rAAV-CAG-ChR2 on the BSM. Pups were raised until 2-3 months of age, to perform optogenetic stimulation on top of the spinal cord (rostral to caudal) while in parallel monitoring EMG activity in the BSM. (B) Leftpanel: Representative spinal cord segment (lumbar segment 3, L3) of a 2 month old mouse that was infected at the age of P4-P6 with a rAAV-CAG-ChR2 (blue) in the BSM. Identification of spinal cord segments based on the atlas was achieved via a Nissl stain (purple). Right panel: corresponding EMG recordings (upper trace: TA in the leg; lower trace: BSM) observed while shining blue light on top of the spinal cord segment shown in the left panel. EMG recordings were aligned to histology by placing an electrolytic lesion at the spot with the

largest BSM response recorded (see panel E). Scale bar 200 µm. Scale bar inset 20 µm. (C-F) Same as B for the remaining spinal cord segments depicted in A (see dotted lines, from L3-S1). Note that the biggest responses in the BSM EMG were triggered at the location where most BSM-MNs were infected (L6, S1).

In five animals, we successfully performed single cell juxtacellular recordings from photoidentified BSM-MNs (N = 7 cells; Figure 2.6 A, MN trace (Lima et al., 2009)) alongside BSM EMG recordings. Brief blue light stimulation (10 ms, 15 mW) at different frequencies (upper panel: 5 Hz, middle panel: 10 Hz, lower panel: 20 Hz) reliably elicited short latency action potentials (mean latency to spike: 4.643 ms +/- 0.33 ms, Figure 2.6B), followed by BSM EMG potentials. Spike and EMG fidelities (calculated as the number of spikes or EMG responses divided by the number of light pulses) remained stable up to 20 Hz (Figure 2.6 C). Moreover, light evoked BSM-MN activity resulted in characteristic pelvic floor movements that were tightly locked to the laser, resembling the movements observed during ejaculation in a sexually behaving male (Dewsbury, 1975). Together, these results revealed a population of MNs, primarily located in the L6 and S1 spinal segments, whose optogenetic activation induces characteristic EMG potentials in the BSM and ejaculatory-like movements of the pelvic floor.

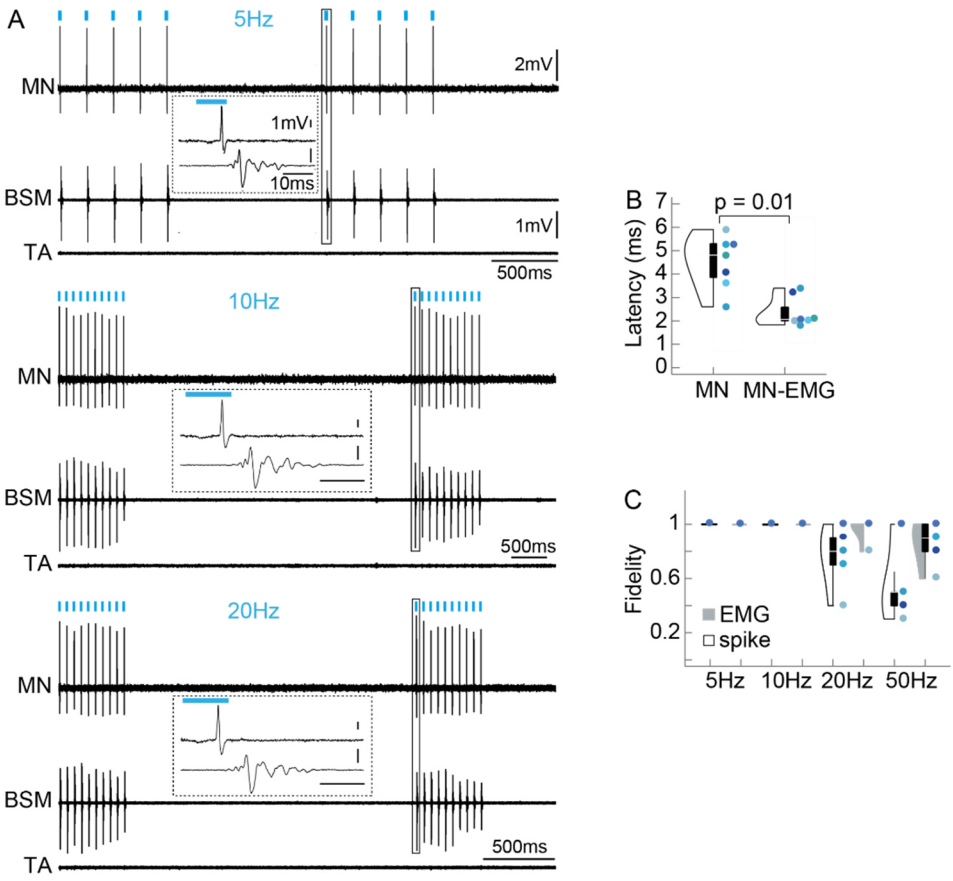

Figure 2.6 Juxtacellular recordings of BSM-MNs while being optogenetically activated, and the consequent BSM response pattern, shows high fidelity to the stimulation protocol. (A) Laser stimulation (10 mW) at 5 Hz (upper panel), 10 Hz (middle panel) and 20 Hz (lower panel) reliably triggered short latency action potentials in a single BSM-MNs. Shortly after the single spikes, BSM EMG potentials were observed (insets) which themselves followed blue laser light applications. No EMG responses were observed in the TA muscle of the leg. (B) Latencies of triggered responses after laser stimulation are plotted for single BSM-MNs (N = 7; mean latency 4.6 ± 0.33 ms) and MN to EMG onset (MN-EMG; mean latency 2.25 ± 0.25 ms). Student's t-test p = 0.01 (violin plots elements: see Methods). (C) Fidelity of spike and EMG activity are shown for the different frequencies of stimulation tested (dark grey: EMG fidelity; black: spike fidelity; violin plots elements: see Methods).

2.2.2 The BSM-MNs receive direct input from a group of lumbar spinal cord Galanin-positive (Gal+) neurons

We next aimed to identify the presynaptic partners of BSM-MNs. To do so, we started by injecting the BSM of adult mice with pseudorabies virus (PRV, Kaplan strain (Boldogkői et al., 2009; Saleeba et al., 2019; Strack & Loewy, 1990)) (Figure 2.7 A). Similar to the FG and retro-AVV injections, PRV-labelled neurons were primarily found in the dorsomedial part of the ventral horn of the L6 segment (Figure 2.7 B). In the rat, BSM-MNs have been reported to receive input from Gal+ interneurons located around the central canal in the lamina X of the L3/L4 spinal segments (Truitt & Coolen, 2002). Consistent with these findings, dense PRV labelling was observed around the central canal in the L2/L3 spinal segments that overlapped with post-hoc immunohistochemical labelling of galanin (Figure 2.7 C), revealing the existence of a similar population of Gal+ cells in the mouse.

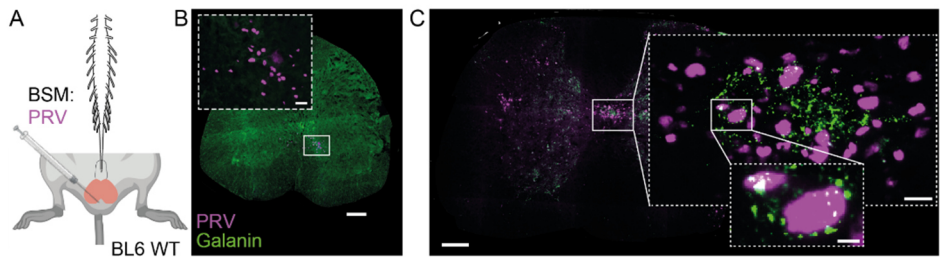

Figure 2.7 The BSM-MNs receive direct input from a group of lumbar Gal+ cells. (A) Experimental setup: PRV injections were done in the BSM of 6 C57BL6 mice. (B) PRV-labelled cells were found at the same major location of FG-positive MNs (see Figure 2.1). Scale bar 200 µm. Scale bar inset 20 µm. (C) PRV injections into the BSM led to prominent labelling around the central canal at the L2/3 spinal segments. Post-hoc immunohistochemical staining against galanin revealed that the PRV labelled cluster was intermingled with galanin-positive immunohistochemical signal surrounding the central

canal at the L2/3 spinal segments (Green: Galanin, Purple: PRV, Scale bar spinal cord section: 200 µm, Scale bar inset 1: 20 µm).

To specifically access the Gal+ population, we utilised a mouse line where Cre recombinase is expressed under the control of the galanin promoter (Gal-cre mice) (Gong et al., 2003, 2007). Gal-cre mice were crossed with a reporter mouse line carrying the gene for the red fluorescent protein TdTomato (Madisen et al., 2010), resulting in progeny expressing the fluorescent protein in all Gal+ neurons (Figure 2.8). Immunohistochemical staining for galanin in the progeny from the Gal-cre x TdTomato cross confirmed the specificity of this mouse line (Figure 2.8 B-D). TdTomato-positive neurons were observed along the rostral caudal axis of the spinal cord, namely in laminae X (around the central canal, N = 10, Figure 2.8 C' and C''), with the highest cell density located in the L2/L3 spinal segments (Figure 2.8 E).

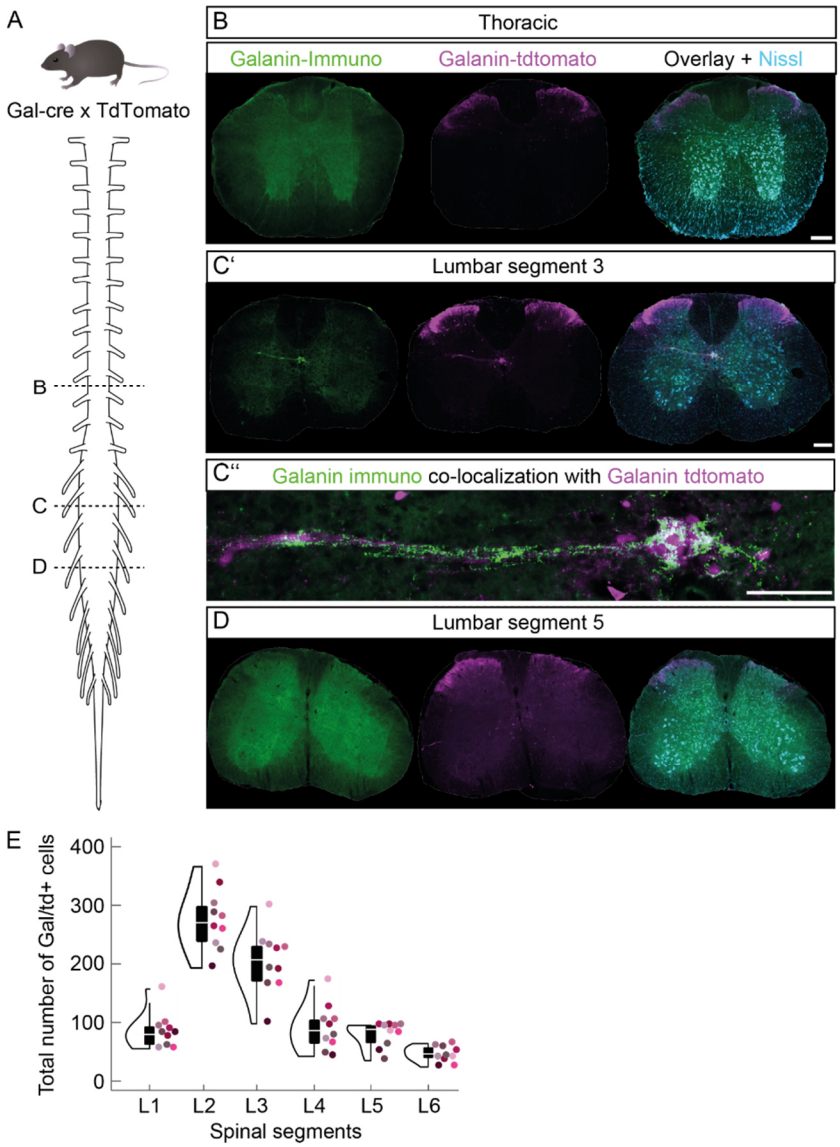

Figure 2.8 Gal+ cells are mainly present around the central canal of the L2/L3 spinal segments. (A) Upper panel: Crossing a Gal-cre line with a tdTomato reporter line, and counterstaining the processed spinal cord sections for galanin, revealed a tight overlap between the tdTomato signal and the galanin signal. Lower panel: Scheme of spinal cord. (B) Example staining, in the thoracic part depicted in A, for Galanin (left, green) in a Gal-cre x TdTomato animal (purple, middle). The Nissl stain (cyan) served as an identification parameter for the spinal cord segments. Note that there is no Galanin signal around the central canal. Scale bar 200 µm. (C') Same as B but for the L3 segment. Note the presence

of a prominent cluster of Galanin expressing cells (shown with the immunostaining, green, and the tdTomato signal, purple, of the Galanin-reporter line) around the central canal. (C") Overlay of the Galanin immunohistochemical signal (green) with the tdTomato signal in the Gal-cre x TdTomato cross reveals an overlap of both signals (see zoom in). Scale bar 100 µm. (D) Same as B but for the L5 spinal segment. Note again the absence of Galanin positive cells around the central canal. (E) Total cell counts (N = 10) of all Gal-cre x TdTomato positive (Gal-tdT+) cells (y-axis) along the rostral-caudal lumbar spinal cord (x-axis) confirmed the presence of a prominent cluster of Gal-cre x TdTomato cells at the L2/3 spinal segments (violin plots elements: see Methods).

The mouse Gal+ neurons also expressed enkephalin, cholecystokinin, gastrin releasing peptide and substance P, similar to the rat Gal+ neurons (Coolen et al., 2003; Kozyrev et al., 2012; Nicholas et al., 1999), as all four peptides were present and overlapped with the Gal+ cells surrounding the central canal in the L2/L3 spinal segments (Figure 2.9).

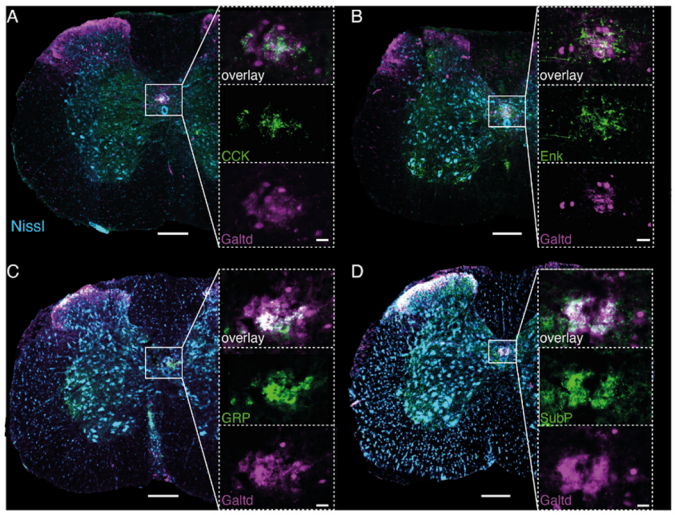

Figure 2.9 Immunohistochemical characterization of the Gal+ cells. (A) Immunohistochemical staining for Cholecystokinin (CCK; green) in the L2/3 spinal segments obtained from a Gal-cre x dTomato (Gal-td, pink) male mouse. A Nissl stain

(cyan) was performed to identify the spinal cord segment. Scale bar spinal segment 200 µm. Scale bar insets 20 µm. (B) Same as A but immunohistochemical processing was done for Enkephalin (Enk). (C) Same as A but a post-hoc staining for Gastrin-releasing peptide (GRP) was performed. (D) Same as A but immunohistochemical staining against Substance P (SubP) was performed.

To determine if the results obtained with the PRV injections are really due to the existence of a monosynaptic connection between the Gal+ cells and the BSM-MNs (Saleeba et al., 2019), we took a two-pronged approach. First, we aimed to identify the location of the synaptic terminals of the lumbar Gal+ cells by injecting a Cre-dependent AAV carrying a green fluorescent protein (GFP)-tagged form of synaptophysin (a synaptic vesicle protein, present in neuronal terminals (Sürmeli et al., 2015)) into the L2/L3 spinal segments of Gal-cre x TdTomato mice (Figure 2.10 A, N = 7). To visualise the BSM-MNs, mice were simultaneously injected with FG in the BSM (Figure 2.10 A). GFP-labelled terminals belonging to Gal+ cells (green channel, Figure 2.10 B) were found around FG+ BSM-MNs (blue channel, Figure 2.10 B) in all 7 animals (Figure 2.10 C). On average, a total of 79% ± 2% FG+ labelled cells overlapped with synaptophysin-labelled terminals (Figure 2.10 C) indicating that the Gal+ neurons in the L2/L3 spinal segments contact the BSM-MNs directly. Furthermore, this approach revealed other projection targets of the Gal+ cells (Figure 2.10 D-H), including the intermediolateral nucleus (IML) and the central autonomic nucleus (CAN) in the lower thoracic and L1 spinal segments (Figure 2.10 E), as well as the sacral parasympathetic nucleus (SPN) (Figure 2.10 H). The IML and CAN are known to contain sympathetic preganglionic cells that provide sympathetic outflow mainly through the hypogastric and pelvic nerves to the visceral organs (Baron & Janig, 1991; Giuliano et al., 1997; Hancock & Peveto, 1979; Nadelhaft & McKenna, 1987). The parasympathetic preganglionic cells clustered in the SPN at

the S2-S5 spinal segments (Figure 2.10 H) innervate the pelvic organs, including the prostate (Orr & Marson, 1998), urethra (Vizzard et al., 1995) and penis (Marson & Carson, 1999). The dorsolateral nucleus (DLN) located at the S1/S2 segments, known to consist of MNs innervating the ischiocavernosus muscle, the most important muscle for erection (Schmidt & Schmidt, 1993), also contained GFP-labelled terminals of the Gal+ cells (Figure 2.10 G). All the regions containing GFP-labelled terminals were also labelled after PRV injection in the BSM (Figure 2.11), except for the DLN which contains ischiocavernosus MNs. These results suggest that the areas sending information to the Gal+ cells receive reciprocal input and confirm that the PRV initial infection was restricted to the BSM.

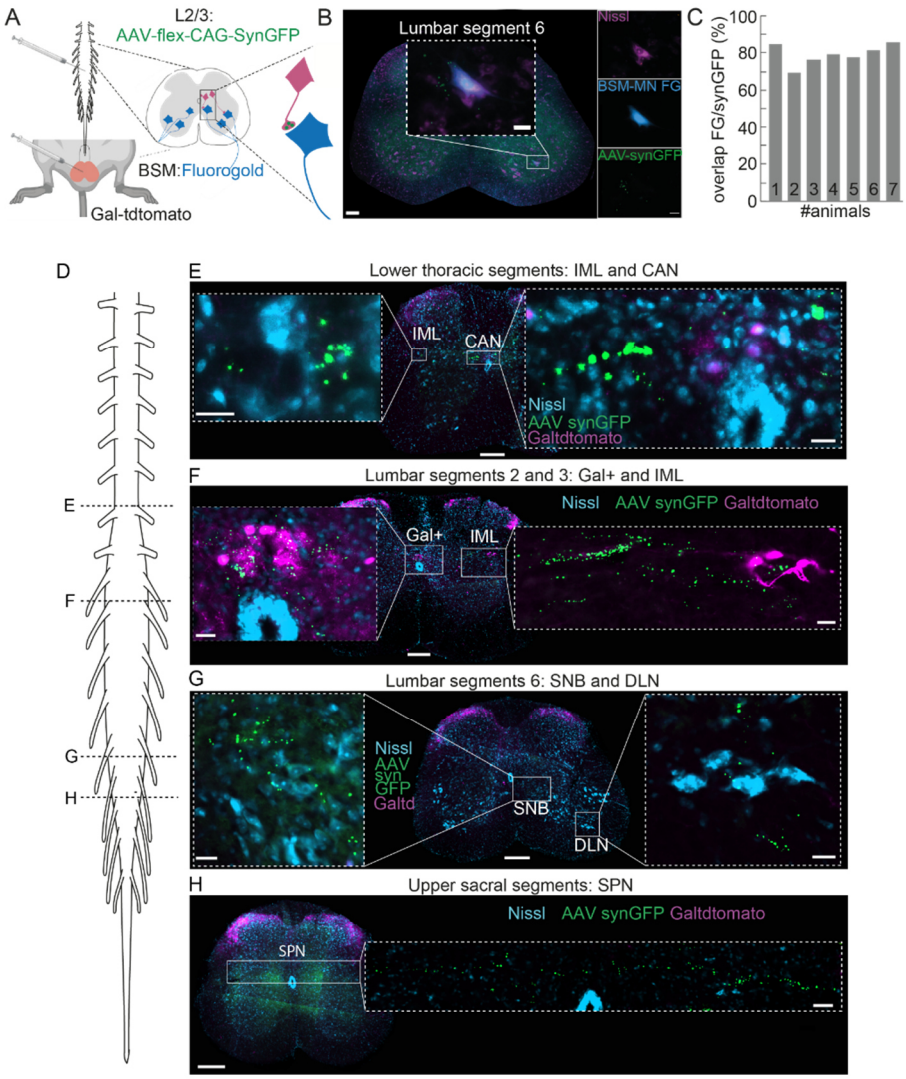

Figure 2.10 Spinal projection targets of the Gal+ cells revealed with a marker for postsynaptic boutons (synaptophysin delivered through an AAV-flex-SynGFP virus). (A) Anatomical connection between Gal+ cells and BSM-MNs was investigated through the co-injection of FG into the BSM and a cre-dependent AAV carrying a GFP-tagged synaptophysin (AAV-flex-CAG-SynGFP) into the L2/3 spinal segments of Gal-cre x TdTomato animals (N = 7). (B) Example image of a spinal cord section obtained from an animal that received FG and AAV-flex-CAG-SynGFP injections. Inset shows a FG-positive BSM-MN that co-localizes with GFP-positive postsynaptic boutons. (C) Quantification of

percentage of FG-positive BSM-MNs showing co-expression of GFP-positive postsynaptic terminals for all 7 injected Gal-cre x TdTomato male mice (mean percentage 79.31 ± 2.1 %). (D) Scheme of spinal cord. (E) GFP-labelled synaptic terminals of Gal+ cells were found at the location of the central autonomic nucleus (CAN) and intermediolateral nucleus (IML) at lower thoracic segments. Both nuclei are known to contain sympathetic preganglionic cells. Scale bar 200 µm. Scale bar insets 20 µm. (F) Prominent GFP-labelled boutons were found at the location of Gal+ cells and at the IML of the L2/3 spinal segments. Scale bar 200 µm. Scale bar inset 50 µm. (G) At the L6 segment, GFP-positive synaptic terminals were dominantly found at the spinal nucleus of bulbocavernosus (SNB) that contains the BSM-MNs and at the dorsolateral nucleus (DLN) which contains the MNs controlling the ischiocavernosus muscle. (H) In upper sacral segments GFP-positive terminals were diffusely found in regions containing parasympathetic preganglionic cells (SPN, sacral parasympathetic nucleus).

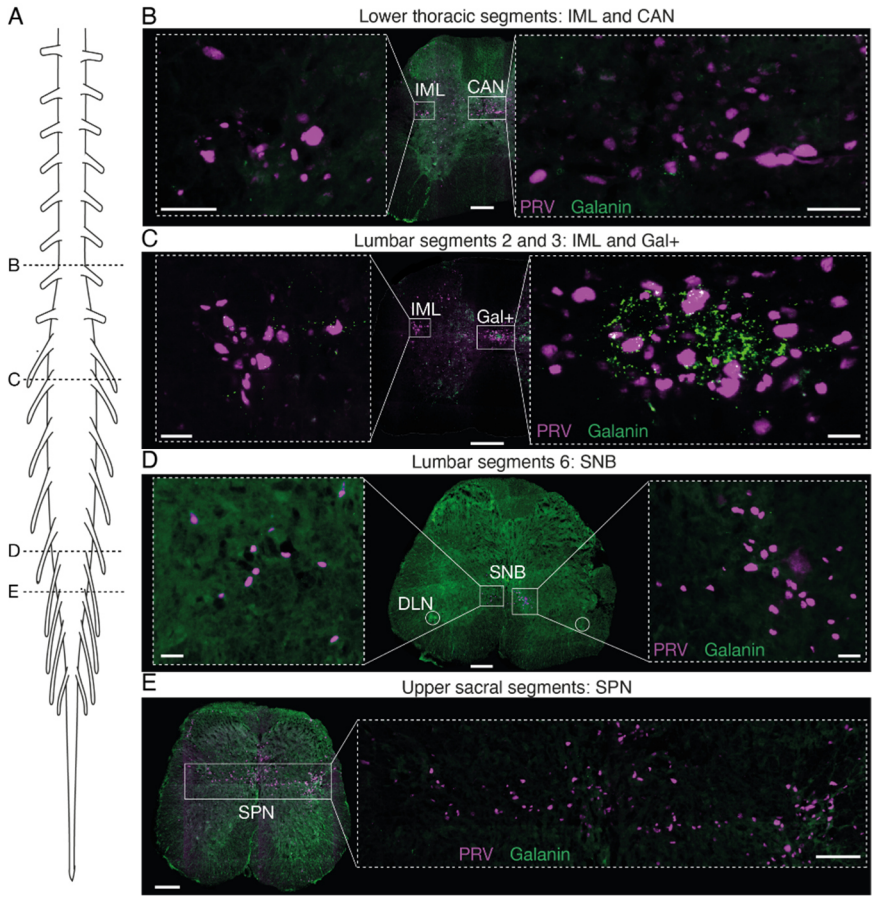

Figure 2.11 PRV injections into the BSM reveal similar anatomical sites as the ones obtained with the injection of AAV-flex-SynGFP at the location of the Gal+ cells. (A) Spinal cord scheme. (B) PRV-positive labelled cells were found at the location of the intermediolateral (IML) and central autonomic nucleus (CAN) at lower thoracic segments. Scale bar 200 µm. Scale bar inset 20 µm. (C) Prominent PRV labelling was encountered at the central canal and at the IML in L2/3 segments. Scale bar 200 µm. Scale bar inset 20 µm. (D) Clusters of PRV cells were present only in the spinal nucleus bulbocavernosus (SNB), that contains the BSM-MNs, at the L6 segment, but not on the dorsolateral nucleus (DLN, white circle), containing the MNs controlling the ischiocavernosus muscle, which shows the specificity of the PRV approach to trace the MNs innervating the BSM. Scale bar 200 µm. Scale bar inset 50 µm. (E) In the upper sacral segments, PRV labelling could be seen along the spinal parasympathetic centres (SPN). Scale bar 200 µm. Scale bar inset 100 µm.

To obtain physiological evidence supporting a direct synaptic connection between the Gal+ cells and the BSM-MNs, we performed *in vitro* whole-cell patch clamp recordings from cholera toxin-B (CTB-594) retrogradely-labelled BSM-MNs in acute spinal cord slices of mouse pups (P2-P6) expressing ChR2 under the galanin promoter (Gal-Chr2, progeny from the cross between the Gal-cre mouse and the ChR2 mouse) (Madisen et al., 2012) (Figure 2.12 A). It is important to note that using adult sexually mature animals for this approach is very challenging, as MNs undergo rapid cell death when performing spinal cord slices beyond a certain age, likely due to their complex dendritic branching (Burke & Rudomin, 1977).

An optical fibre (0.5 mm diameter) was placed close to the central canal (Figure 2.12 A) to illuminate the terminals of the Gal+ cells. A total of 21 CTB-positive BSM-MNs were recorded in Gal-ChR2 pups (N = 7), of which 18 reliably responded to laser illumination (Figure 2.12 B-F). Short laser pulses led to dominant excitatory postsynaptic potentials (EPSPs) and/or action potentials in CTB-positive BSM-MNs (see upper traces in Figure 2.12 D and E). Repeating laser stimulation after the superfusion of a high cation containing aCSF, to isolate monosynaptic transmission (Falgairolle & O'Donovan, 2019), resulted in much smaller EPSPs in BSM-MNs (middle traces in Figure 2.12 D and E). Blocking neural transmission via the pharmacological manipulation of NMDA (through AP5) and AMPA (through DNQX) receptors (lower traces in Figure 2.12 E) abolished light-triggered EPSPs in BSM-MNs. In contrast to the BSM-MNs, other large CTB-negative lumbar MNs (N = 16) did not respond to laser illumination (1 out of 16 responded, Figure 2.12 F). Taken together, these findings provide evidence for a population of Gal+ neurons present in the laminae X of the L2/L3 spinal segments in mice, which is monosynaptically connected to BSM-MNs via glutamatergic transmission.

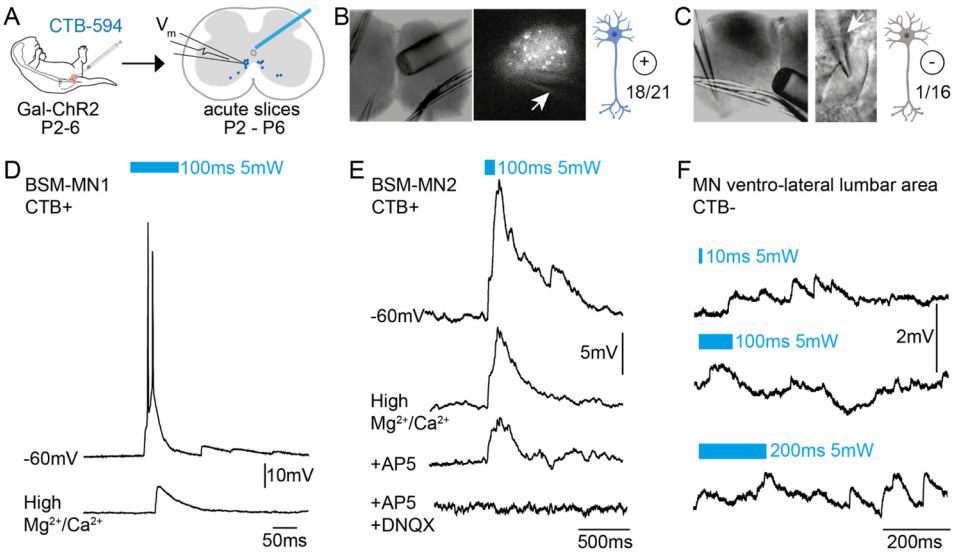

Figure 2.12 In vitro whole cell patch clamp recordings of BSM-MNs while stimulating the Gal+ cells terminals show their monosynaptic connection. (A) Experimental setup for establishing the functional connectivity between the Gal+ cells and BSM-MNs; in vitro whole cell recordings from choleratoxin-B (CTB, tagged with 594 fluorophore) retrogradely labelled BSM-MNs in acute spinal cord slices of Gal-Chr2 pups aged P2-P6. (B) Example spinal cord slice showing the location of fibre and pipette placement (left panel) during the recording of a CTB-positive cell (middle panel). A total of 21 CTB-positive cells were recorded, of which 18 were connected to Gal-ChR2+ fibres running through the dorsal grey commissure above the central canal (right panel). (C) Example spinal cord slice showing the location of fibre and pipette placement (left panel) during the recording of a control cell, a large MN located at the lateral ventral horn and CTB-negative (middle panel). A total of 16 CTB-negative cells were recorded out of which 1 seemed to be connected to Gal-Chr2+ fibres running through the dorsal grey commissure above the central canal (right panel). (D) Example of a whole-cell recording from CTB-positive BSM-MN. Upper trace: a 100 ms laser stimulation led to a short latency Excitatory Postsynaptic Potential (EPSP) and action potentials. Lower trace: High-concentration of Mg+ and Ca2+ in the ACSF lowered the amplitude and latency of the light triggered EPSP. (E) Second example of a CTB-positive BSM-MN is shown, same as L. Lower trace: Application of NMDA and AMPA receptor blockers abolished the light-evoked EPSP, indicating that the neural transmission between Gal+ cells and BSM-MNs is glutamatergic. (F) Example of a whole-cell recording of a CTB-negative MN. In contrast to the high number of CTB-positive cells

responding to laser stimulation, only in 1 out of 16 CTB-negative cells did the stimulation (Upper trace: 50 ms, Middle trace: 100 ms, Lower trace: 200 ms) led to an EPSP.

2.2.3 Gal+ neurons and BSM-MNs receive sensory input from the penis

It has been hypothesised that once the ejaculatory threshold is reached, genital input can activate the spinal circuitry controlling the ejaculatory reflex (Allard et al., 2005). This model is supported by anatomical evidence, as previous studies have reported connections between the sensory branch of the pudendal nerve and putative rat Gal+ neurons (Larsson & Sodersten, 1973). However, to the best of our knowledge, functional connectivity has never been established. Therefore, next we investigated whether the BSM-MNs and Gal+ cells receive sensory feedback from the penis.

We first replicated an experiment previously conducted in rats (Carro-Juárez & Rodríguez-Manzo, 2000, 2005; Larsson & Sodersten, 1973) (where the penis is stimulated electrically or through air puffs) in male mice that were either intact (Figure 2.13 A and B) or spinalized (Figure 2.13 C and D) while monitoring the BSM activity in parallel through EMG. Consistent with findings in rats, we observed prominent BSM EMG activity when stimulating (200 Hz, 100 pulses, 6 V; 5 Hz, 3 x 5 pulses of 100 ms, 6 V) the penis in a spinalized preparation, whereas penile stimulation in intact mice resulted in minimal BSM activation (Figure 2.13 B and D). Penile stimulation-triggered BSM responses were significantly larger in amplitude (Figure 2.13 E) and duration (Figure 2.13 F) in spinalized mice compared to non-spinalized mice, although the onset of BSM responses did not differ (Figure 2.13 G). These experiments further support the existence of supraspinal inhibition of the spinal circuitry, but do not yet

confirm whether penile sensory information is physiologically integrated at the level of Gal+ cells and/or BSM-MNs.

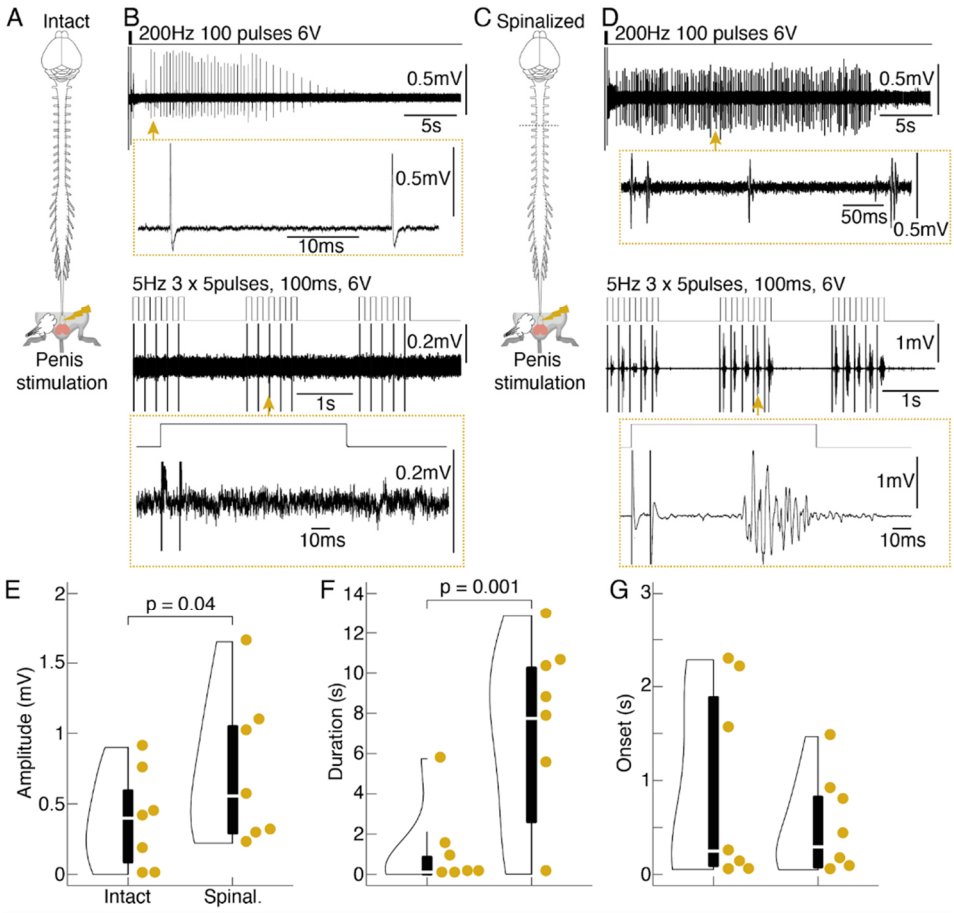

Figure 2.13 Mechanical and electrical stimulation of the penis leads to more pronounced BSM EMG activity in a spinalized anaesthetised in vivo preparation. (A) Experimental design: stimulation of the penis was achieved with either current application using a nerve cuff electrode or with an airpuff, pointed to the penis that was pulled out. The anaesthetised preparation was intact, meaning that the connection with the brain was kept. (B) Example EMG traces obtained in an animal in which the connection to the brain was kept intact and electrical stimulation was applied to the penis. Upper panel: train stimulation. Lower panel: 5 Hz stimulation. Note that the train stimulation triggered modest

BSM responses while the 5 Hz stimulation did not trigger any activity in the BSM EMG. (C) Same as A but the anaesthetised preparation was spinalized, meaning that the connection to the brain was cut. (D) Same as B but for the spinalized preparation. Note that both the train stimulation and 5 Hz stimulation triggered striking BSM responses. (E) Violin plot comparing the amplitude of BSM responses upon sensory penile stimulation in an intact vs. spinalized (spinal.) preparation (N = 7). Penis stimulation led to significantly bigger BSM amplitudes in spinalized preparations in comparison to the intact preparations. Every dot represents an animal. (F) Same as E but the duration of BSM responses is plotted. Penis stimulation led to significantly longer BSM responses in spinalized preparations in comparison to the intact preparations. (G) Same as E but the onset of BSM responses is shown. No significant difference was found.

To address this question, we used an optogenetic approach and mapped light-induced local field potentials (LFP) of ChR2 infected BSM-MNs in the lumbar spinal cord of adult male mice combined with BSM-EMG recordings (Figure 2.14 A). Prominent time-locked LFP deflections were observed when illuminating above the BSM-MNs-containing spinal segments (Figure 2.14 B, blue trace, Vm) which were followed by BSM activity (Figure 2.14 B, black trace, BSM EMG). After mapping the optimal location of laser induced BSM-MN LFP deflections and BSM EMG activity, the position of the glass pipette capturing LFP deflections was maintained while applying brief air puffs of 5 Hz (10 ms, 1 bar) to the pulled-out penis, or the leg as a control (Figure 2.14 C). Air puff stimulations led to larger LFP deflections when applied to the penis (Figure 2.14 C, blue trace) compared to leg puffs (Figure 2.14 C, yellow trace), a result that was consistent at the population level (Figure 2.14 D). Plotting the light-induced BSM-MNs LFPs against the LFP deflections induced by penis puffs (blue) or the leg puffs (yellow) showed a higher correlation between the light-induced LFPs and the penis puffs (Figure 2.14 E). These results hint to the BSM-MNs receiving sensory input from the penis.

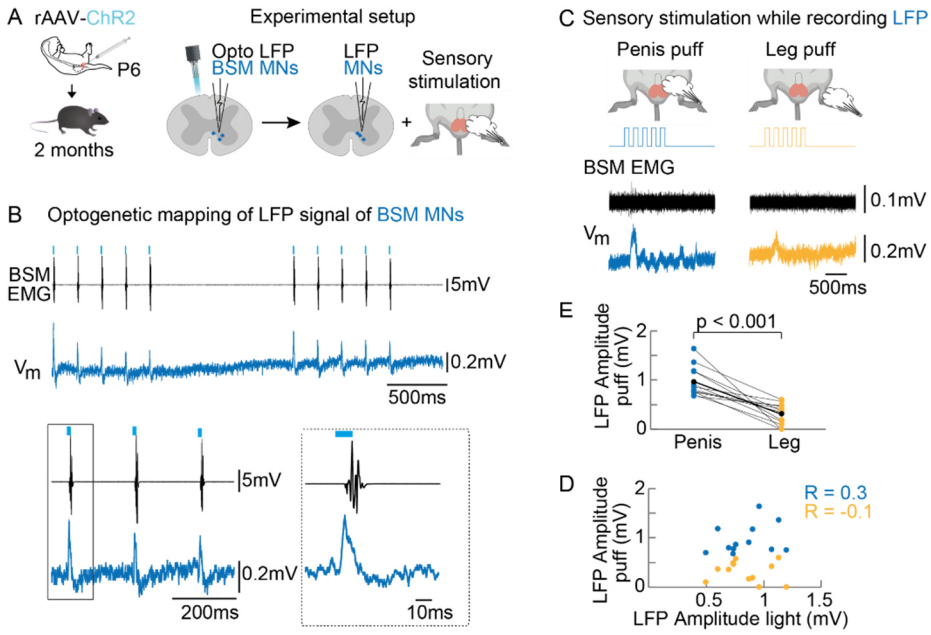

Figure 2.14 BSM-MNs receive sensory input from the penis. (A) Light-induced local field potentials (LFPs) were mapped in adult male mice whose BSM-MNs were infected with ChR2 at young age (rAAV-CAG-ChR2 injections into the BSM at P3-P6). Once the position with the most prominent light triggered LFPs was detected, the glass pipette was left at that position and sensory puff stimulations of penis and leg were conducted. (B) Example traces for optogenetically induced LFP activity of BSM-MNs. BSM (black) and LFP responses (blue) were tightly locked to the laser onset. (C) The pipette was kept at the position where the highest LFP responses were encountered. Subsequently sensory airpuff stimulation of penis (left, dark blue) and leg (right, yellow) were conducted while monitoring LFP and EMG responses in animals whose BSM-MNs were infected with ChR2. Example traces were obtained from the same animal and correspond to the LFP traces depicted in A2. (D) The highest light-induced LFP responses are plotted against the penis/leg puff induced LFP responses revealing that penis puff-induced LFPs (blue) are more strongly correlated with the light induced LFP than the leg puff-induced LFP responses (yellow). Every dot is the pooled data of an animal (N = 12). (E) Penis puff responses (blue) led to significantly higher amplitudes (mean 0.96 ± 0.27 mV) in LFP than leg puff responses (yellow; mean amplitude 0.31 ± 0.09 mV). Student's t-test $p < 0.001$.

We repeated the same experiment in male mice expressing ChR2 under the Gal promoter (Gal-ChR2), as we mapped light induced LFP signals at the location of the Gal+ cells (Figure 2.15 A) while monitoring BSM activity in a spinalized preparation. Optogenetic stimulation at the L2/L3 spinal segments evoked prominent BSM responses (Figure 2.15 B, black trace) in line with time-locked LFP deflections (Figure 2.15 B, pink trace). We then performed air puff stimulations on the penis or leg while maintaining the LFP capturing pipette at the spot of the most effective light-induced LFPs (Figure 2.15 B, right panel). Penile sensory stimulation elicited significantly larger LFP responses (Figure 2.15 C, pink trace) compared to leg airpuffs (Figure 2.15 C, yellow trace and Figure 2.15 D). Moreover, light-induced LFPs were more correlated with LFPs induced by penis puffs than those elicited by leg puffs (Figure 2.15 E) indicating that penile sensory inputs can reach the Gal+ cells present at the L2/L3 spinal segments. These findings provide evidence that both the BSM-MNs and the Gal+ population are the recipients of penile sensory information.

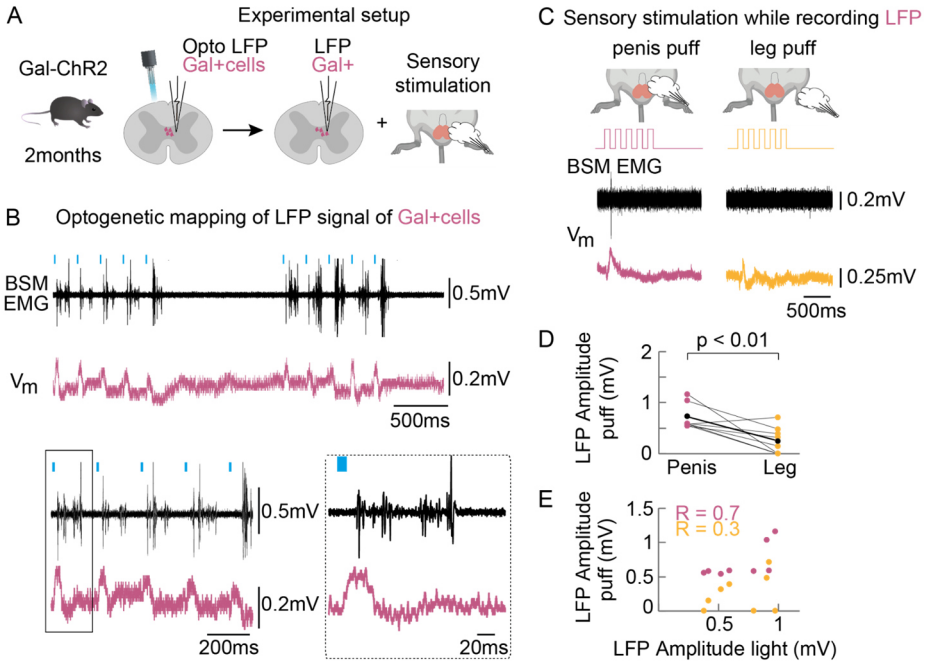

Figure 2.15 Gal+ neurons receive sensory input from the penis. (A) Light-induced LFPs were first mapped in Gal-ChR2 mice. Afterwards the mapping pipette was left at the location where the strongest light triggered LFPs were encountered. Subsequent sensory stimulation of penis and leg were conducted while monitoring LFP and EMG activity in parallel. (B) Example traces for optogenetically induced LFP activity in Gal-ChR2 animals (pink) while BSM activity (black) was monitored in parallel. Note the light-locked responses of the BSM with parallel timed LFP activity (putative Gal+ population activity around the central canal in L2/3). (C) Example traces for penis (pink) and leg (yellow) puff induced LFPs correspond to the traces shown in B2. (D) Highest light-induced LFP responses are plotted against the penis/leg puff induced LFP responses revealing that penis puff induced LFPs (pink) are more strongly correlated with the light induced LFP than leg puff induced LFP responses (yellow). Every dot is the pooled data of an animal (N = 8). (E) Penis puff responses (pink) led to significantly bigger LFPs (mean amplitude 0.73 ± 0.09 mV) than leg puffs (yellow; mean amplitude 0.25 ± 0.09 mV). Student's t-test p = 0.0035.

2.3 Discussion

Ejaculation, and sperm expulsion more specifically, are essential components of a successful sexual encounter (Dewsbury, 1972). Therefore, unravelling the neuronal circuits controlling this behaviour is essential for better understanding potential disorders associated with altered ejaculatory patterns (Carson & Gunn, 2006).

In this chapter we used male mice to trace the spinal circuit involved in sperm expulsion. We used the BSM as an entry point, being the main muscle responsible for contracting to eject sperm. We traced the MNs controlling this muscle as well as a group of Gal+ cells that are monosynaptically connected to them. We further described the BSM-MNs functional properties as well as the sensory input that both BSM-MNs and Gal+ cells are receiving from the pelvic area. To our knowledge, the results in this chapter are the first to describe this circuit in mice and to use state of the art techniques to further investigate the properties of said circuit.

2.3.1 Anatomical and functional characterization of BSM-MNs

Using the classical tracer Fluorogold, we began by showing the spinal distribution of the BSM-MNs along the rostral caudal axis, finding them to be distributed, from L3 to the S1 segments, with the highest density located on the L6 and S1 segments. Even though unexpectedly widely distributed, the location and total number of BSM-MNs is in accordance with previous studies (Sengelaub & Forger, 2008; Wagner & Clemens, 1989). With the use of immunohistochemical markers, namely osteopontin, ChAT and VLGUT1, in combination with an evaluation of the soma size, we concluded that the majority of BSM-MNs are principal alpha

motor neurons, as it has been described for other striated muscles (Friese et al., 2009).

Using optogenetics, we specifically drove BSM-MNs activity and, as expected, elicited pronounced BSM muscle potentials. These responses were time locked to the stimulus and present even after several rounds of optogenetic stimulation. Furthermore, we observed prominent pelvic floor movements, upon stimulation. These movements resemble the pelvic floor movements observed when a behaving animal is performing the deep thrust associated with ejaculation. This further supports the idea that the BSM-MNs and the consequent BSM activity are indeed the main players in sperm expulsion during copulation (Elmore & Sachs, 1988).

2.3.2 Anatomical and functional characterization of Gal+ cells

We next performed PRV tracing combined with immunohistochemical stainings and found a cluster of Gal+ cells located around the central canal at lumbar segments 2 and 3. This population of Gal+ cells shares a similar immunohistochemical profile to the rat putative SEG, but is found in a slightly different location; while the rat SEG is located at the L3 and L4 segments, our Gal+ cluster is situated between the L2 and L3 (Truitt & Coolen, 2002). Even though PRV has not been previously used in mice to study the muscles of the pelvic floor, it was used successfully in the rat to identify the spinal ejaculation circuitry (Dobberfuhl et al., 2014; Xu et al., 2005, 2006). To further establish the monosynaptic connection between the Gal+ cells and BSM-MNs we labelled the synaptic terminals of the former by using a Cre-dependent AAV, expressing a GFP tagged form of synaptophysin. We found that around 80% of all BSM-MNs overlapped with labelled Gal+ cells terminals. Interestingly, we also observed that the

Gal+ cells project to other spinal cord locations, namely, the CAN, IML and SPN (the first two being the location of the pelvic sympathetic centres, and the third the parasympathetic one). Previous studies with rats using PRV injections in the pelvic organs, namely the prostate (Orr & Marson, 1998), testis (Gerendai et al., 2000), ductus deferens (Gerendai et al., 2003) and penis (Marson et al., 1993) revealed labelling of the autonomic centres followed by labelling of the lumbar spinal cord in the dorsal grey commissure, the location of the Gal+ cells. With our dual genetic based approach, based on retrograde (PRV) and anterograde (AAV expressing synaptophysin) methods, we are, to our knowledge, the first to show a reciprocal connection between the autonomic centres and the Gal+ cells in mice, that could be the basis to coordinate sperm emission.

To functionally prove the monosynaptic connection between the BSM-MNs and the Gal+ cells we performed whole cell patch clamp recordings of CT-B+ BSM-MNs in spinal cord slices obtained from pups (P0-P4) from a Gal-cre line crossed with ChR2. Optogenetic stimulation of Gal+ cells terminals triggered light specific EPSPs in BSM-MNs but not in CT-B-negative MNs. This data further supports that the Gal+ cells and BSM-MNs are functionally monosynaptically connected.

2.3.3 Sensory innervation of Gal+ neurons and BSM-MNs

Sensory innervation of the pelvic floor was also assessed in this paper. With penis air puff stimulation, we measured LFP responses in the spinal cord, specifically in the areas richest in Gal+ cells and BSM-MNs. We observed that air puff penis stimulation induced reliable responses in both spinal locations, which indicates direct sensory feedback from the penis and the pelvic area to these key cell groups. This is in accordance with

previous studies in rats that show a connection between the sensory branch of the pudendal nerve and Gal+ cells (McKenna & Nadelhaft, 1986). Anatomically, this connection is well-positioned for sending sensory information from the pelvic area to the Gal+ cells to trigger ejaculation.

2.4 Materials and Methods

2.4.1 Experimental model and subject details

All experimental procedures were carried out in strict accordance with the guidelines of the European Committee Council Directive and were approved by the Animal Care and Users Committee of the Champalimaud Neuroscience Program, the Portuguese National Authority for Animal Health (Direcção Geral de Veterinária; approval number 0421/000/000/2022) and by the local ethic committee of the University of Bordeaux and the French Agriculture and Forestry Ministry for handling animals (approval number 2016012716035720). For tracing from the BSM (FG and PRV), BL6 (*Mus musculus domesticus*, C57BL/6J) male mice aged 3-6 months were used. For tracing from the spinal cord, Gal-cre x TdTomato (*Mus musculus domesticus*, B6;129S6-Gt(ROSA)26Sortm9(CAG-tdTomato) Hze/J) male mice aged 3-6 months old were obtained from Jackson Laboratories. For the airpuff/electrical sensory stimulation of the penis, Gal-ChR2 (*Mus musculus domesticus*, B6;129S-Gt(ROSA)26Sortm32(CAG-COP4 *H134R/EYFP)Hze/J) male mice aged 3-6 months old were obtained from Jackson Laboratories. For the pup muscle injections, BL6 male mice pups aged P3-P6 were used. For the pup optogenetic and electrophysiology experiment, Gal-ChR2 male mice pups aged P2-P6 were used. All animals were bred and

maintained in our animal facility. Except for the optogenetic experiment in pups, all animals were weaned at 21 days and housed in same-sex groups in stand-alone cages (1284L, Techniplast, 365 × 207 × 140 mm) with access to food and water *ad libitum*. Mice were maintained on an inverse 12:12 light/dark cycle and experiments were performed during the dark phase of the cycle, phase of higher animal activity. Immediately after surgery, male mice were kept single-housed until the experiment was over.

2.4.2 Bulbospongiosus muscle injections

Mice were anaesthetised with 3% isoflurane in oxygen and put into the mouthpiece of a stereotaxic device (Kopf, Tujunga, CA, USA). After that, mice were turned into a supine position to facilitate access to the BSM. After shaving the anogenital area and cleaning with Betadine (MEDAPharma) and 70% ethanol, a small incision in the scrotum area was made. At this point, an analgesic (buprenorphine, 0.05-0.1 mg/kg, intraperitoneal injection) was administered. The BSM was exposed after removing fat and conjunctive tissue. Pulled capillaries (length 3 1/2 inches [9 cm]; inner diameter 0.53, outer diameter 1.14 mm; tip diameter 40 µm; DrummondScientific, Broomall, PA, USA) were used to inject 1,5 µl of 2% Fluorogold (FG) at a rate of 13.8 nL per pulse, and a frequency of 0.2 Hz. In total, 5 BSM sites were injected with FG (three in the dorsal and two in the ventral portion of the BSM). A waiting time of 5 min prior to and 10 min after injection was kept. The glass pipette was pulled out slowly and the skin sutured. All mice were single housed post-surgery, for 1 to 2 weeks, until perfusion. A total of 12 male mice was used for anatomical investigation of BSM motor neurons using FG.

Another 6 male mice were injected with PRV-Ka-gEI-mCherry (PRV (Boldogkői et al., 2009)) in the BSM. The male was similarly anaesthetised with 3% isoflurane in oxygen and put into the mouthpiece of a stereotaxic device. After that, mice were turned into a supine position to access the BSM, and after disinfecting, a small incision was made to expose the muscle. Using a glass pipette as described above, 1 µl of PRV was injected once into the BSM at a rate of 13.8 nL per pulse, and a frequency of 0.2 Hz. A waiting time of 5 min prior to and 10 min after injection was kept, after which the pipette was pulled and the incision sutured. All mice were single housed post-surgery, for 3-4 days, until perfusion.

2.4.3 Pup viral injections

To infect the BSM-MNs with the light activated channel, channelrhodopsin-2 (ChR2), young animals needed to be used as it has been shown that viral tracers are not able to infect the motor end plate beyond a certain age (Stepien et al., 2010). Pups (P3-P6) were briefly separated from their litter and mother, and cryo-anaesthetised. After all reflexes were gone, pups were placed on ice and a small incision below the penis was made to access the BSM. Pulled capillaries (length 3 1/2 inches [9 cm]; inner diameter 0.53, outer diameter 1.14 mm; tip diameter 15-20 µm; DrummondScientific, Broomall, PA, USA) were used to inject 1 µl of retroAAV-CAG-hChR2-H134R-tdTomato (28017-AAVrg, Addgene) into the BSM at a rate of 18.4 nl/pulse per second.

After injection, the incision was glued and the pups placed onto a heating pad. Once all reflexes were recovered, the pups were put back to their litter and mother. Injected pups were raised until 2-3 months of age before performing the acute optogenetic experiments as described above.

2.4.4 Spinal cord stereotaxic viral injections

Mice were anaesthetised with 3% isoflurane in oxygen and spinally fixed into a stereotaxic frame using adapted vertebrae clamps (Kopf, Tujunga, CA, USA). During surgery, anaesthesia was maintained using 1.5% isoflurane. Injection sites (lumbar segments 2/3) were targeted by using vertebral landmarks as described in (Harrison et al., 2013). Muscle and fat tissue were gently removed in order to get a better sight onto the spinal cord. The injection pipette was inserted in between the thoracic vertebrae T11 and T12 before having made a small puncture into the dura mater that allowed for better insertion of the injection pipette. Pulled capillaries (length 31/2 inches [9 cm]; inner diameter 0.53, outer diameter 1.14 mm; tip diameter 40 µm; DrummondScientific, Broomall, PA, USA) were used to inject the AAVs at 100 µm medial from the midline and at a depth of 750-850 µm from the spinal cord surface, at a rate of 0.1 Hz with 2.3-4.6 nL per pulse. For the AAV1-CAG-floxed-SynGFPrev-WPRE (N=7), 30 nL were injected. Before and after the pressure injection a waiting time of 10 min was kept. Afterwards, the pipette was retracted, eventual bleeding stopped and the skin sutured. Analgesic (burprenorphine 0.1 mg/kg) was administered post surgery at all times. After sufficient time for viral expression (3 weeks), animals were deeply anaesthetised and perfused transcardially with saline, followed by a cold 4% paraformaldehyde solution (PFA) in 0.01 mol/L PBS. Spinal cords were removed from the spine and kept for 1 h in 4% PFA before transferring them for another hour into 0.01 M PBS. Subsequently spinal cords were stored overnight in 30% sucrose in 0.01 M PBS, 0.1% azide in order to cryo-protect the tissue. Spinal cords were embedded in frozen section medium and frozen for half an hour at -80 °C in 2-methylbutane solution before mounting them in the cryostat. Spinal cord sections were cut and mounted on a poly-lysine-coated glass slide at 50 µm.

2.4.5 Electrophysiology

In vivo anaesthetised optogenetic stimulation

For acute electrophysiological experiments, mice (N = 10) underwent optogenetic stimulation of the BSM-MNs (BL6 mice infected with an AAV expressing ChR2 on the BSM). Mice were anaesthetised by injection of an initial dose of 100 mg/kg ketamine and 7.5 mg/kg xylazine. Respiration, blink and pinch reflex were observed throughout the experiment and, if needed, animals were injected with an extra shot (25%) of ketamine/xylazine mixture or a 25% dose of ketamine alone. The animal's back, scrotum and right leg were shaved and cleaned with ethanol. Electromyogram electrodes were inserted into the BSM or tibialis anterior (TA) muscles and glued using Vetbond. The back skin was cut along the rostral caudal axis and the spine was fixed into stereotaxic spinal clamps (Kopf). Muscle and conjunctive tissue was removed before performing a laminectomy along the rostral caudal axis. Spinalization was performed in between the thoracic segments 5 and 6. An optrode (diameter: 1 mm) was moved on top of the spinal cord, in the rostral caudal axis, while monitoring EMG recordings and documenting movements. An electrolytic lesion was placed at the position where the light pulses led to the most prominent BSM EMG responses. We tested a variety of stimulation protocols (single, 5 Hz, 10 Hz, 20 Hz, 50 Hz, 100 Hz) and laser powers (5 mW – 40 mW).

Eventual activity in the BSM and TA was monitored via EMG recordings using a custom-made amplifier (x 1000) and filtered at 2 kHz. Data acquisition and analysis were performed using spike2 software (CED Cambridge).

In vivo *juxtacellular recordings of photoidentified cells*

Single in vivo juxtacellular recordings were performed as described in (Lima et al., 2009). Briefly, a glass electrode (resistance ranging from 4 to 6 MΩ) made of borosilicate glass tubes (Hilgenberg) was first lowered at the position where optogenetic stimulations led to the highest activity in the BSM. Pipettes were filled with a ringer solution. Extracellular local field potential recordings were captured while shining the light. Subsequently, cells were searched for by applying a negative current pulse and using an audio monitor (Grass Technologies, AM10) while steps were made in 1.5 µm increments with a micromanipulator (Luigs & Neumann SM-5, Germany) and potential increases in resistance were carefully observed. When spiking activity was detected, electrophysiological recordings were performed in line with optogenetic stimulation protocols (single, 5 Hz, 10 Hz, 20 Hz, 50 Hz) and EMG monitoring. Recordings were amplified (Dagan BVC-700A, Dagan, Minneapolis, MN), low-pass filtered at 10 kHz and sampled at 50 kHz by a data-acquisition interface (Power 1401, CED, Cambridge, England) and controlled and analysed by the spike2 software (CED, Cambridge, England).

In vitro *patching of identified BSM MNs in new born male Gal-ChR2 animals*

New-born male Gal-ChR2 mice aged postnatal day (P2) to P6 were used in accordance with the guidelines of the French Agriculture and Forestry Ministry for handling animals. The protocol was approved by the local ethics committee of the University of Bordeaux (approval number 2016012716035720). To record specifically from identified MNs innervating the BSM, a crystal of cholera toxin β-subunit conjugated to

AlexaFluor 594 (Thermo Fisher Scientific, C34777) was inserted into the BSM with an insect pin 20–24 h before slice preparation procedure in cryo-anaesthetised mouse pups. Following the labelling process, spinal cord slices were prepared using the following procedure: mice were anaesthetised using isoflurane until all reflexes were gone. After decapitation, the spinal cord was dissected out in an ice-cold sucrose-based saline solution containing the following: 2 mM KCl, 0.5 mM $CaCl_2$, 7 mM $MgCl_2$, 1.15 mM NaH_2PO_4, 26 mM $NaHCO_3$, 11 mM glucose and 205 mM sucrose. The saline was bubbled with 95% O_2, 5% CO_2. Transverse slices (350 µm) of the lower lumbar enlargement and first sacral segments were cut with a vibratome and then transferred to a holding chamber. Slices were allowed to recover in oxygenated aCSF (130 mM NaCl, 3 mM KCl, 2.5 mM $CaCl_2$, 1.3 mM $MgSO_4$, 0.58 mM NaH_2PO_4, 25 mM $NaHCO_3$, 10 mM glucose) for at least 1 hour at 30 °C. Whole-cell current-clamp recordings from BSM-MNs, identified by their 594 fluorescence, were made under visual control with a Multiclamp 700B amplifier. Recording glass microelectrodes (4–7 MΩ) were filled with the following: 120 mM K-gluconate, 20 mM KCl, 0.1 mM $MgCl_2$, 1 mM EGTA, 10 mM HEPES, 0.1 mM $CaCl_2$, 0.1 mM GTP, 0.2 mM cAMP, 0.1 mM leupeptin, 77 mM d-mannitol and 3 mM Na_2-ATP, with a pH of 7.3. All of the experiments were performed at room temperature (~23 °C). Data acquisition and analysis were performed using the Axograph software. Experiments were discarded if series resistance increased more than 20% during a given recording period. Polysynaptic transmission was decreased using a high cation solution containing 7.5 mM $CaCl_2$ and 8 mM $MgSO_4$ (Liao and Walters, 2002). Throughout recording episodes, GABAergic and glycinergic inputs were blocked with gabazine and strychnine (1 µM each), respectively (Clarac et al., 2004; Taccola et al., 2004). A stimulating optrode connected to an optogenetic laser box (Prizmatrix) was placed above the central canal at the dorsal grey

commissure and light pulses were applied at different lengths. Excitatory postsynaptic currents (EPSCs) were recorded from MNs held at −60 mV in current clamp mode. The input resistance of MNs (Rin) was determined from the slope of the voltage-current curve within the linear portion of current traces. AHP parameters were measured after single action potential evoked by short depolarizing current steps (7 ms, 0.25 nA) in current clamp conditions in MNs held at −60 mV by injection of bias current.

2.4.6 Sensory stimulation of the penis and local field potential recordings of photo-identified cells

For sensory stimulation of the penis in parallel with BSM activity monitoring by EMG, the surgical procedure was performed as described above (In vivo *anaesthetised optogenetic stimulation*). To stimulate the penis electrically (by wrapping a nerve cuff electrode around the penis) or mechanically (by locally applying an airpuff) the penis was gently pulled out. Electrical (6V) and mechanical (0.5-1 mbar) stimulations of the penis were done at either 200 Hz (100 pulses) or 5 Hz (3 x 5 pulses, 100 ms). Stimulation protocols were first run in an anaesthetised male mouse with an intact brain-spinal connection before disrupting the latter by performing a spinalization between the thoracic segments 9 and 10. Electrical and/or mechanical stimulation protocols were then repeated in the spinalised preparation (N = 7).

For local field potential (LFP) recordings of optogenetically tagged Gal+ cells or BSM-MNs, a glass electrode (resistance ranging from 4 to 6 MΩ) made of borosilicate glass tubes (Hilgenberg) was lowered at the position of the Gal+ cells or the BSM-MNs and optogenetic stimulations were

performed until encountering the maximal light triggered LFP response. Subsequently the glass pipette was left in the place at which the highest light triggered LFP response of BSM-MNs or Gal+ cells was encountered. Finally the penis and leg were mechanically stimulated with a locally applied airpuff (5 Hz; 5 pulses, 100 ms) while monitoring LFP responses and EMG responses in BSM and TA muscles. Analysis was performed in spike2 and data plotted in Excel and Matlab.

2.4.7 Nissl stain

The slides were washed 2 times in 0.01 M PBS to remove the excess of frozen section medium. Afterwards, the sections were rehydrated for 40 min in PBS 0.1 M, pH 7.2 (PBS 10x) and permeabilized for 10 min with 0.1% Triton-X (T9284-100ML, SigmaAldrich) in PBS 10x. The tissue was washed 2 times for 5 min with PBS 10x before incubating them for 20 min with a 1:100 Neurotrace staining solution (in PBS 10x; (NeuroTrace™ 500/525 Green Fluorescent Nissl Stain, N21480, ThermoFisher Scientific; or NeuroTrace™ 530/615 Red Fluorescent Nissl Stain, N21482, ThermoFisher Scientific; or NeuroTrace™ 640/660 Deep-Red Fluorescent Nissl Stain, ThermoFisher Scientific). Subsequently the tissue was washed with 0.1% Triton-X in PBS 10x for 10 min. After washing 2 times 5 min with PBS 10x, the slides were rinsed with distilled water, dried and coverslipped with Mowiol.

2.4.8 Immunohistochemistry

Immunohistochemical labelling was performed using standard procedures. Briefly, spinal cord sections, which were labelled either for

Gastrin releasing peptide (Gastrin Releasing Peptide (GRP) (Porcine) - Antibody, Phoenix Pharmaceuticals, H-027-13), Substance P (Anti-Substance P Receptor Antibody, Sigma-Aldrich, AB15810), Enkephalin (Anti-Enkephalin/ENK antibody, Abcam, ab85798), CCK (Polyclonal Rabbit anti-Human CCK / Cholecystokinin Antibody, LSBio, LS-C190673), Osteopontin (Mouse Osteopontin/OPN Antibody, R&D Systems, AF808), VGLUT1 (VGLUT 1 antibody, Synaptic Systems, 135 304) or Galanin (Anti-Galanin Antibody, Milipore, AB2233), were firstly washed 2 times for 5 min with PBS 0.01 M to remove the excess OCT. Afterwards, they were washed 2 times for 10 min with PBS 10x and preincubated for 1.5 hours at room temperature in a blocking solution (PBS 10x, 1% bovine serum albumin, and 0.3% Triton X-100). Afterwards, primary antibodies were diluted in the same blocking solution at a proportion of 1:100. The primary antibody was incubated on the glass slides overnight at room temperature. Incubation with the primary antibody was followed by 5 times 10 min washing with PBS 10x. Subsequently, we proceeded to detect the primary antibody with a secondary antibody coupled to different fluorophores (Alexa Fluor 488, 594 or 647, Abcam/Thermo Fisher Scientific). The secondary antibody was diluted (1:500) in the blocking solution and the reaction was allowed to proceed for 2 hours in the dark at room temperature. In some cases, a Nissl stain was performed as described above. After the staining procedure, sections were washed 5 times for 10 min with PBS 10x, rinsed with distilled water, dried and coverslipped with Mowiol mounting medium.

2.4.9 Statistical Analysis

Statistical analysis was performed with homemade code in Matlab and Python (scipy and statsmodels). All error ranges represent standard error

of the mean. For two-sample comparisons of a single variable, Student's t test was used, unless in cases when the underlying distributions were non-Gaussian (Shapiro-Wilk test, $p<0.05$), where a two-tailed Mann-Whitney-U Test was performed. When multiple variables were compared, a Kruskal Wallis test or a Wilcoxon-Signed-Rank test were used since the data did not follow a Gaussian distribution. Probabilities of the null hypothesis $p<0.05$ were judged to be statistically significant. Elements of violin plots: centre line, median; box limits, upper (75) and lower (25) quartiles; and whiskers, 1.5x interquartile range.

2.5 Author contributions

A.R.M., C.L. and S.Q.L designed the experiments and the analysis. A.R.M. performed the muscle, pup and spinal cord injections. A.R.M. and L.F. performed immunohistochemistry and histological image acquisition. C.L. performed the electrophysiology experiments and the optogenetic stimulations. C.L., C.Q. and S.B. performed the in vitro patching experiments.

3 Functional description of the spinal circuit controlling the BulboSpongiosus Muscle

In the previous chapter, we showed the location and properties of the BSM-MNs and their presynaptic partners, the Gal+ cells in the upper lumbar spinal cord. This knowledge allowed us to dig deeper into the circuit and further characterise the role of the BSM and Gal+ cells in ejaculation and sexual behaviour in general. In this chapter we describe how electrical and optogenetic stimulation of Gal+ cells leads to robust BSM activation. Gal+ cells activation reliably follows light stimulation and it is only visible in animals that were spinalised beforehand, pointing to a strong inhibition from the brain impinging on this spinal circuit. Furthermore, we observed that repeated Gal+ cells stimulation led to a reduced BSM muscular activity, which may reflect an entrance in the refractory period after a certain threshold of Gal+ cells activation.

Interestingly, this also depends on the internal state of the male. If the animals underwent a sexual encounter, where they were allowed to perform 5 mounts with intromissions, the BSM activity was mainly similar to the sexually naive group. However, if the animals were allowed to ejaculate beforehand, BSM activity was mainly absent after electrical stimulation of Gal+ cells, pointing to an integration of the animal's internal state already at the level of the spinal cord. In order to further understand the role of the BSM in sexual behaviour, we recorded the BSM EMG activity in vivo in sexually behaving animals. We observed that this muscle is active with each intromission and massively active during sperm expulsion. When comparing both EMG signals we observed that both the amplitude and frequency of these signals are similar, pointing again to the importance of the Gal+ cells in regulating BSM contractions during sexual behaviour in mice.

3.1 Introduction

Research about the neuronal control of sexual behaviour has been mainly focused on understanding how the brain drives the motivation and receptivity (Georgiadis et al., 2012) for the behaviour to start, as well as on the brain signals that drive the spinal cord to execute the specific motor patterns for copulation (Hull et al., 2006; Pfaus, 1999; Wagner & Clemens, 1991). However, not much is known about the spinal circuits themselves when it comes to sexual behaviour. Most studies in the past have focused on anatomical studies that describe the presence of an SEG in the lumbar spinal cord that is capable of driving ejaculation in male rats (Truitt & Coolen, 2002). Yet one question remains, how are these SEG Gal+ cells actually integrating external cues, the internal state of the animal and the brain control signals in order to timely achieve ejaculation?

Electrical stimulation of the SEG in rats led to a full ejaculatory reflex, with the emission of sperm. However, this was only achieved in spinalised anaesthetised animals, that is, with the connection to the brain severed before electrical stimulation (Borgdorff et al., 2008). This suggests that SEG cells are under inhibition from the brain, namely the brainstem (Marson & McKenna, 1992), which suppresses the ejaculatory reflex and prevents ejaculation to happen in an untimely manner. Ablation studies, where the Gal+ cells were pharmacologically inhibited, lead to impairments in ejaculation but no other phases of the copulatory sequence (Truitt & Coolen, 2002), once more supporting the dogma that the spinal cord circuit acts only as a reflex arc.

In this chapter, we aim at answering these questions. To do so, we started by replicating the electrical stimulation experiments previously conducted in rats and were successful in inducing BSM activity in the mouse. Interestingly, and contrary to most previous data, we observed that Gal+

cells in mice can integrate the internal state of the animal. First, there is a repression of the BSM activity with repeated Gal+ cells stimulation. Secondly, their levels of activity depend on the animal's recent sexual history, with animals that ejaculated right before the stimulation showing very poor BSM activity after Gal+ cells electrical stimulation. Besides, we went one step further by proving that these effects are specifically induced by Gal+ cells by performing optogenetic stimulations in Gal-ChR2 animals and observing similar patterns of BSM activation. Finally, we are the first to show that specific optogenetic stimulation of Gal+ cells lead to BSM patterns of activation that are physiologically relevant, as we showed by comparing to EMG BSM recording in sexually behaving animals.

3.2 Results

3.2.1 Electrical stimulation of the spinal cord location harbouring the Gal+ neurons leads to BSM activity and suggests peripheral regulation of sexual excitation

To further explore the role of Gal+ cells in the control of BSM activity in mice, we investigated whether the artificial activation at their location could trigger BSM activity. First, we performed electrical stimulations along the rostrocaudal lumbar spinal cord by inserting a tungsten electrode at various depths (550 µm – 850 µm), while concurrently measuring BSM activity using EMG recordings, in sexually naive, spinalized animals (SN, N = 8), and simultaneously monitored the activity of the TA leg muscle to assess the specificity of our protocol (Figure 3.1 A). The site with the strongest electrically triggered BSM responses was labelled by electrolytic lesions and immunohistochemical staining for galanin (Figure 3.1 B). Successful BSM muscle activity was elicited

(Figure 3.1 B and Figure 3.2) when stimulations (40 µA, 200 Hz, 100 pulses) were applied near the Gal+ cluster, located in the L2/L3 spinal segments (Figure 3.1 C), at a depth of 850 µm, which aligns with the location of the central canal (Figure 3.1 D and Figure 3.2 C,D).

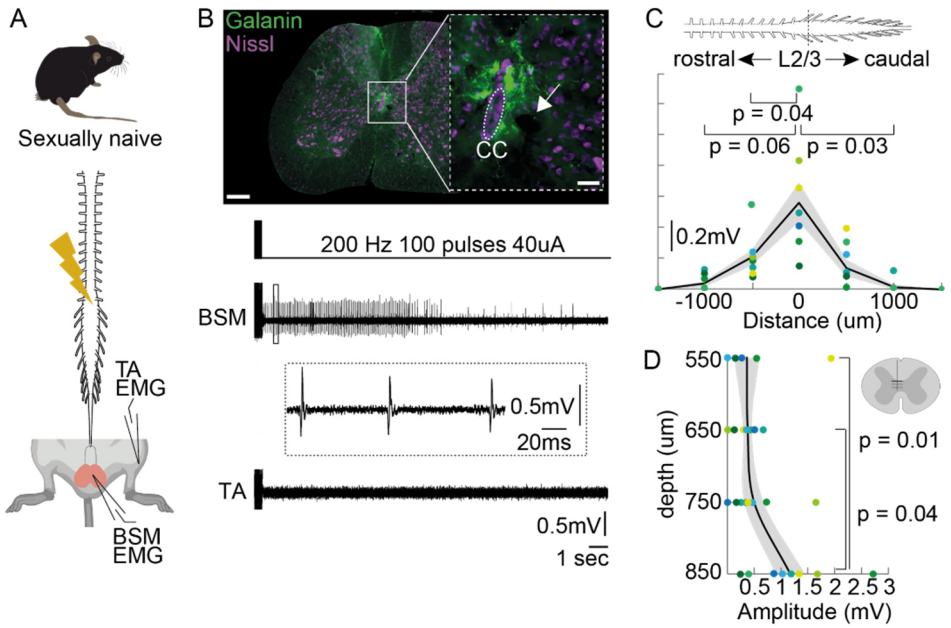

Figure 3.1 Electrical stimulation of the lumbar spinal cord location harbouring the Gal+ cells leads to BSM activity in a spinalised anaesthetised preparation. (A) Electrical stimulations (200 Hz, 100 pulses, 40 µA) were performed along the rostrocaudal lumbar spinal cord in adult anaesthetised and spinalized C57BL6 mice (left panel) while performing EMG recordings in the BSM and a control leg muscle (TA - Tibialis anterior). (B) Electrolytic lesions were placed at the location where electrical current applications led to the most prominent BSM potentials (upper panel, see inset and white arrow; Green: immunohistochemical staining for Galanin, Purple: Nissl stain). Lower panel: representative traces of the EMG activity (BSM and TA) during electrical current application at the lesion site. First current application led to high amplitude and high frequency discharges in the BSM (but not in the leg muscle). (C) Diagram showing the triggered BSM activity along the rostrocaudal spinal cord axis. Largest BSM responses were encountered at the L2/3 spinal segments (mean amplitude 0.56 ± 0.13 mV). Data refers to individual animals (N = 8). Mean amplitudes: at 500 µm rostral to L2/3 0.2 ± 0.05

mV; 500 µm caudal to L2/3 0.14 ± 0.05 mV; at 1000 µm rostral to L2/3 0.04 ± 0.02 mV; at 1000 µm caudal to L2/3 0.01 ± 0.003 mV. P-values result from a two-tailed Mann-Whitney-U Test. (D) BSM amplitudes plotted against the depth of the stimulation sites. Differently coloured dots refer to individual animals (N = 8). Mean amplitudes: at 550 µm 0.36 ± 0.23 mV, at 650 µm 0.37 ± 0.083; at 750 µm 0.49 ± 0.18 mV; at 850 µm 1.17 ± 0.27 mV. P-values result from a two-tailed Mann-Whitney-U Test.

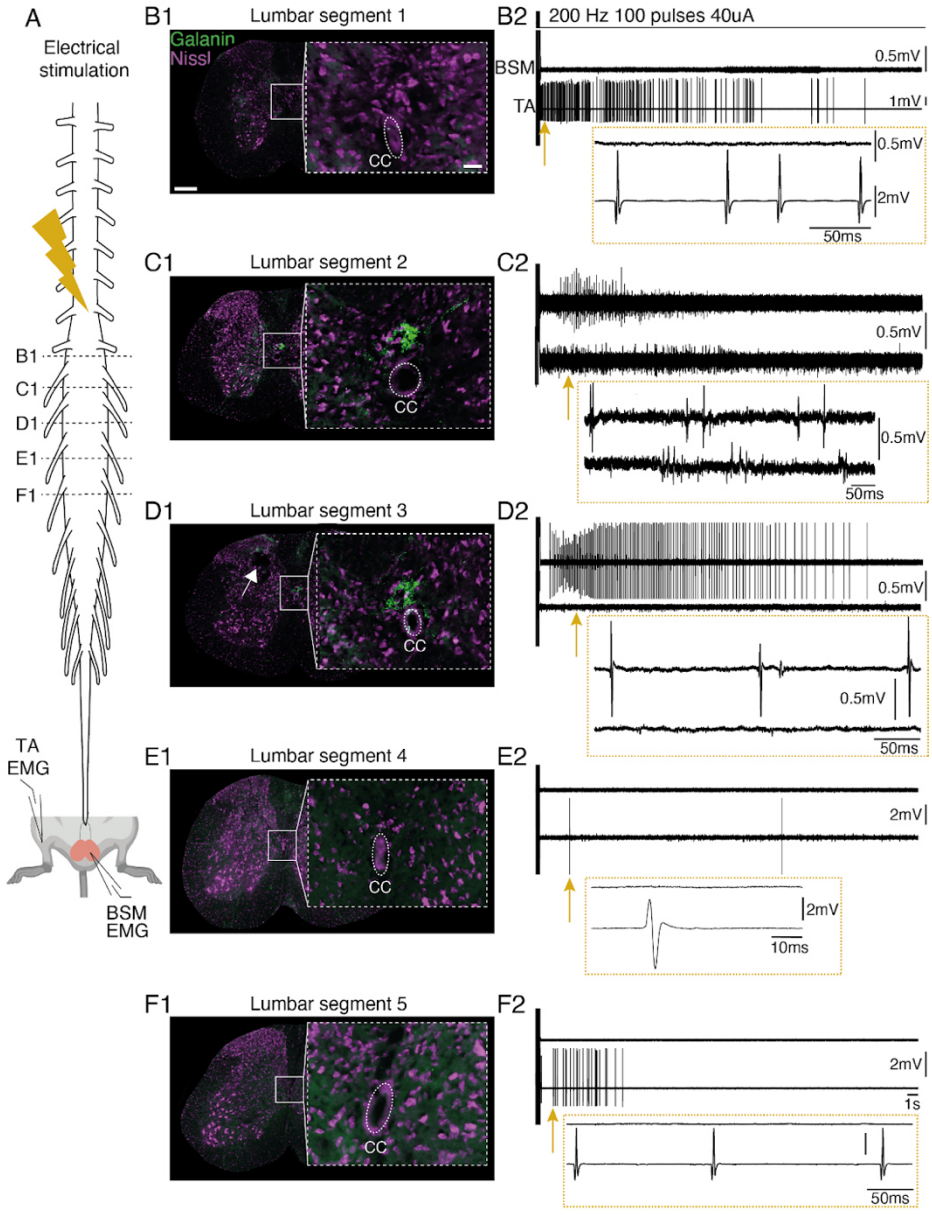

Figure 3.2 Electrical stimulation along the rostrocaudal lumbar spinal cord in an anaesthetised preparation. (A) Experimental design: anaesthetised animals were clamped into the spinal frame and the spine was opened. A tungsten electrode was inserted along the rostrocaudal axis at different depths and current was applied while BSM activity was monitored in parallel. (B1 - F1) Representative post-hoc histological sections along the rostrocaudal axis of the spinal cord are shown. Note the electrolytic lesion at the

L3 segment (D1). Green: Galanin. Purple: Nissl. (B2 - F2) Representative electrophysiological traces with BSM (upper trace) and leg (lower trace, TA, tibialis anterior) responses triggered at the stimulation site shown in B1 - F1. Note that BSM responses were most prominent at locations (C2, D2) where Galanin labelling was observed post hoc around the central canal (C1, D1) while TA responses randomly occurred along the rostrocaudal axis.

The electrically triggered BSM responses were significantly higher and longer in spinalized preparations compared to non-spinalized ones (Figure 3.3), suggesting descending inhibition from the brain. This finding aligns with our previous results from the mechanical/electrical stimulation of the penis experiments (Chapter 2) and prior studies in rats (Carro-Juárez & Rodríguez-Manzo, 2008; Coolen et al., 2004).

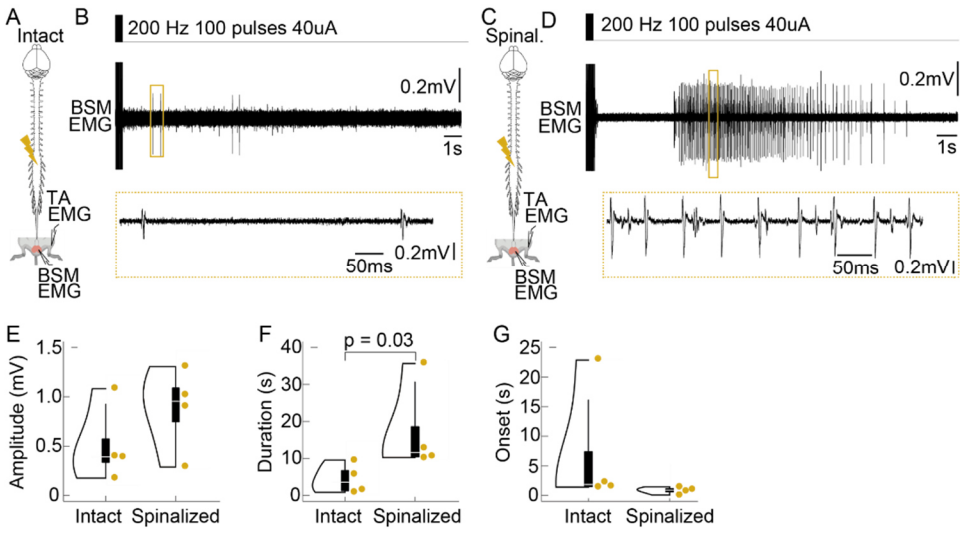

Figure 3.3 Electrically triggered BSM responses in a spinalized vs non-spinalized preparation. (A) Experimental design: electrical stimulations at the location of Gal+ cells in L2-L3 segments (see yellow flash) were conducted in anaesthetised mice in which the connection to the brain has been kept intact while in parallel monitoring BSM activity using

EMG recordings (N = 4). (B) Example EMG trace obtained in an animal in which the connection to the brain was kept intact and electrical stimulation was applied with a tungsten electrode. (C) Same as A, but a spinalization was performed between thoracic segments 5 and 6 (N = 4, same animals). (D) Same as C, but EMG trace is recorded from an animal in which a spinalization was performed prior to stimulation. Note the difference in BSM activity. (E) Violin plots showing the BSM EMG amplitude triggered with electrical stimulation in intact anaesthetised mice (mean amplitude 0.51 ± 0.19 mv) compared to spinalized mice (0.87 ± 0.21 mV). P = 0.48 resulting from a Mann-Whitney U-Test. (F) Same as E but the duration of the BSM EMG activity is plotted, which was markedly longer in the spinalized (mean duration 17.33 ± 0.21 s) vs. intact (mean duration 4.41 ± 2.02 s) anaesthetised preparations. P = 0.03 resulting from a Mann-Whitney U-Test. (G) Same as E but the onset of triggered BSM responses is depicted (mean onset for intact 7.0 ± 5.28 s; vs mean onset for spinalized 0.84 ± 0.28 mice). P = 0.05 resulting from a Mann-Whitney U-Test.

However, unlike what was observed in the rat, where repeated electrical stimulations led to consistent BSM responses (Borgdorff et al., 2008), repeated stimulations in mice resulted in decreased BSM responses (see Methods Details; Figure 3.4; BSM 2nd and 3rd). Quantification of the EMG responses (Figure 3.4 B-D) showed significantly larger and longer potentials during the first train of stimulation (mean amplitude 0.99 mV +/- 3.6 mV, 1st vs 2nd amplitude p = 0.04, 1st vs. 3rd amplitude p = 0.02; mean length 8.83 ms +/- 1.4 ms; 1st vs 2nd length p = 0.09, 1st vs. 3rd length p = 0.02; Mann-Whitney-U Test) compared to the second (mean amplitude 0.5 mV +/- 0.25 mV; mean length 4.22 s +/- 1.47 s) and third trains (mean amplitude 0.06 mV +/- 0.04 mV; mean length 1.74 s +/- 1.31 s) of current application, while the onset of the responses did not change (mean onset of 1st 3.9 +/- 1.83 s, mean onset of 2nd 6.03 +/- 3.02 s, mean onset 3rd 0.54 +/- 0.13 s; Figure 3.4 D). The reduction in response during repeated stimulation was not due to deterioration of the preparation (Figure 3.5).

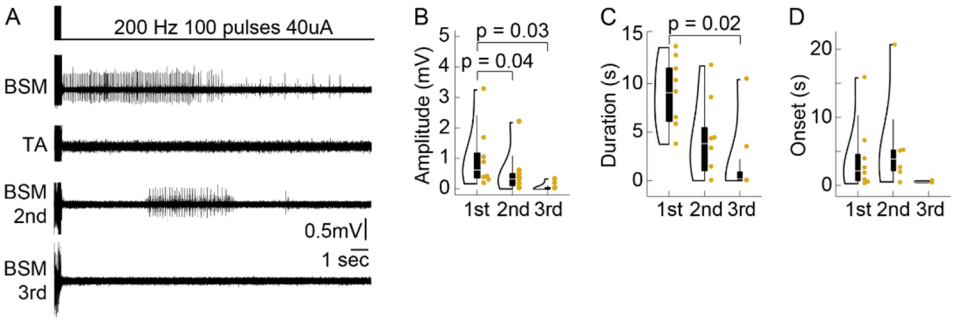

Figure 3.4 Repeated electrical stimulation of the spinal cord location of the Gal+ cells leads to a decrease in the BSM EMG responses. (A) Representative traces of the EMG activity (BSM and TA) during electrical current application. While the first current application led to high amplitude and high frequency discharges in the BSM (but not in the leg muscle), second current applications led to a reduced response (in this example, BSM activity was not observed during the third current application). (B) Violin plot illustrating the amplitudes of electrically triggered BSM activity (N=8) during the 1st (mean amplitude 0.99 ± 0.36 mV), 2nd (mean amplitude 0.5 ± 0.25 mV) and 3rd (mean amplitude 0.06 ± 0.04 mV) rounds of current application, with boxplots (elements: see Methods). P-values result from a two-tailed Mann-Whitney-U Test. (C) Same as B, but the duration of the BSM activity is plotted. Mean durations: for 1st stimulation 8.8 ± 1.3 s; after 2nd current application 4.2 ± 1.46 s; after 3rd stimulation 1.74 ± 1.3 s. P-values result from a two-tailed Mann-Whitney-U Test. (D) Same as B, but the onset with which BSM activity was triggered is plotted. Mean onset of EMG: after 1st current application 3.99 ± 1.83 ms; after 2nd stimulation 6.02 ± 3.01 ms; after 3rd current application round 0.54 ± 0.13 ms. A non-parametric anova led to no significance (P = 0.21; Wilcoxon-Signed-Rank Test).

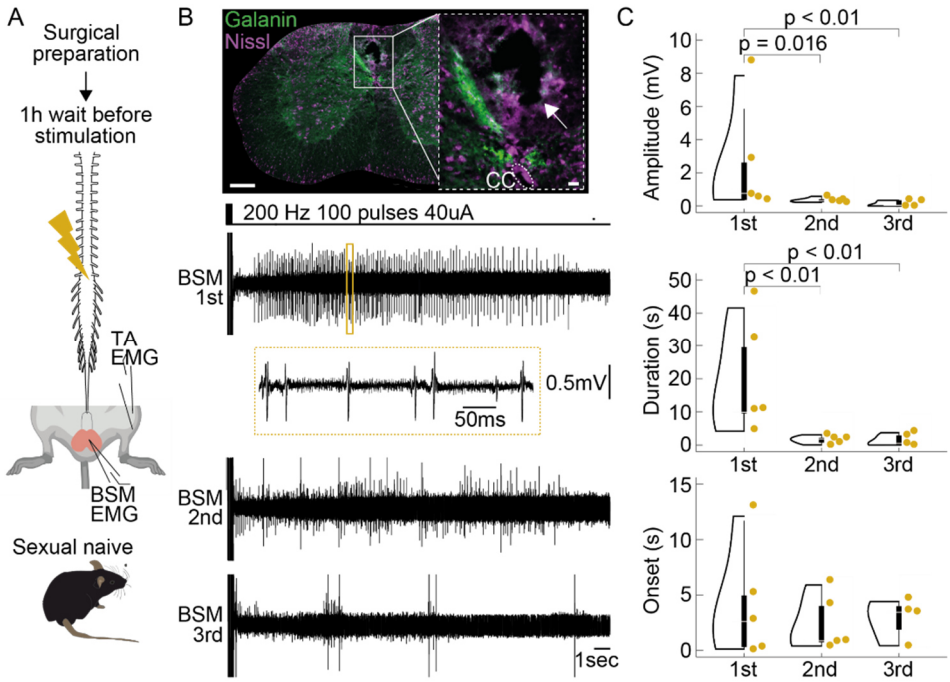

Figure 3.5 Electrically triggered BSM activity does not depend on the duration of the time of spinal cord exposure after the laminectomy. (A) Experimental design: anaesthetised animals (N = 5) were clamped into the spinal frame and the spine was exposed. Before starting with the electrical stimulation protocol, a waiting window of 1 h was respected in order to reveal that the observed depression in the BSM activity with repeated trains of stimulation was not due to deterioration of the prep (due to the interval between opening the spinal cord and the application of the last stimulation protocol). (B) Upper panel: Histological section showing the electrolytic lesion (white arrow) that has been placed at the location on which electrical stimulation triggered the highest BSM activity. Green: Galanin. Purple: Nissl. Scale bar 200 µm. Scale bar inset: 50 µm. Lower panel: Electrical stimulation protocol (200 Hz, 100 pulses, 40 µA) led to pronounced BSM activity (BSM 1st) at the location of Galanin clusters. The same depression in BSM activity (as depicted in Figure 3.4) was observed during the 2nd and 3rd rounds of stimulation. (C) Quantitative analysis of BSM responses triggered after 1 h of waiting time. Amplitude (upper panel; mean amplitudes: 1st 2.48 ± 1.39 mV; vs. 2nd 0.35 ± 0.06 mV; vs. 3rd 0.13 ± 0.08 mV; 1st vs. 2nd P = 0.016 and 1st vs. 3rd P = 0.0078 resulting from a Mann-Whitney U-Test) and duration (middle panel; mean durations: 1st 18.9 ± 7.08 s; vs. 2nd 1.61 ± 0.51; vs. 3rd 1.4 ± 0.76 s; 1st vs. 2nd P = 0.007 and 1st vs. 3rd P = 0.008 resulting from a Mann-Whitney U-Test) of BSM activity decreased upon 2nd and 3rd stimulation rounds while the

onset with which BSM activity was elicited remained stable (lower panel; mean onsets: 1st 4.01 ± 2.2 s; vs. 2nd 2.38 ± 1.08 s; vs. 3rd 2.75 ± 0.9 s; P = 0.98 resulting from a Kruskal Wallis test).

In addition to the intriguing depressing response observed with repeated electrical stimulations, the structure of the electrically elicited BSM activity in mice differed from previously recorded EMG responses during ejaculation in anaesthetised rats (see (Borgdorff et al., 2008)). Moreover, we did not observe the expulsion of sperm or seminal fluid in any of our mouse experiments. To rule out the hypothesis that the lack of sperm emission in mice was due to a technical issue, we replicated the experiment by Borgdorff et al., 2008 in anaesthetised rats. As expected, the application of electrical current (Figure 3.6 A) at the L3/L4 spinal segments (as confirmed by electrolytic lesions; Figure 3.6 B) resulted in the characteristic activity pattern in the rat BSM (N = 5; Figure 3.6 C) and the expulsion of sperm (Figure 3.6 D).

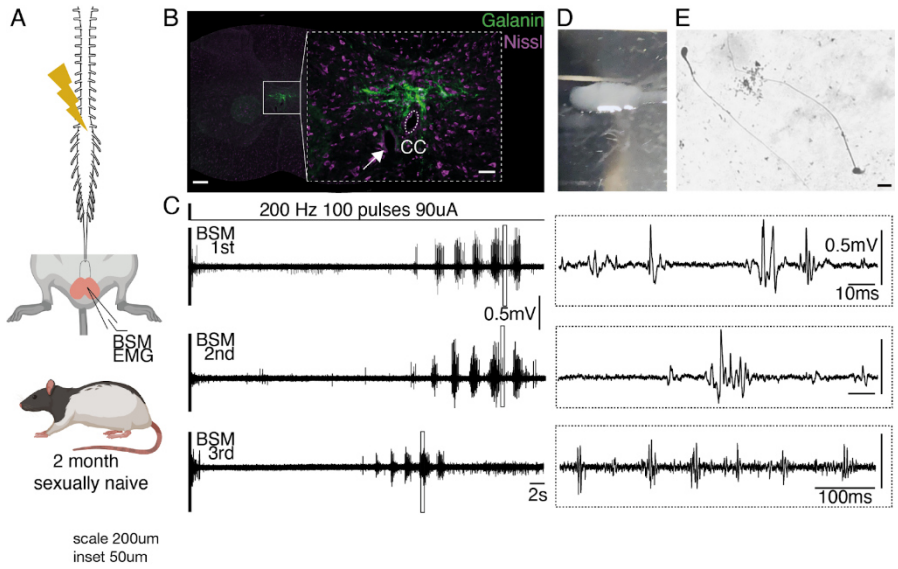

Figure 3.6 Repeated electrical stimulation of the rat spinal cord at the location of the spinal ejaculation generator leads to stable BSM activity and to the emission and expulsion of sperm. (A) Similar to the mice experiment, the tungsten electrode was moved along the rostrocaudal axis of the spinal cord in an anaesthetised rat (sexually naive, 2 months) while the BSM activity was monitored in parallel using an EMG. (B) Histological section of the L3 spinal segment where BSM activity was elicited and ejaculation triggered by current application. Note a similar expression pattern of Galanin (green) around the central canal (CC) when compared to mice. An electrolytic lesion (white arrow) was placed at the shown location. Purple: Nissl stain. Scale bar 200 µm, inset 50 µm. (C) Example BSM EMG trace for the first current application at the location shown in B, note the characteristic rhythmic pattern in the BSM with a long onset. The 2nd and 3rd current application (BSM 2nd, BSM 3rd) led to a very similar activity pattern in the BSM, contrary to mice. (D) Current applications at the L3/4 spinal segments not only led to a characteristic activity pattern in the BSM, but also to the expulsion of sperm. Cloudy liquid (sperm) was collected on an objective slide which was diluted for post-hoc staining. (E) Sperm was made visible by performing a Papanicolaou staining protocol. Scale bar 10 µm.

To explore how electrically induced BSM activity relates to natural physiological conditions, we conducted in vivo EMG recordings of BSM activity in sexually behaving mice (Figure 3.7 A). BSM activity was detected at various stages during the sexual interaction (Figure 3.7 B). Notably, distinct BSM contractions were observed with each male thrust (Figure 3.7 C), with the strongest bursts occurring as the penis exited the vagina. In contrast, no BSM contractions were present during probing behaviour (the period after mounting and before penile intromission, when the male is performing shallow thrusts, trying to locate the female's vagina, Figure 3.7 D). These findings support the hypothesis that the BSM might be involved in maintaining an erection (as the BSM is active during intravaginal thrusts) but not in initiating it.

Interestingly, no BSM activity was detected during the shuddering phase, the brief period immediately following the last thrust leading to ejaculation, characterised by rapid pelvic movements and lasting less than 3 seconds (McGill & Coughlin, 1970) (Figure 3.7 B). Since ejaculation consists of two stages - emission and expulsion - we hypothesise that the shuddering phase corresponds to the emission phase, during which sperm is deposited in the urethra while the penis is less erect (Soukhova-O'Hare et al., 2007). The subsequent expulsion of sperm is driven by BSM contractions observed immediately after the shuddering phase (Figure 3.7 B,E). This hypothesis, suggesting that sperm emission occurs during shuddering and expulsion afterward, is supported by previous studies in mice (McGill & Coughlin, 1970), which found that separating males from females during this phase prevented pregnancy and led to sperm expulsion at the tip of the penis outside the vagina.

As expected, the BSM activity recorded immediately after the shuddering phase showed the highest EMG activity, with bursts averaging a mean

amplitude of 0.732 mV, lasting more than 6 seconds (Figure 3.7 F). Based on the same separation studies in mice (McGill & Coughlin, 1970) sperm expulsion is thought to occur during the first 1-2 seconds immediately after the shuddering phase occurs. Therefore, after sperm expulsion, the post-shuddering phase activity is probably related to flipping and cupping movements of the penis (McGill & Coughlin, 1970). Importantly, the dynamics of BSM EMG activity in freely moving animals mirrored those elicited by direct optogenetic stimulation of the BSM MNs and by sensory stimulation of the penis. Similar patterns were also observed during electrical stimulation of the location containing Gal+ neurons, including comparable amplitudes and durations, and oscillatory patterns (Figure 3.7 G). These consistent results across experiments further support that we are observing expulsion-like patterns in the BSM, but no sperm emission, when artificially activating the Gal+ cells in anaesthetised *in vivo* preparations.

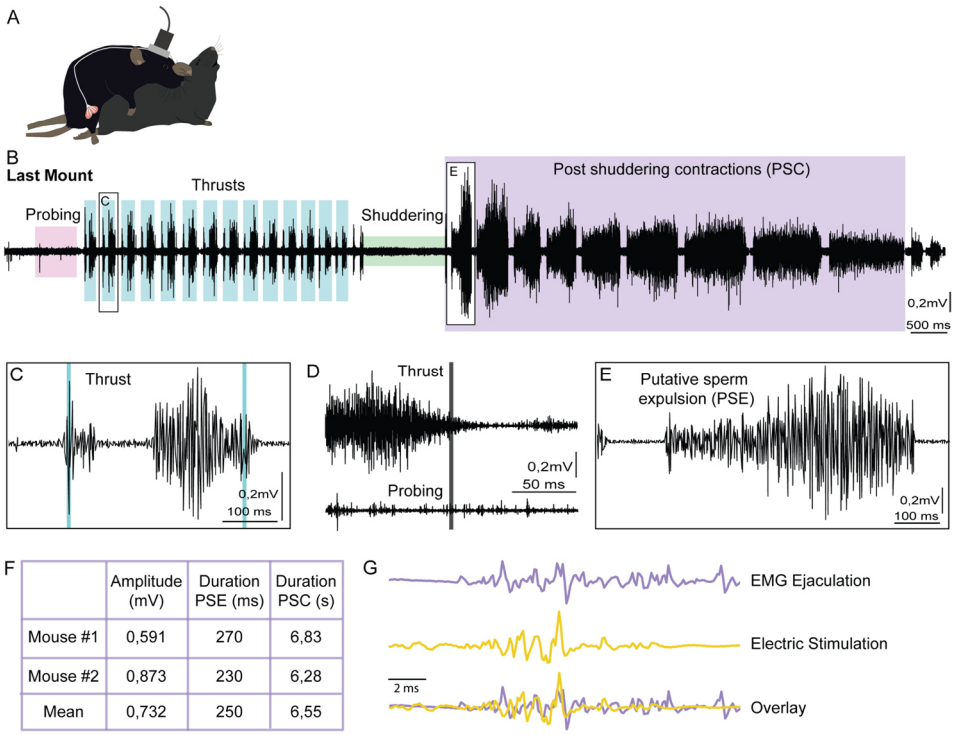

	Amplitude (mV)	Duration PSE (ms)	Duration PSC (s)
Mouse #1	0,591	270	6,83
Mouse #2	0,873	230	6,28
Mean	0,732	250	6,55

Figure 3.7 BSM EMG in vivo recordings in sexually behaving animals shows the muscle activity in different phases of the behaviour. (A) Experimental design: In vivo BSM EMG recordings in behaving mice while performing copulatory behaviour allowed access to the BSM contraction patterns during the different phases of a sexual encounter (N=2). (B) EMG trace from the BSM activity in the last mount of a sexual behaviour session, showing the muscular activity during Probing, Thrusts, Shuddering and the Post Shuddering Pelvic Contractions. (C) Close up from the highlighted Thrust in (A), showing the detailed BSM EMG activity. Note the two bursts of activity concordant with the point where the thrust is deeper (first blue trace) and when the thrust is shallower (second blue trace). (D) Comparison between the thrusts and probing events, aligned to the end of the behavioural bout. Mean EMG trace for all the events in one animal in one recording channel. (E) Close up from the highlighted Post Shuddering Pelvic Contractions in (A), showing the detailed BSM EMG activity. According to work from McGill and Coughlin, we believe that this is the burst that leads to the expulsion of sperm, hence calling it putative sperm expulsion. (F) Quantitative analysis of BSM responses in terms of amplitude of the Post Shuddering Pelvic Contractions (mean of 0,732 mV), their duration (mean of 6,55s) and the duration of the putative sperm expulsion burst (mean of 250 ms) (N=2). (G)

Comparison between the oscillatory pattern of the BSM EMG signal recorded in vivo during expulsion and the BSM EMG signal after electrical stimulation of the Gal+ cells.

As previously described, mice and rats display distinct reproductive strategies, particularly in the number of ejaculations each species can achieve in a short time: while rats can ejaculate 7-8 times in a short period before reaching sexual exhaustion, mice, similar to humans, generally enter a refractory period after a single ejaculation, which in the case of C57Bl6 mice (the genetic background used in this study) can last several days (Turley & Rowland, 2013). We speculated that the inability to elicit stable BSM activity with repeated electrical stimulations in mice might be due to the first round of stimulation inducing a refractory state similar to that following ejaculation.

To test this hypothesis, we allowed male mice to have sex prior to the electrical stimulation experiments. One group of males was allowed to reach ejaculation (Ejaculation, N = 8; Figure 3.8 A upper panel), while another group was allowed to perform 5 mounts with intromission and intravaginal thrusting (5 Mounts, N = 7, Figure 3.8 B upper panel). Electrical stimulation of the spinal cord in the Ejaculation group evoked less BSM activity (Figure 3.8 A, lower panel) compared both to the Sexually Naive group (Figure 3.4), and the 5 Mounts group (Figure 3.8 B, lower panel). The mean amplitude of the BSM activity was significantly higher in the 5 Mounts group (Figure 3.8 C), while the duration of the BSM activity was significantly shorter in the Ejaculation group compared to the other two groups (Figure 3.8 D). Although there was no difference in the mean onset of the BSM events between the Sexually Naive and Ejaculation groups (Figure 3.8 E), the number of events was significantly lower in the Ejaculation group compared to the other two (Figure 3.8 F),

further suggesting that after ejaculation, electrical stimulation of the spinal cord cannot elicit high BSM activity.

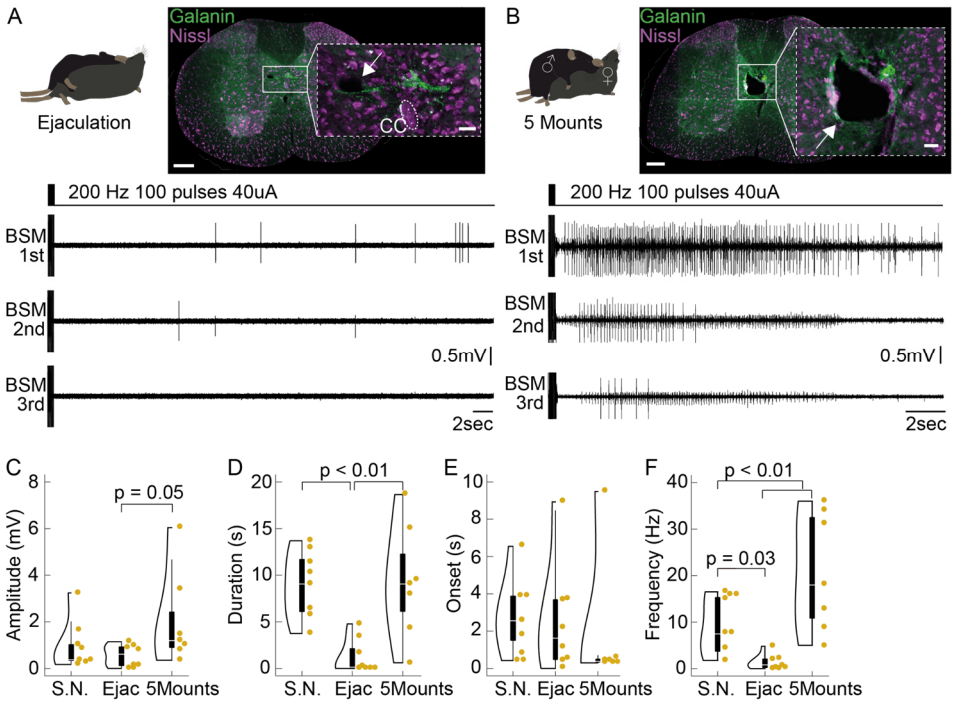

Figure 3.8 Electrical stimulation of the spinal cord at the Gal+ cells location immediately after a sexual encounter leads to markedly different BSM responses to the ones observed in a sexually naive animal. (A) Example BSM EMG traces of 1st, 2nd and 3rd current applications, recorded from an animal that ejaculated prior to the electrical stimulation experiment. Note that the BSM activity pattern during 1st and 2nd round of current application is markedly different from the sexually naive animal (Figure 3.4). (B) Same as H, but traces are obtained from an animal that was allowed to perform 5 mounts with vaginal thrusting prior to the electrical stimulation experiment. BSM activity is comparable to the sexually naive male (Figure 3.4). (C) Violin plot illustrating the amplitudes of electrically triggered BSM activity in sexually naive males (N = 8, mean amplitude 0.99 ± 0.36 mV), males that reached ejaculation (Ejac, N = 8, mean amplitude 0.57 ± 0.16 mV) or executed 5 mounts with vaginal thrusting (N = 7, mean amplitude 2.03 ± 0.76 mV), with boxplots (elements: see Methods). Data refers to the mean amplitude on

the stimulation site with the highest response during first rounds of current applications. P-values result from a two-tailed Mann-Whitney-U Test. (D) Same as C, but the duration of the BSM activity is plotted. Mean duration: in sexually naive animals 8.8 ± 1.3 s; in the Ejac group 1.26 + 0.26 s; in the group with 5 mounts 10.43 + 1.82 s. P-values result from a two-tailed Mann-Whitney-U Test. (E) Same as C, but the onset of BSM activity is depicted. Mean onset: sexually naive 3.99 ± 1.83 ms; Ejac 2.56 ± 1.04 ms; 5 mounts 0.88 ± 0.48 ms). No significance was found using a non parametric anova, Wilcoxon-Signed-Rank Test; P = 0.2. (F) Same as C, but the frequency of BSM activity is shown. Mean frequency: sexually naive 8.79 ± 2.2 Hz; Ejac 1.39 ± 0.56 Hz; 5 mounts 20.81 ± 4.8 Hz). P-values result from a two-tailed Mann-Whitney-U Test.

Taken together, these experiments suggest that electrical stimulation of the mouse spinal cord in the area where the Gal+ neurons are located can only evoke the second and final phase of the ejaculatory process (expulsion), but not the emission phase. The differing outcomes of the electrical stimulations based on the male's internal state (Sexually Naive vs. 5 Mounts vs. Ejaculation) imply that the properties of neuronal circuits in this spinal cord region are modulated by copulation and ejaculation, suggesting that the spinal circuitry may be involved in controlling the refractory period in addition to ejaculation.

3.2.2 Optogenetic stimulation of the lumbar Gal+ neurons leads to BSM activity

To address the inherent lack of specificity in electric stimulation experiments and to unequivocally link the activity of Gal+ cells, BSM-MNs and the BSM, we genetically restricted the neuronal population being stimulated to the Gal+ neurons by crossing the Gal-cre mouse line with the ChR2 line (Gal-ChR2 (Madisen et al., 2012)). To activate the Gal+ neurons, we placed an optical fibre on top of the spinal cord of

anaesthetised spinalized mice and delivered brief pulses of blue light along its rostrocaudal axis (Figure 3.9 A, N = 10). Light delivery (20 mW, 200 Hz, 100 pulses with 10 ms duration) led to comparable responses to the ones elicited via electrical stimulation (Figure 3.9 B-D). As expected, BSM activity was only observed in response to illumination at the location with the highest ChR2 expression (revealed by either DiI injections or an electrolytic lesion, Figure 3.9 B, Figure 3.10), specifically above the L2/L3 spinal segments (Figure 3.9 C,D), the region previously shown to harbour the highest density of Gal+ cells. No responses were observed when light stimulation was performed on negative litter mates of the Gal-ChR2 cross (data not shown).

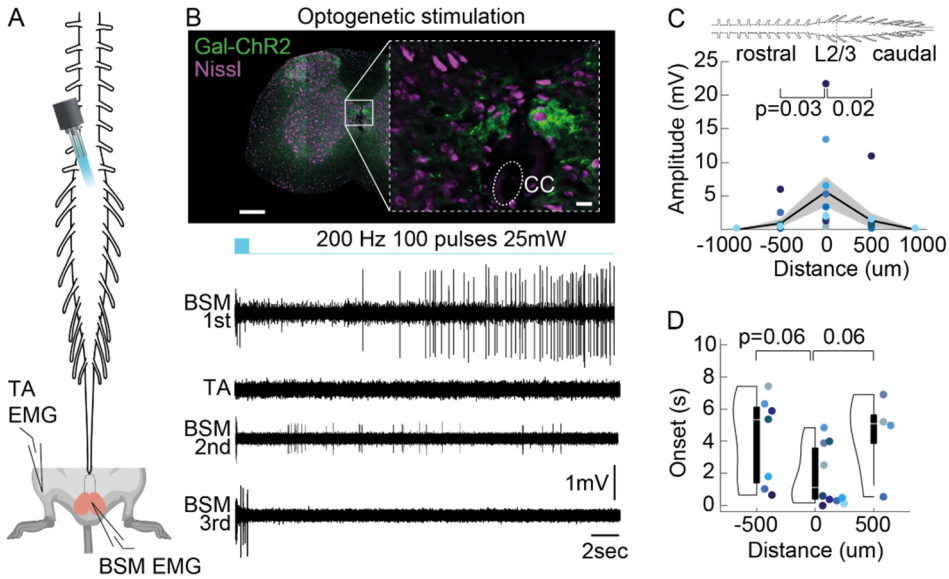

Figure 3.9 Optogenetic stimulation of the Gal+ cells leads to BSM activity similar to the one observed with electrical stimulation. (A) Optogenetic stimulations (200 Hz, 100 pulses / 10 ms, 20 mW) were performed on top and along the rostrocaudal lumbar spinal cord in adult anaesthetised and spinalized Gal-Chr2 males (left panel) while performing EMG recordings in the BSM and a leg muscle (TA - Tibialis anterior). (B) Electrolytic lesions were placed at the location where optogenetic stimulation led to the most prominent BSM potentials (upper panel, see inset and white arrow; Green: Galanin-ChR2,

Purple: Nissl stain). Scale bar of spinal cord section 200 µm. Inset, 20 µm. Lower panel: representative traces of the EMG activity (BSM and TA) during optogenetic application on top of the lesion site. Note that it led to a similar activity pattern compared to the electrical stimulations: while the first laser application led to high amplitude and high frequency discharges in the BSM, but not in the leg muscle (TA), the second round of light delivery led to a reduced response, and BSM activity was not detected during the third round of optogenetic stimulation. (C) Diagram showing the light-triggered BSM activity along the rostrocaudal spinal cord axis. Largest BSM responses were encountered at the L2/3 segments (mean amplitude 5.61 ± 2.31 mV, N=10). Note that responses are more restricted to the L2/3 spinal segments where the cluster of Gal+ cells was found, around the central canal (mean amplitudes: 500 µm rostral to L2/3 0.99 ± 0.58 mV, 500 µm caudal to L2/3 1.35 ± 1.06 mV). P-values result from a two-tailed Mann-Whitney-U Test. (D) Violin plots with boxplots (elements: see Methods) illustrating the latencies with which BSM responses were triggered as a function of distance (N=10). Shorter latencies were achieved at 0 µm which corresponds to the L2/3 spinal segments (0.02 ± 0.006 s). P-values result from a two-tailed Mann-Whitney-U Test. In 7 out of 10 animals BSM responses were triggered at 500 µm rostral to L2/3 whereas only in 4 animals BSM responses were triggered at 500 µm caudal to L2/3 (see individual dots).

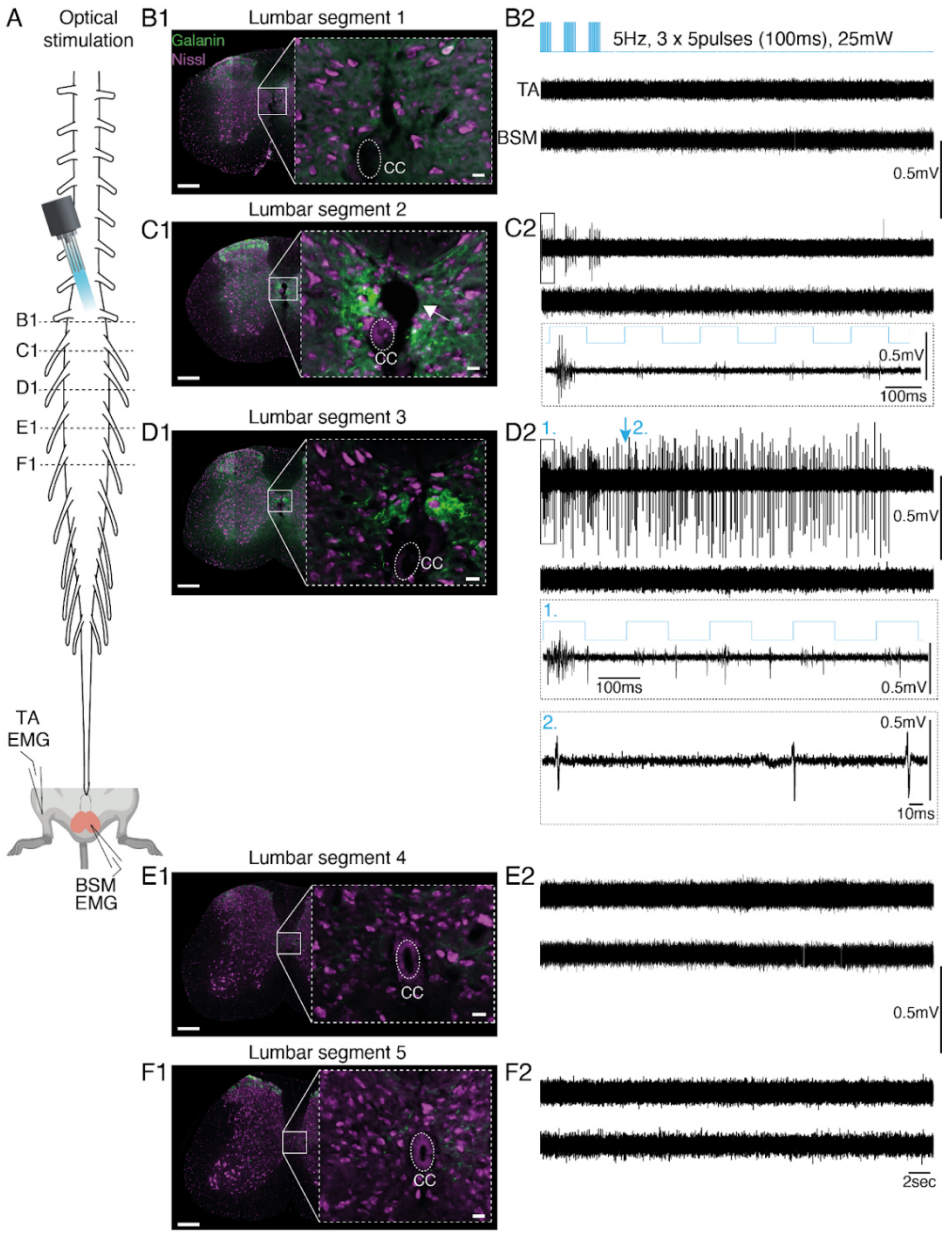

Figure 3.10 Optogenetic stimulation of the Gal+ cells along the rostrocaudal axis in an anaesthetised preparation. (A) Experimental design: anaesthetised Gal-ChR2 animals were clamped into the spinal frame, the spine was opened and animals were spinalized. An optical fibre was placed on top of the spinal cord and moved along the rostral caudal axis to deliver blue light while in parallel BSM activity was monitored. (B1 - F1) Representative post-hoc histological sections along the rostral caudal axis of the spinal

cord are shown. Note the electrolytic lesion at the lumbar segment 2 which corresponds to the location where the biggest and longest BSM responses were triggered. Green: Galanin ChR2. Purple: Nissl. (B2-F2) Representative electrophysiological traces with BSM and leg (TA, tibialis anterior) responses triggered at the optogenetic stimulation site shown in B1 -F1. Note that BSM responses were most prominent at locations (C2, D2) where Galanin ChR2 labelling was observed post hoc around the central canal (C1, D1) while TA responses were never observed. In D2 also notice the inset (1.) denoting the response during optogenetic stimulation and inset (2.) with an example of response after the stimulation train is over.

Consistent with the results obtained from electric stimulations, optogenetically-evoked BSM responses were markedly higher in amplitude and longer in duration in spinalized compared to intact preparations (Figure 3.11), further supporting the idea that the Gal+ cells may be subject to tonic descending inhibition (Marson & McKenna, 1990, 1992).

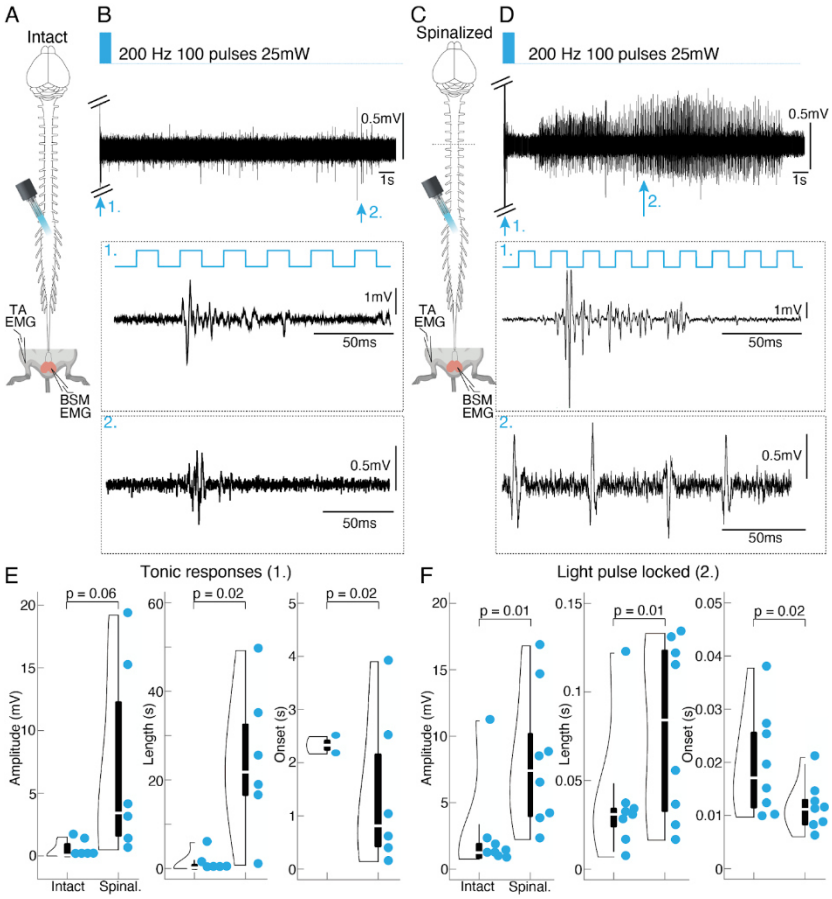

Figure 3.11 Optogenetic activation of Gal+ cells triggered BSM responses in a spinalized vs non-spinalized preparation. (A) Experimental design: optogenetic stimulations were conducted in the Gal+ cells location in anaesthetised mice in which the connection to the brain has been kept intact while in parallel monitoring BSM activity using EMG recordings (N = 8; same animals used for intact and spinalization experiments). (B) Example EMG trace obtained in an animal in which the connection to the brain was kept intact and optogenetic stimulation was applied with an optrode on the spinal cord surface (above the midline). (C) Same as A but a spinalization was performed between thoracic segments 5 and 6. (D) Same as B but EMG trace is recorded from an animal in which a spinalization was performed prior to stimulation. Note the difference in BSM activity. (E) BSM EMG amplitude (left), length (middle) and onset (right) triggered with an optogenetic train stimulation in intact anaesthetised mice compared to spinalized mice. Note that amplitudes (mean amplitude intact 0.45 ± 2.6 mV vs. mean amplitude spinalized 7.13 ± 2.6 mV; P = 0.06 resulting from a Student's t-test) and lengths (mean length intact 1.13 ±

6.7 s vs. mean length spinalized 24.1 ± 7.01 s; P = 0.007 resulting from a Student's t-test) were markedly increased after spinalization while the onset with which BSM responses were triggered was shortened after spinalization (mean onset intact 2.32 ± 0.5 s vs. mean onset spinalized 1.42 ± 0.6 s; P = 0.02 resulting from a Student's t-test). Only in 2 out of 8 animals responses were triggered before spinalization. (F) Same as E but parameters are depicted for the 5Hz optogenetic stimulations. The same phenomena was observed. Light triggered BSM responses showed an increase in amplitude (left; mean amplitude intact 2.5 ± 1.24 mV vs. mean amplitude spinalized 8.11 ± 1.83 mV; P = 0.01 resulting from a Student's t-test) and length (middle; mean length intact 0.04 ± 0.01 s vs. mean length spinalized 0.08 ± 0.02 s; P = 0.05 resulting from a Student's t-test) and a decrease in onset (right; mean onset intact 0.02 ± 0.003 s vs. mean onset spinalized 0.01 ± 0.003 s; P = 0.02 resulting from a Student's t-test) after the connection to the brain was cut.

Furthermore, optogenetically elicited BSM responses exhibited similar dynamics to those evoked by electrical stimulation. Both methods resulted in a decrease in amplitude and duration with consecutive trains of stimulation (Figure 3.12 A, B), while the onset of triggered responses remained unchanged (Figure 3.12 C).

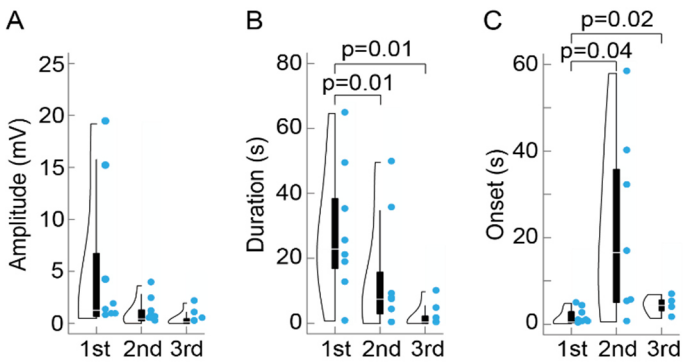

Figure 3.12 Amplitude, duration and onset quantification of BSM responses after consecutive optogenetic activation of Gal+ cells, shows a decrease in the BSM response. (A) Violin plots illustrating the amplitudes of optogenetically triggered BSM signal during 1st (mean amplitude 5.5 ± 2.6 mV), 2nd (mean amplitude 1.48 ± 0.86 mV) and 3rd rounds (mean amplitude 0.41 ± 0.23 mV) of laser application, with boxplots

(elements: see Methods, N=8). P-values result from a two-tailed Mann-Whitney-U Test. Every dot represents the BSM responses obtained from an animal. (B) Same as A, but the duration of BSM activity is plotted. Mean durations: after 1st 29.33 ± 7.28 s; 2nd 15.59 ± 6.43 s; and 3rd 2.27 ± 1.24 s, laser application. P-values result from a two-tailed Mann-Whitney-U Test. (C) Same as B, but the onsets with which BSM activity was initiated are plotted. Mean onset of BSM EMG: after 1st 1.18 ± 0.02 s; 2nd 25.25 ± 0.1; and 3rd 4.28 ± 0.1 s, laser application. P-values result from a two-tailed Mann-Whitney-U Test.

In addition to these bursts of activity, we used lower stimulation frequencies to trigger time locked BSM responses (N = 12; 20 mW, 5 Hz-50 Hz, 15 pulses; Figure 3.13). In a subset of animals, we successfully conducted juxtacellular recordings in photo-identified single Gal-ChR2 neurons (Figure 3.13 A, N=7 cells), revealing response dynamics upon optogenetic stimulation in individual Gal+ cells and the consequent dynamics of the BSM with time locked triggered activity. The mean latency to spike for Gal+ cells was 10.6 ms ± 1.7 ms, followed by light triggered BSM EMG with a mean latency of 6.7 ms ± 0.09 ms. Notably, the mean latency to spike for photo-identified BSM-MNs was 4.5 ms ± 0.4 ms; Figure 3.13 B), further supporting the existence of a monosynaptic connectivity between Gal+ cells and BSM-MNs, as demonstrated above through in vitro recordings. Spike and EMG fidelities (calculated as the number of spikes or EMG responses divided by the number of light pulses) were stable up to 10 Hz (Figure 3.13 C). Importantly and similar to the tonic discharges observed above, a decrease in amplitude (Figure 3.13 D) and duration (Figure 3.13 E) was observed with consecutive lower frequency optogenetic stimulation, with a constant onset of triggered responses (Figure 3.13 F).

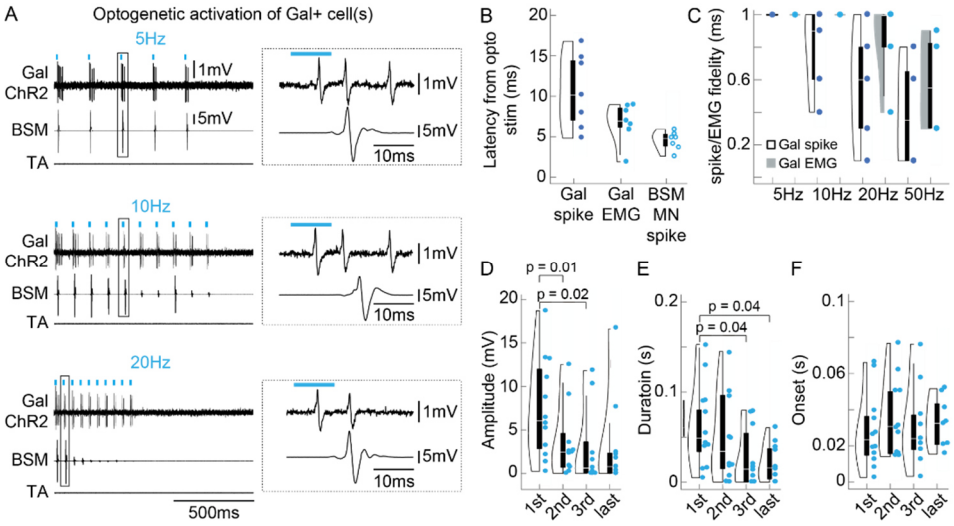

Figure 3.13 Juxtacellular recordings of Gal+ cells while being optogenetically activated, and the consequent BSM response pattern. (A) In addition to tonic BSM responses as observed during the electrical stimulations, optogenetic stimulations also led to timely locked BSM responses, capable of following stimulation frequencies up to 20 Hz (N = 12). In a subset of animals (4 out of 12) we recorded photo-identified single Gal-ChR2 neurons (N = 7 cells). Upper left panel: Juxtacellular recording of a Gal-ChR2 cell in parallel with EMG recordings of the BSM (2nd trace) and the TA muscle of the leg (3rd trace) during a 5 Hz laser stimulation. Upper right panel: zoom in of the indicated box illustrating the spike and EMG onset. Middle and lower panels: same as upper panel but for a 10 Hz and 20 Hz, respectively, laser application (pulses of 10 ms length) of the same cell shown in the upper panel. (B) Violin plot with boxplots (elements: see Methods) illustrating the latency for optogenetically triggered spikes in Gal-ChR2 single cells (Gal spike), the latency between spike onset of Gal-ChR2 single cells and BSM EMG onset (Gal EMG), and the latency to spike of single photo-identified BSM-MNs (BSM MN spike). Data refers to 7 single Galanin cells obtained from 4 Gal-ChR2 animals and to 7 single BSM-MNs obtained from 6 animals that received retro AAV injections with ChR2 as pups (see Chapter 2, Figure 2.6). (C) Same as B, but the Gal-ChR2 spike and Gal-EMG fidelity (with which a laser pulse triggered a single spike or EMG response) is plotted. (D) Violin plots illustrating the amplitudes of optogenetically time-locked (5Hz) BSM signals (N=12) during 1st (mean amplitude 7.45 ± 1.64 mV), 2nd (mean amplitude 3.59 ± 1.17 mV), 3rd (mean amplitude 2.93 ± 1.26 mV) and last rounds (mean amplitude 3.98 ± 1.98 mV) of laser application, with boxplots (elements: see Methods). P-values result from a two-tailed Mann-Whitney-U Test. Every dot is an individual animal. 11 out of 12 animals showed

BSM responses upon 2nd laser application, in 9 out of 12 animals BSM responses were triggered upon 3rd laser application and in 8 out of 12 animals, laser application led to BSM responses during last rounds of stimulation (5th laser applications). (E) Same as D, but the duration of BSM signals is plotted. Mean durations: after 1st 0.06 ± 0.01 s; 2nd 0.05 ± 0.01; 3rd 0.03 ± 0.01; and last 0.03 ± 0.06 laser application. P-values result from a two-tailed Mann-Whitney-U Test. (F) Same as D, but the onset with which locked laser light triggered a BSM response. Data refers to 5 averaged onsets. Mean onsets: after 1st 0.03 ± 0.005 s; 2nd 0.03 ± 0.006; 3rd 0.03 ± 0.006; and last 0.03 ± 0.005 s, laser application.

Finally, the decrease in BSM activity observed with the electric and optogenetic stimulation of Gal+ cells contrasts sharply with the responses evoked by direct optogenetic activation of BSM-MNs. Direct optogenetic stimulation of BSM-MNs resulted in consistent responses in single BSM-MNs and in the BSM across repeated rounds of stimulation (Chapter 2, Figure 2.4 to Figure 2.6) and no observed depression of the response as in the stimulation of the Gal+ cells. This suggests that the depression in BSM activity upon consecutive stimulation of Gal+ neurons may be due to an alteration in synaptic transmission between the Gal+ cells and BSM-MNs, rather than changes in the intrinsic properties of BSM-MNs.

3.3 Discussion

The spinal control of ejaculation has been primarily thought as a reflex arc that receives constant descending inhibition from the brain (Marson & McKenna, 1992). In this chapter we start to show that the spinal cord may have a more complex role in ejaculation and sexual behaviour in general.

By electrically and optogenetically stimulating the Gal+ cells, and consequently driving BSM activity, we observed that the response of the

muscle is dependent on two things: 1) the short term stimulation history of Gal+ cells, since repeated stimulation leads to a decrease in the BSM contraction; and 2) the internal state of the animal, considering that electrical stimulation of animals that experienced an ejaculation beforehand lead to no muscle activity. To our knowledge, these results are the first to describe such an integration at the level of the spinal cord and point to a more intricate role of Gal+ cells during sexual behaviour in male mice.

3.3.1 Repeated stimulation of Gal+ cells leads to decreased BSM activation

To further describe the functional connection between the Gal+ cells and the BSM-MNs we used an anaesthetised *in vivo* preparation and electrically stimulated the spinal cord along the rostral caudal lumbar axis while in parallel monitoring BSM activity using an EMG. As expected, we were able to electrically elicit BSM activity at a very restrictive location that corresponded to the position of the Gal+ cells, as it had been previously done for the rat (Borgdorff et al., 2008). Very strikingly and different from the rat, however, was the result of decreased BSM activity when stimulating a second and a third time that let us to wonder whether a certain activity level of Gal+ cells initiates the refractory period in mice, a state of sexual satiety (Valente et al., 2021). Specific optogenetic Gal+ cells stimulation in the same type of preparation supports this hypothesis: after having induced prominent BSM activity in the first train of stimulation, we were not able to induce the same amount of activity in the BSM when shining light a second or third time. Interestingly, contrary to these results, direct optogenetic activation of BSM-MNs (Chapter 2) always led to sustained BSM activity, regardless of how many times we would stimulate

the MNs, indicating that once a certain activity level in Gal+ cells has been reached (with optogenetic or electrical stimulations), a mechanism is put into place to suppress their activity, or the activity of the synapse between Gal+ cells and BSM-MNs.

3.3.2 Gal+ cells integrate the internal state of the animal

To further understand the reasons behind the depression in the BSM activity with repeated Gal+ cells activation, we performed the electrical stimulation experiment in male mice that had undergone sexual behaviour: males were either allowed to perform 5 mounts with intromissions or do the full repertoire of sexual behaviour until reaching ejaculation. While the 5 mounts with intromission group showed very similar BSM activation patterns when comparing to sexually naïve animals, BSM activity in the ejaculation group was very scarce, thereby supporting the hypothesis that the refractory period may be already reflected and set in the periphery (Turley & Rowland, 2013). Furthermore, there is evidence that rats' sexual behaviour performance is also reflected at the spinal cord level as it has been shown that artificially triggered expulsion is accelerated in rats that were characterised as rapid ejaculators in a natural setting compared to those that would ejaculate on a 'sluggish' timescale or that would show a rather slow ejaculatory behaviour (Borgdorff et al., 2009).

3.4 Materials and Methods

3.4.1 Experimental model and subject details

All experimental procedures were carried out in strict accordance with the guidelines of the European Committee Council Directive and were approved by the Animal Care and Users Committee of the Champalimaud Neuroscience Program, the Portuguese National Authority for Animal Health (Direcção Geral de Veterinária; approval number 0421/000/000/2022) and by the local ethic committee of the University of Bordeaux and the French Agriculture and Forestry Ministry for handling animals (approval number 2016012716035720). For electrical stimulation experiments and EMG recordings in behaving animals, BL6 (*Mus musculus domesticus*, C57BL/6J) male mice aged 3-6 months were used. For the spinal cord optogenetic stimulation, Gal-ChR2 (*Mus musculus domesticus*, B6;129S-Gt(ROSA) 26Sortm32 (CAG-COP4*H134R/EYFP)Hze/J) male mice aged 3-6 months old were obtained from Jackson Laboratories. For electric stimulation of the spinal cord, Long Evans (Crl:LE Long-Evans) male rats were ordered from Charles Rivers. Finally, as a sexual stimuli, after ovariectomy and hormonal priming, C57BL6 female mice aged 3-6 months were used. All the animals were bred and maintained in our animal facility. All animals were weaned at 21 days and housed in same-sex groups in stand-alone cages (1284L, Techniplast, 365 × 207 × 140 mm) with access to food and water *ad libitum*. Mice were maintained on an inverse 12:12 light/dark cycle and experiments were performed during the dark phase of the cycle, phase of higher animal activity. After initiation of sexual behaviour training or immediately after surgery, male mice were kept single-housed until the experiment was over.

3.4.2 Electromyogram electrodes implantation for chronic recordings in sexually behaving animals

For chronic BSM EMG recording in behaving mice, animals were implanted with myomatrix arrays kindly made available to us from Sam Sober's Lab and CAMBER (Chung et al., 2023). Mice were anaesthetised with 3% isoflurane in oxygen and mouth fixed into a stereotaxic frame (Kopf, Tujunga, CA, USA), allowing the rotation of the body to implant the arrays in the bulbospongiosus muscle. During surgery, anaesthesia was maintained using 1.5% isoflurane. Three incisions were made to implant the array: first in the pelvic area, then above the animal's right hind leg and finally a midline incision in the scalp. The skin was carefully separated from the muscle using scissors, using the three incisions to insert the scissors, and finally allowing to subcutaneously guide the arrays' connector from the pelvic area to the skull to be later secured. Once each thread has been routed subcutaneously and positioned near the BSM, the animal is turned into a supine position and each thread is inserted into the muscle using a suture needle. A suture (size 8-0) was tied to a hole in the array and the needle was then passed through the BSM and used to pull the attached array thread into the muscle. The array was then secured within the muscle by suturing it to the BSM, using additional holes on the array. Afterwards, the incision in the pelvic area was closed and the animal was turned to access the skull. The skull was carefully cleaned and disinfected and the array's connector was secured to it using dental cement. If necessary, the incision on the skull was sutured and, after guaranteeing that all the array was under the skin, the incision above the hind leg was also sutured. All mice were single housed post-surgery and used for behaviour afterwards.

3.4.3 Nissl stain

The slides were washed 2 times in 0.01 M PBS to remove the excess of frozen section medium. After that the sections were rehydrated for 40 min in PBS 0.1 M, pH 7.2 (PBS 10x) and permeabilized for 10 min with 0.1% Triton-X (T9284-100ML, SigmaAldrich) in PBS 10x. The tissue was washed 2 times 5 min with PBS 10x before incubating them for 20 min with a 1:100 Neurotrace staining solution (in PBS 10x; (NeuroTrace™ 500/525 Green Fluorescent Nissl Stain, N21480, ThermoFisher Scientific; or NeuroTrace™ 530/615 Red Fluorescent Nissl Stain, N21482, ThermoFisher Scientific; or NeuroTrace™ 640/660 Deep-Red Fluorescent Nissl Stain, ThermoFisher Scientific). Subsequently the tissue was washed with 0.1% Triton-X in PBS 10x for 10 min. After washing 2 times 5 min with PBS 10x, the slides were rinsed with distilled water, dried and coverslipped with Mowiol.

3.4.4 Immunohistochemistry

Immunohistochemical labelling was performed using standard procedures. Briefly, spinal cord sections, which were labelled for Galanin (Anti-Galanin Antibody, Milipore, AB2233), were firstly washed 2 times for 5 min with PBS 0.01 M to remove the excess OCT. Afterwards, they were washed 2 times for 10 min with PBS 10x and preincubated for 1.5 hours at room temperature in a blocking solution (PBS 10x, 1% bovine serum albumin, and 0.3% Triton X-100). Afterwards, the primary antibody was diluted in the same blocking solution at a proportion of 1:100. The primary antibody was incubated on the glass slides overnight at room temperature. Incubation with the primary antibody was followed by 5 times 10 min washing with PBS 10x. Subsequently, we proceeded to detect the primary antibody with a secondary antibody coupled to different

fluorophores (Alexa Fluor 488, 594 or 647, Abcam/Thermo Fisher Scientific). The secondary antibody was diluted (1:500) in the blocking solution and the reaction was allowed to proceed for 2 hours in the dark at room temperature. In some cases, a Nissl stain was performed as described above. After the staining procedure, sections were washed 5 times 10 min with PBS 10x, rinsed with distilled water, dried and coverslipped with Mowiol mounting medium.

3.4.5 Electrophysiology

In vivo electrical stimulations and optogenetic stimulations

For acute electrophysiological experiments, mice (N = 8) and rats (N = 4) were anaesthetised by injection of an initial dose of 100 mg/kg ketamine and 7.5 mg/kg xylazine. Respiration, blink and pinch reflex were observed throughout the experiment and, if needed, animals were injected with an extra shot (25%) of ketamine/xylazine mixture or a 25% dose of ketamine alone. The animal's back, scrotum and right leg were shaved and cleaned with ethanol. Electromyogram electrodes were inserted into the BSM or tibialis anterior (TA) muscles and glued using Vetbond. The back skin was cut along the rostral caudal axis and the spine was fixed into stereotaxic spinal clamps (Kopf). Muscle and conjunctive tissue was removed before performing a laminectomy along the rostral caudal axis. Spinalization was performed in between the thoracic segments 5 and 6. For electrical stimulations, a 1 MΩ tungsten electrode (World Precision Instruments) was lowered at each microstimulation site (ranging from ~550 µm to ~950 µm of depth in the dorsal ventral axis, in each spinal cord segment), and currents ranging from 50 µA to 140 µA were injected using a stimulus isolator (Model no. A365RC, World Precision Instruments) while possible movements were documented. Various stimulation protocols were tested (single, 5 Hz, 50 Hz). Eventual activity in the BSM and TA was monitored

via EMG recordings using a custom-made amplifier (x 1000) and filtered at 2 kHz. Data acquisition and analysis were performed using spike2 software (CED Cambridge). Tungsten electrodes were moved along the rostral caudal axis of the spinal cord and electrolytic lesions were placed at the location where the biggest EMG responses were encountered. After having mapped the BSM responses along the rostral caudal axis, consecutive electrical stimulations were performed at the spinal cord sites where prominent BSM responses were encountered previously. Inter-stimulus intervals of consecutive electrical stimulations ranged from 15 to 5 min.

In a subset of animals undergoing electrical stimulations (N = 15), sexual behaviour (see below) was performed prior to the acute recordings. Animals either ejaculated (N = 8) or performed 5 mounts with intromission (N = 7), before they were anaesthetised.

During control experiments, the animals were prepared as above but a waiting time of 1 h was kept before the first stimulation to control that the observed effects are not due to a rundown of the preparation.

For optogenetic stimulations of the Gal+ cells (N = 13 of Gal-ChR2 male mice) and BSM-MNs (N = 10 of C57BL6 mice infected with an AAV expressing ChR2 on the BSM) the experimental procedure was similar except the fact that an optrode (diameter: 1 mm) was moved on top of the spinal cord, in the rostral caudal axis, while monitoring EMG recordings and documenting movements. Likewise, an electrolytic lesion was placed at the position where the light pulses led to the most prominent BSM EMG responses. We tested a variety of stimulation protocols (single, 5 Hz, 10 Hz, 20 Hz, 50 Hz, 100 Hz) and laser powers (5 mW – 40 mW).

In vivo juxtacellular recordings of photoidentified cells

Single in vivo juxtacellular recordings were performed as described in (Lima et al., 2009). Briefly, a glass electrode (resistance ranging from 4 to 6 MΩ) made of borosilicate glass tubes (Hilgenberg) was first lowered at the position where optogenetic stimulations led to the highest activity in the BSM. Pipettes were filled with a ringer solution. Extracellular local field potential recordings were captured while shining the light. Subsequently, cells were searched for by applying a negative current pulse and using an audio monitor (Grass Technologies, AM10) while steps were made in 1.5 µm increments with a micromanipulator (Luigs & Neumann SM-5, Germany) and potential increases in resistance were carefully observed. When spiking activity was detected, electrophysiological recordings were performed in line with optogenetic stimulation protocols (single, 5 Hz, 10 Hz, 20 Hz, 50 Hz) and EMG monitoring. Recordings were amplified (Dagan BVC-700A, Dagan, Minneapolis, MN), low-pass filtered at 10 kHz and sampled at 50 kHz by a data-acquisition interface (Power 1401, CED, Cambridge, England) and controlled and analysed by the spike2 software (CED, Cambridge, England).

3.4.6 Behaviour

Sexual priming prior electrical stimulations

Male mice were single-housed and trained in sexual behaviour, with a primed ovariectomised female, until ejaculation was reached in 3 sessions. Afterwards, the animals were divided into two groups: one group was allowed to perform 5 mounts with intromissions (N = 7) and the second group was allowed to perform the whole repertoire of sexual behaviour until reaching ejaculation (N = 8). Immediately after the

behaviour, the animals were anaesthetised and used for in vivo electrical stimulations as described above.

In vivo BSM EMG recordings

Male mice were single-housed and trained in sexual behaviour, with a primed ovariectomised female, until ejaculation was reached in 3 sessions. Afterwards the animals were implanted with EMG probes in the BSM as described above. Following a recovery period of 2 weeks post surgery in their home cages, the animals were put on an experimental box, where they had a 10 min habituation, after which a primed ovariectomised female was introduced. The animals were allowed to perform the full repertoire of sexual behaviour until ejaculation was reached and they were transferred back to their home cage. If the animals did not initiate behaviour, the experiment was stopped after 30 min and the sexual experimental paradigm was repeated for at least two more weeks. At the end of the experiment the animals were sacrificed and the probes recovered to reuse in future experiments. BSM recordings were conducted using an RHD 16-Channel bipolar-input recording headstage (Intan Technologies), connected to an Acquisition Board (Open Ephys), using a sampling rate of 30 KHz. The board and cameras were controlled using a bonsai script (Bonsai Visual Reactive Programming) and the data was band-passed between 850-7,000 Hz and further analysed using Matlab.

Ovariectomy and hormonal priming

All female mice (N=20) used as sexual stimuli were ovariectomised. Briefly, female mice were anaesthetised using 3% isoflurane in oxygen and placed into a mouth piece allowing for continuous isoflurane anaesthesia. After all reflexes were gone, an incision was made at the

centre of the lower back. The skin was separated from the muscle towards both sides of the back. After that, on one side, levelled with the hindlimb, the ovary fat pad was located and a small incision was made in the muscle above this area. The ovary was gently pulled and the connection between the ovary and the uterus was cut using a cauterizer. The same procedure was repeated for the second ovary. Finally, the incision in the back was sutured and the animal was allowed to fully recover on a heating pad. After two weeks of recovery, the animals underwent hormonal priming during which they received an oestrogen (1 mg/ml, Sigma E815 in sesame oil) injection 2 days prior to the sexual behaviour experiment and a progesterone (5 mg/ml, Sigma P0130 in sesame oil) injection 4h before the experiment was scheduled. Hormonal priming with oestrogen and progesterone was conducted before each experiment.

3.4.7 Quantification and Statistical Analysis

Behavioural Analysis

The *in vivo* EMG BSM recordings behavioural experiments were carefully recorded using two point grey cameras (Teledyne FLIR), at 60 frames per second. The cameras acquired a top and front video of the cage and were controlled using a bonsai script (Bonsai Visual Reactive Programming). Afterwards, the videos were analysed using Python Video Annotator (developed at the Champalimaud Foundation). A wide range of behaviours was annotated, namely: sniffing of the anogenital area of the female; mount attempts (when the male was not able to perform intromissions) mounts with probing (shallow pelvic movements when the male is trying to intromit but still has not inserted the penis); mounts with intra-vaginal thrustings; intra-vaginal thurstings (when the male successful inserted the penis in the female's vagina); and finally ejaculation (time

between the beginning of shivering and the moment the male dismounted the female). The duration, in frames, for each behaviour was then aligned to the camera timestamps, acquired during video recording. Analysis of behavioural timestamp data was performed using a python script in Spyder 3.3.6 (Python).

Statistical Analysis

Statistical analysis was performed with homemade code in Matlab and Python (scipy and statsmodels). All error ranges represent standard error of the mean. For two-sample comparisons of a single variable, Student's t test was used, unless in cases when the underlying distributions were non-Gaussian (Shapiro-Wilk test, $p<0.05$), where a two-tailed Mann-Whitney-U Test was performed. When multiple variables were compared, a Kruskal Wallis test or a Wilcoxon-Signed-Rank test were used since the data did not follow a Gaussian distribution. Probabilities of the null hypothesis $p<0.05$ were judged to be statistically significant. Elements of violin plots: centre line, median; box limits, upper (75) and lower (25) quartiles; and whiskers, 1.5x interquartile range.

3.5 Author Contributions

A.R.M., C.L. and S.Q.L designed the experiments and the analysis. A.R.M. performed in vivo EMG BSM recording in sexually behaving animals and the ovariectomies. A.R.M, H.M and N.G.C performed the EMG data and behavioural analysis. C.L. performed the electrophysiology experiments and the electrical and optogenetic stimulation experiments. A.R.M. and C.L. did the sexual behaviour priming for the electric stimulation experiments. A.R.M. and L.F. performed immunohistochemistry and histological image acquisition.

4 Characterization of the spinal circuit controlling the BSM in behaving animals

After anatomically and functionally characterising the spinal circuit responsible for sperm expulsion in mice, we decided to study the role of Gal+ cells in awake behaving animals. Firstly, we assessed the pattern of activation of Gal+ cells during different stages of sexual behaviour using cFos. We observed that Gal+ cells are increasingly active as the behaviour evolves, but their activity peaks when the male ejaculates. This is in accordance with our freely moving EMG BSM recordings that show BSM activity in several stages of the behaviour. With this in mind, we decided to ablate this cluster of spinal Gal+ cells using a chemogenetic strategy based on the Diphtheria Toxin receptor to test the potential differences in male mice sexual behaviour. Interestingly, animals with a reduced number of Gal+ cells showed striking differences in the latency

to ejaculate and in the copulatory sequence, once again pointing to the role of Gal+ cells in more than just controlling ejaculation. Taken together, these results show the presence of a spinal circuit that, contrary to previously believed, does not work simply as a spinal reflex, but integrates the internal state of the animal and controls different steps of the copulatory sequence.

4.1 Introduction

In mice, copulation can be divided into several behavioural epochs that depend on different central and peripheral neuronal control. When a male and a female begin a sexual encounter the first cues are mainly olfactory, with anogenital investigations being the main component at the beginning of the copulatory sequence (Dulac & Wagner, 2006). Eventually, the male will attempt to mount the female, initiating the consummatory part of the copulatory behaviour. If the female is receptive she will accept the male's attempts and he will be able to perform an intromission followed by several vaginal thrusts until they separate again ending that mount bout. These mounts with intromission will be repeated a variable number of times until a final one is reached and ejaculation takes place (Dewsbury, 1972, 1975; Valente et al., 2021). Interestingly, ejaculation is the turning point in the sexual encounter, since it marks the moment that the male enters in the refractory period and is no longer interested in the female (Valente et al., 2021). Despite its profound impact on male behaviour, still little is known about the spinal and brain circuits that control ejaculation.

As mentioned before, one of the key players inducing ejaculation is a spinal circuit composed of Gal+ cells that control the BSM (Truitt & Coolen, 2002). However, there is still an important question to be answered: what is the role of this population of Gal+ cells in behaving animals?

Given that most previous studies focused on anatomy (Dobberfuhl et al., 2014; Veening & Coolen, 2014) or were conducted in anaesthetised animals (Borgdorff et al., 2008), it remains to be determined exactly what is the role of these cells in sexually behaving animals. One study reports that Gal+ cells are partially active upon mounts with intromissions, but are mainly active after at least one ejaculation in rats, as observed with the

colocalization with the immediate early gene, cFos (Truitt et al., 2003). However, pharmacological ablation of these cells lead to specific impairments in ejaculation but not other components of the copulatory sequence (Truitt & Coolen, 2002). This again points to the role of the Gal+ cells as a spinal reflex centre and not as integrators of external cues and capable of controlling other aspects of copulation.

In this chapter we investigate further the role of Gal+ cells in copulation. We start by studying their levels of activation with different behavioural epochs by using cFos. We show that Gal+ cells are progressively active with copulation and arousal, but are more strongly active after ejaculation takes place. Besides, by chemogenetically ablating Gal+ cells, we observed that they not only affect ejaculation and the latency for ejaculation to take place, but they also impair other aspects of the copulatory sequence.

4.2 Results

4.2.1 The lumbar population of Gal+ neurons becomes increasingly active during sexual behaviour

Given the unexpected finding that the outcome of electrical stimulation of the spinal cord on BSM activity was dependent on the behavioural state of the male, suggesting the involvement of Gal+ cells during other phases of copulatory behaviour, we used the expression of the immediate early gene *cFos* to establish a link between behaviour and neuronal activity (Krukoff, 1999). For this purpose, we compared the induction of the cFos protein in the Gal+ cells of the L2/L3 spinal segments of male mice that ejaculated (sexual interaction with a receptive female until ejaculation, Ejaculation, N=6) with the induction in males that were either alone in a

clean cage (Cage control, N=7) or had varying degrees of interaction with a female (10 minutes with a receptive female but no penile insertion as intromission was interrupted whenever the male attempted copulation, Sexually Aroused, N=5; or five mounts with intromission and intravaginal thrusting, 5 Mounts, N=5) (Figure 4.1 A-D).

To specifically quantify the number of active Gal+ cells, we used male progeny from the Gal-cre x TdTomato cross and performed post-hoc immunohistochemical quantification of the TdTomato signal and cFos induction in the L2/L3 spinal segments for each condition. As expected, given the direct contact to the BSM-MNs, significantly more double-positive neurons were found in the Ejaculation group, compared to the other three conditions (Cage control, $p < 0.0001$, Sexually Aroused, $p < 0.0001$ and 5 Mounts, $p< 0.0001$ Student's t-test, Figure 4.1 E). Unexpectedly, we observed similar levels of activation between the Sexually Aroused and 5 Mounts groups, with both conditions exhibiting significantly higher levels of double-positive neurons compared to the Cage control ($p < 0.01$, Student's t-test).

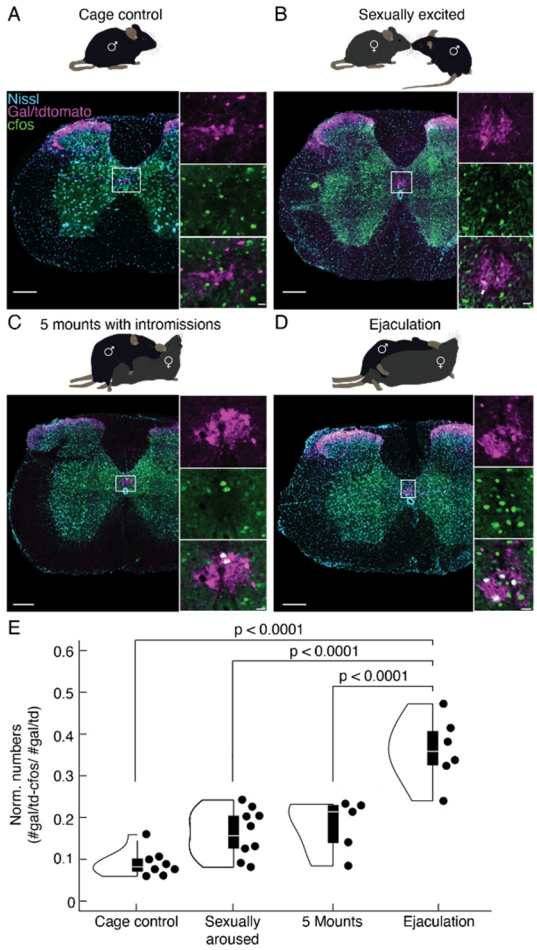

Figure 4.1 The lumbar population of Gal+ cells becomes increasingly active during sexual behaviour. (A) Upper panel: Males in the Cage control group were alone in their home cage or in the behaviour box for 10 min (N = 6). Lower panel: Example spinal cord section at the L2/3 segments (revealed by Nissl stain, blue). Note no overlap between the cFos signal (green) and the Galanin signal (purple; see larger insets). Scale bar spinal cord section 200 µm, scale bar inset 20 µm. (B) Upper panel: Males in the Excited group were allowed to interact with a hormonally primed ovariectomised female for 10 min, but attempts of copulation were interrupted (N = 7). Lower panel: Example spinal cord section at the L2/3 segments. (C) Upper panel: Males in the 5 Mounts group: were allowed to perform 5 mounts with vaginal thrusting (N = 5). Lower panel: Example spinal cord section at the L2/3 segments. (D) Upper panel: Males in the Ejaculation group were allowed to engage in sexual behaviour until they ejaculated (N = 6). Lower panel: Example spinal cord section at the L2/3 segments. (E) Normalised cell numbers (number of double labelled

cells, cFos+ and Gal+; divided by the total number of Gal+ cells) for the four groups. Depicted p values from Student's t-test (violin plots elements: see Methods).

To test if the activation observed in the Sexual Aroused group was specific to an interaction with a female, we conducted a separate experiment evaluating cFos activation levels after introducing a male intruder in the cage with the test animal and compared it to the Cage control and Sexually Aroused groups. The interaction with the intruder male, which involved bouts of aggressive behaviour and male-directed mounting, elicited similar levels of cFos activation in the Male and Sexually Aroused groups (Figure 4.2). Given the high arousal state of the male in these two conditions, this result suggests that the activity of the Gal+ cells may be related to the internal state of the male and not just with the ejaculatory reflex.

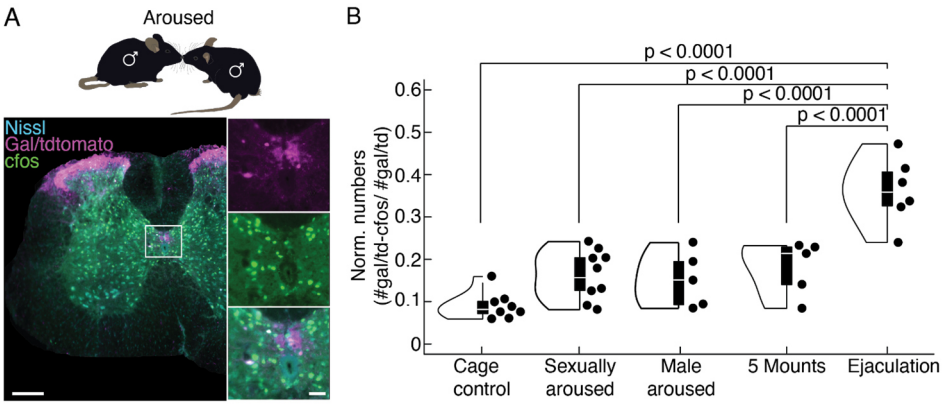

Figure 4.2 Activation of the Gal+ population with different social interactions, namely a male-to-male interaction. (A) Upper panel: Males in the Male aroused group were allowed to interact with a naive young male (5 weeks old) for 10 min or 10 attack bouts (N = 5). Lower panel: Example spinal cord section at the L2/3 segments. (B) Normalized cell numbers (number of double labeled cells, cfos+ and Gal+; divided by the total number of Gal+ cells) for the five groups (groups depicted in Figure 4.1 with the

addition of the Male aroused group). Depicted p values from Student's t-test (violin plots elements: see Methods).

4.2.2 Genetic ablation of the lumbar Gal+ neurons disrupts male sexual behaviour

Our results so far suggest that the population of lumbar Gal+ cells might have a role before the ejaculatory threshold. To determine the function of this spinal population during a full sexual interaction, we used a genetic approach to specifically ablate the Gal+ cells by expressing the diphtheria toxin receptor (DTR, (Azim et al., 2014)). A conditional AAV carrying the DTR construct (AA8V-FLEX-DTR-GFP, Salk) was injected into the L2/L3 spinal segments of sexually trained males derived from the Gal-Cre x TdTomato cross (Figure 4.3; DTR group; N = 12). The control group, of the same genotype and also sexually trained, underwent a sham surgery at the same spinal location (SHAM group; N = 7).

After a recovery period and a second session of sexual behaviour, both groups (DTR and SHAM) received an intraperitoneal injection of diphtheria toxin (DT). One week after DT treatment, the effect of the genetic ablation on sexual behaviour was tested in the presence of a sexually receptive female. Males of both groups were sacrificed either 90 minutes after ejaculation or 90 minutes after the female was introduced into the testing arena if the male initiated copulation but did not ejaculate. In cases with absent sexual motivation (no mount attempts), the trial was interrupted 30 minutes after the female was introduced, and testing was repeated up to two more times, once a week (Figure 4.3 B and see Methods for detailed experimental procedure).

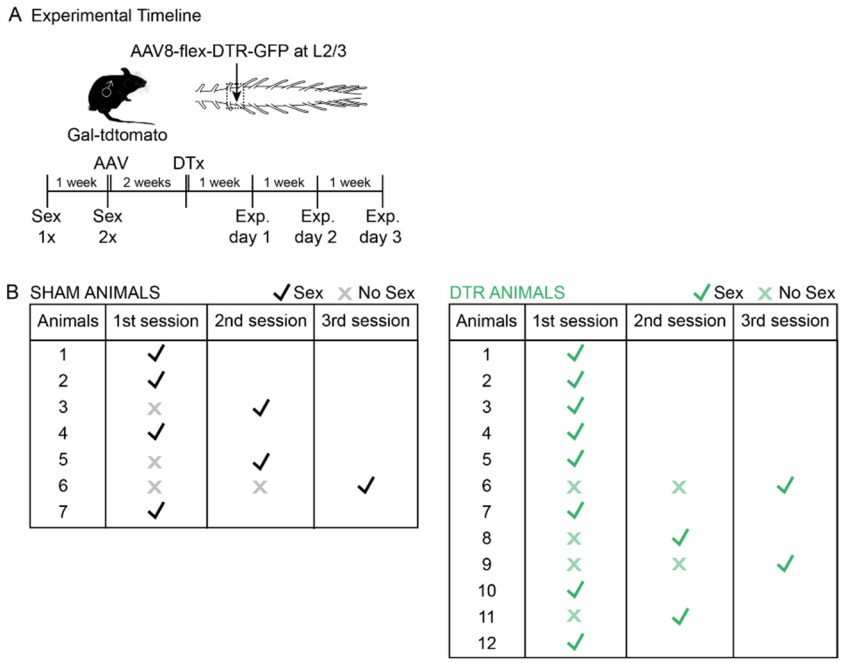

Figure 4.3 Experimental design of the DTR based chemogenetic ablation of the Gal+ cells experiment and number of sessions for each male mice used. (A) Experimental design. Gal-cre x dTomato male mice were sexually trained once before receiving a spinal injection of either a flexed AAV carrying DTR (DTR group) or undergoing a sham surgery (SHAM). Two weeks post-surgery the sexual performance of both groups was tested, after which they received an injection of Diphtheria Toxin (DT). One week after DT injection, the impact of the neuronal ablation on sexual behaviour was investigated. (B) Animals were tested for 3 weeks in a row to assess their capability to perform sexual behaviour after surgery. Both SHAM (left) and DTR (right) animals took different amounts of sessions to initiate the behaviour, but eventually all showed sexual behaviours (mounts, probing, thrustings, and in most cases ejaculation) in the span of three weeks.

Post-hoc immunohistochemical processing of the spinal cords (Figure 4.4 A) allowed us to determine the number of cFos-positive and Gal+ cells in the L2/L3 spinal segments. While the number of cFos-positive cells was comparable between the SHAM and DTR group (Figure 4.4 B), there was

a significant reduction in the number of Gal+ cells (Figure 4.4 C) and in the overlap of Gal+ neurons and cFos-positive cells (Figure 4.4 D and E).

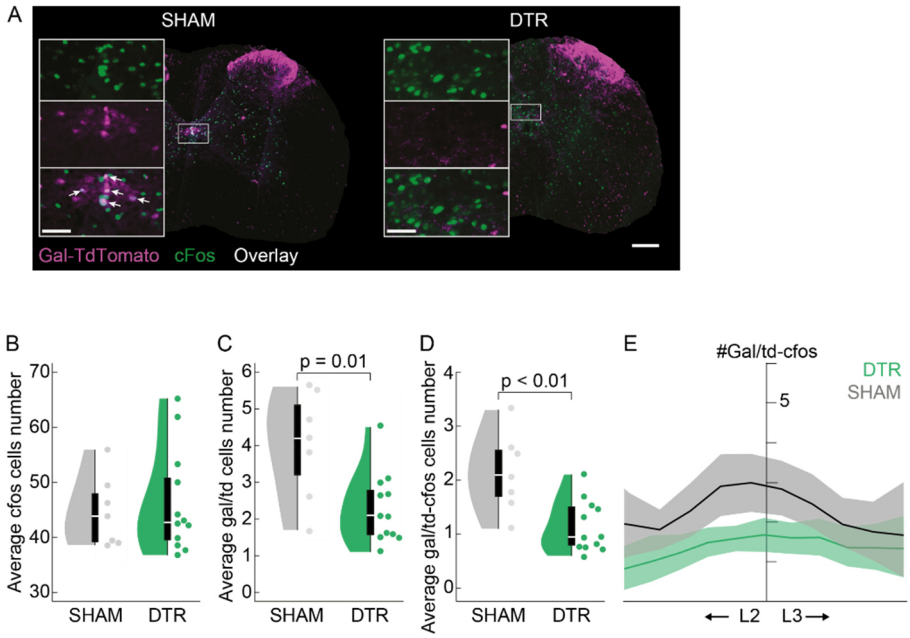

Figure 4.4 Quantification of the ablation success based on the number of Gal+ cells before and after DT application. (A) Left panel: example spinal cord section at the L2/3 segments obtained from an animal of the SHAM group. tdTomato indicating Gal+ neurons (purple) overlap (white) with the immediate early gene cfos (green). Scale bar 200 µm. Inset 50 µm. Right panel: same as for the left panel but for an animal of the DTR group. Note the poor TdTomato signal (purple) around the central canal at the L2/3 spinal segments. (B) Violin plots of cFos cells quantified in the L2/3 spinal segments for the SHAM (gray, mean number 44.6 ± 2.4) and DTR (green, mean number 46.2 ± 2.1) animals. P = 0.7 resulting from a student's t-test (violin plots elements: see Methods). (C) Same as B, but the averaged number of Gal-cre x TdTomato cells is depicted. Note the significantly lower number of Gal-cre x TdTomato cells in the DTR animals (mean number of tdTomato+ cells 2.3 ± 0.28) compared to the SHAM group (4.0 ± 0.6). P = 0.01 resulting from a student's t-test. (D) Same as B, but the averaged number of Gal-cre x TdTomato cells co-expressing cfos is plotted. A significant difference was observed across groups (mean number of Gal-cre xTtdTomato+/cfos+ cells in DTR 1.1 ± 0.14 and SHAM 2.1 ± 0.3

animals, p = 0.01 resulting from a student's t-test). (E) Cumulative curve of Gal-cre x TdTomato cell numbers along the L2/3 spinal segments for SHAM and DTR animals.

Consistent with the previous cFos and electrical stimulation experiments, and further supporting the involvement of these neurons in a more general control of sexual behaviour, the copulatory sequence (Figure 4.5 A) was significantly disrupted in the DTR group. While 3 out of 12 DTR animals did not reach ejaculation (but attempted copulation), and only one ejaculated in less than 10 minutes, all SHAM animals reached ejaculation, with only two taking longer than 10 minutes (Figure 4.5 B), as indicated in the cumulative distribution of the latency to ejaculate from the first mount (Mount with probing - MP - or Mount with Intromission - MI). Individual raster plots for each animal aligned to the first consummatory act (Figure 4.5 C) illustrate no effect on the latency to mount, while the latency to ejaculate from first mount was significantly longer.

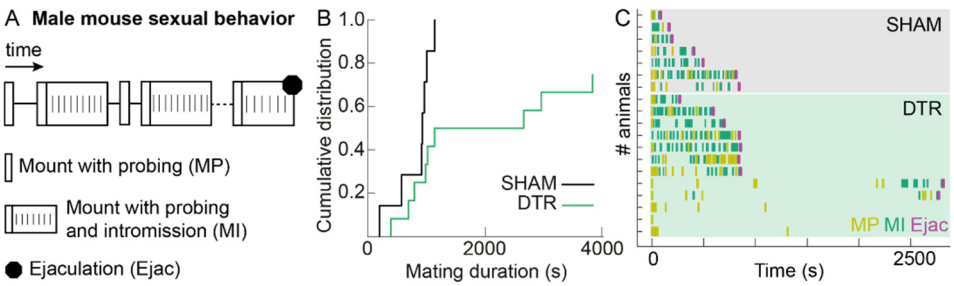

Figure 4.5 Ablation of the Gal+ cells leads to a disruption in the copulatory pattern in male mice. (A) Schematic representation of male sexual behaviour: Mounts with probing (MP), correct positioning of the paws on the female flanks and shallow pelvic thrusting movements trying to locate the vagina; Mounts with Intromission (MI), after the initial probing period of shallow thrusting the male inserts the penis inside the female and executes several deeper thrusts until he dismounts; several MI are executed until the ejaculatory threshold is achieved. (B) Cumulative distribution of the latency to ejaculate

from the first consummatory act (MP or MI) (black SHAM; green DTR). Proportion of animals that ejaculated (y - axis) within a given time (x - axis) is shown. Survival analysis using the Kaplan–Meier estimator shows a significant difference between the SHAM and DTR distributions by the log-rank test (p=0.02). (C) Raster plot aligned to the first consummatory act (MP or MI). Each line represents an animal: SHAM animals on a shaded grey; DTR animals on a shaded green background. Purple line marks Ejaculation (Ejac). Animals are ordered by latency to ejaculate, after separating animals that ejaculated or not.

To identify which aspect of the sexual interaction was disrupted, leading to an increased latency to ejaculate, we further analysed the copulatory sequence (including only DTR animals that ejaculated in the analysis). Sexual motivation did not differ across groups as reflected by the latency to mount (Figure 4.6 A) and the number of anogenital investigations (Figure 4.6 B-D), though there was a trend towards a higher number of anogenital investigations in the DTR group, in particular when considering the number of events during the consummatory phase of the behaviour (after the first mount, Figure 4.6 D).

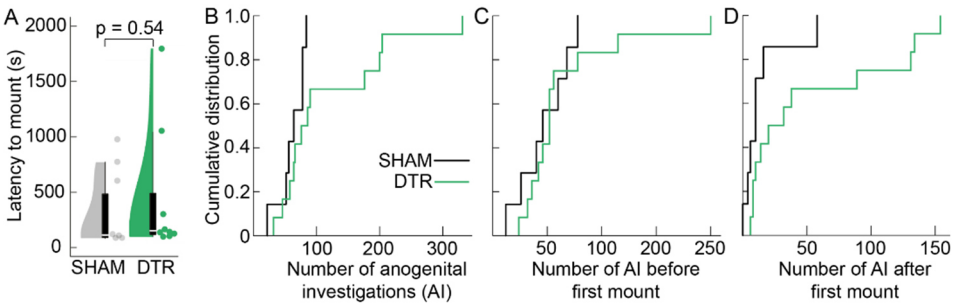

Figure 4.6 The appetitive phase of the sexual encounter does not seem to be affected by the Gal+ cells ablation. (A) Cumulative distribution relative to the number of all anogenital investigations shown by SHAM and DTR animals. No significant difference was found using the Mann-Whitney-Wilcoxon two-sided test (p=0.17) or the two-sample

Kolmogorov-Smirnov test (p=0.15). (B) Cumulative distribution relative to the number of anogenital investigations before the first mount shown by SHAM and DTR animals. No significant difference was found using the Mann-Whitney-Wilcoxon two-sided test (p=0.6) or the two-sample Kolmogorov-Smirnov test (p=0.96). (C) Cumulative distribution relative to the number of anogenital investigations after the first mount shown by SHAM and DTR animals. No significant difference was found using the Mann-Whitney-Wilcoxon two-sided test (p=0.07) or the two-sample Kolmogorov-Smirnov test (p=0.26). (D) Violin plot showing the latency to mount (MP or MI) for SHAM (mean latency 392 ± 181 s) and DTR (mean latency 435 ± 248 s) animals. No significant difference was detected, p = 0.54, Mann-Whitney U-test (violin plots elements: see Methods).

Interestingly the mounting events resulting in penile insertion (MI, Figure 4.5 C), had similar durations across groups (Figure 4.7 A and B), and the number of MI was also similar (Figure 4.7 C), indicating that a comparable amount of genital sensory information was sufficient to trigger ejaculation in both types of males, despite differences in the latency to ejaculate (Figure 4.7 D).

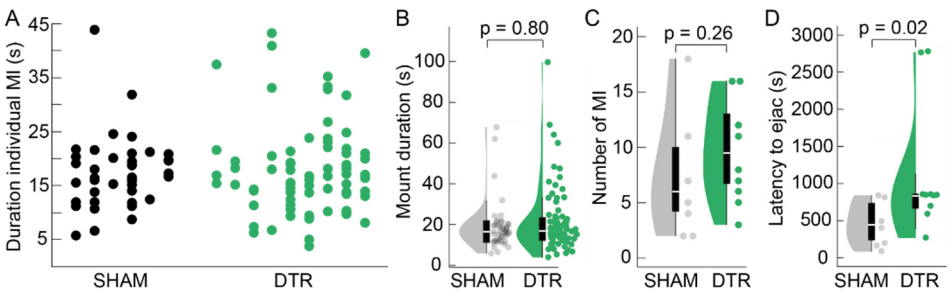

Figure 4.7 Different quantitative factors associated with the mounts do not change with ablation of the Gal+ cells. (A) Duration of individual mounts with thrusts (MI, in seconds) per animal. SHAM and DTR animals show identical values. (B) Violin plot showing the mount duration (all MI events) which is comparable across groups (mean mount duration of SHAM animals 18.9 ± 2 s and DTR animals 21.1 ± 2 s). P = 0.8 resulting from a Mann-Whitney U-test (violin plots elements: see Methods). (C) Number of MTs for SHAM (mean number 7 ± 2.7) and DTR (mean number 9.3 ± 2) animals. P = 0.29 resulting

from a Mann-Whitney U-test (violin plots elements: see Methods). (D) Violin plot showing the latency to ejaculate from the first consummatory act (MP or MI). Mean latency to Ejac for SHAM animals is 427.2 ± 146 s and note that DTR animals take significantly longer to reach ejaculation (mean latency to Ejac 1170.8 ± 392 s). P = 0.002 resulting from a Mann-Whitney U-test (violin plots elements: see Methods).

In contrast, we observed a difference in the number of mounts that did not result in penile insertion: mount attempts where the male performed several shallow pelvic thrust movements trying to locate the female's vagina (which only occurs if the male is sexually motivated, MP; Figure 4.8 A). Surprisingly, the ejaculation duration was similar across all males that ejaculated (from the last thrust until the male dismounted the female, see Methods; Figure 4.8 B), indicating that if the male reached the ejaculatory threshold, sperm expulsion could occur. This contrasts with results from similar experiments in rats, where ablation of rat Gal+ cells disrupted ejaculation, but not copulation (Truitt & Coolen, 2002). In line with the increased number of MP, the time to successful penile insertion after the male placed his paws on the female flanks was also significantly longer in the DTR group (Figure 4.8 C and D).

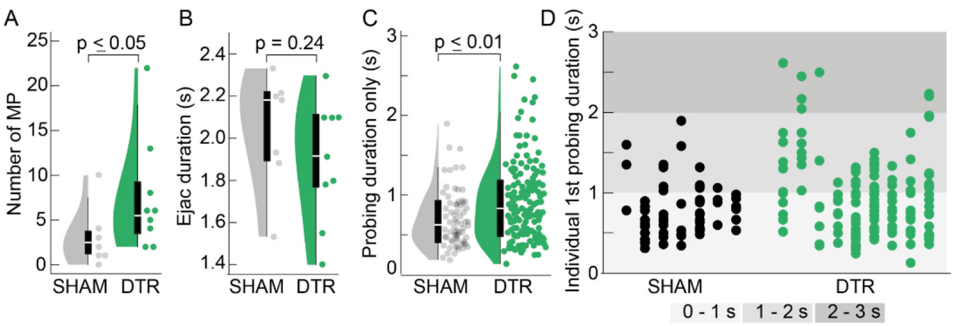

Figure 4.8 Probing is affected by the Gal+ cells ablation, indicating an impairment in the sensory integration associated with probing. (A) Number of MPs for SHAM

(mean number 3 ± 1.6) and DTR (mean number 7.6 ± 2.7) animals. P = 0.03 resulting from a Mann-Whitney U-test (violin plots elements: see Methods). (B) The time window for ejaculation is plotted (from the last thrust until separating from the female). Mean Ejac duration for SHAM animals 16 ± 3 s vs. mean DTR 15.4 ± 2.3 s. P = 0.8 resulting from a Student's t-test (violin plots elements: see Methods). (C) Probing duration for all MI (time from first to the last shallow thrust, before penile insertion). Mean probing duration for SHAM 0.7 ± 0.04 s vs. DTR 0.91 ± 0.04 s. P = 0.002 resulting from a Mann-Whitney U-test (violin plots elements: see Methods). (D) Duration of the first probing event per mount (MP, in seconds) per animal. DTR animals show a higher number of mounts with longer probing durations (namely with more than 2 seconds duration).

Thrusting rate and dynamics of MI were similar across groups (Figure 4.9 A-C), indicating normal pelvic thrusting once penile insertion was achieved. Importantly, erection did not seem affected by the ablation of Gal+ cells, as penile movements were similar in SHAM and DTR animals, with both groups capable of penile insertion and intravaginal thrusts (data not shown).

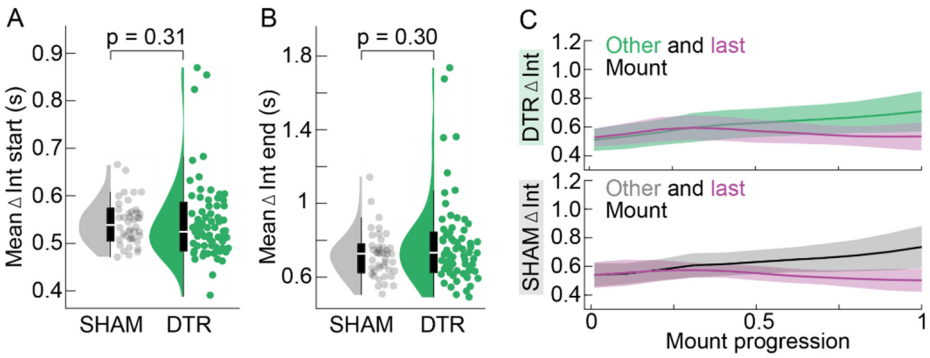

Figure 4.9 The thrusting patterns are not affected by Gal+ cells ablation. (A) Violin plots of all inter-thrust intervals of the first four thrusts of a MI (mean for SHAM 0.54 ± 0.01 s vs. DTR 0.54 ± 0.01 s). P = 0.31 resulting from a Mann-Whitney U-test (violin plots elements: see Methods). (B) Same as A, but the inter-thrust interval of the last four thrusts in a MI is plotted (mean for SHAM 0.69 ± 0.03 s vs. DTR 0.76 ± 0.03). P=0.15 resulting

from a Mann-Whitney U-test. (C) Mean interval with standard deviation is plotted in relation to mount progression for all other MI (light green DTR; grey SHAM) and the last MI leading to ejaculation (purple); a similar pattern of deceleration and acceleration is observed across the two groups.

Finally, to test if the behavioural impairments were due to the extent of the ablation, we assessed the relationship between the number of Gal+ cells or the double-positive neurons (Gal+ and cFos+) and various behavioural parameters. There was no correlation between the number of MI, total number of thrusts, mount duration, or other behavioural parameters and the Gal+ (Figure 4.10A, C, E, G, I) or the double-positive neurons (Figure 4.10 B, D, F, H, J), meaning that the magnitude of behavioural impairments is not explained only by the extent of ablation, but perhaps by other compensatory mechanisms discussed below. Taken together, our results indicate that the ablation of the lumbar Gal+ population leads to an increase in the latency to ejaculate and a significant disruption of the copulatory sequence, supporting a more complex involvement of the spinal cord in controlling sexual behaviour in mice.

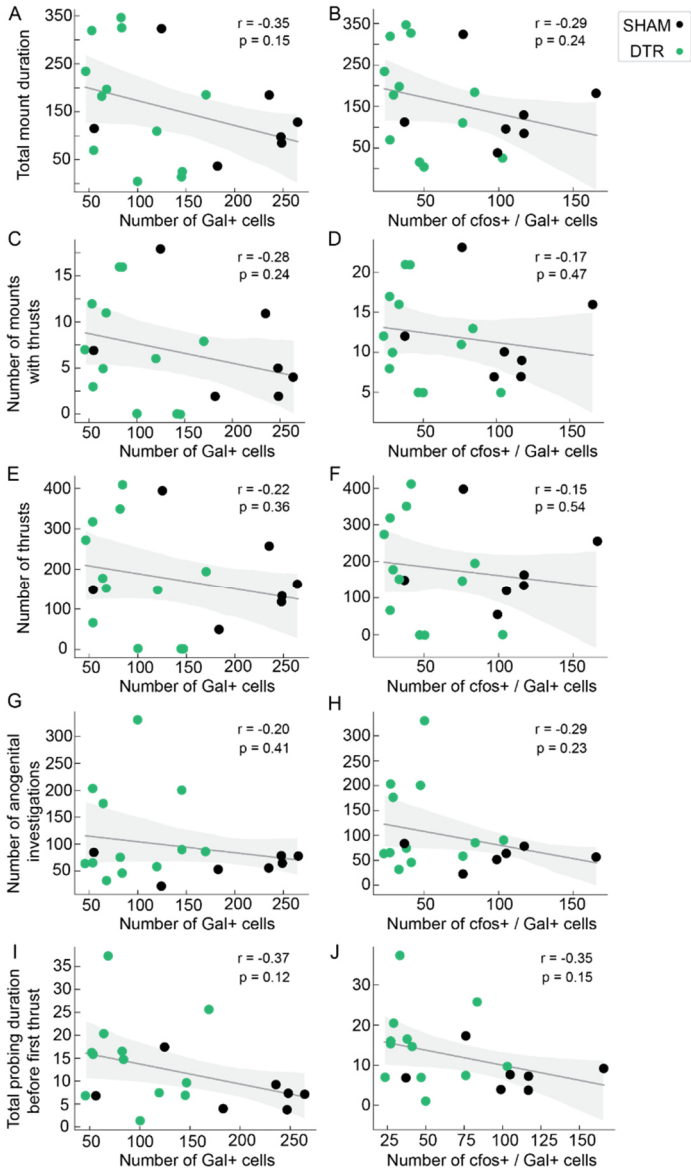

Figure 4.10 No correlation between sexual behaviour measures and amount of Gal+ cell ablation. (A) Total mount duration is plotted against the number of Gal+ cells in SHAM (black) and DTR animals (green). Every dot represents an individual animal. Note that there is no significant correlation between the Gal+ cell numbers and the total mount duration. (B) Total mount duration is plotted against the number of Gal+ and cFos+ cells in SHAM (black) and DTR animals (green). Every dot represents an individual animal. There is no correlation between the number of double positive cells (cFos+ and Gal+) and the total mount duration. (C) Same as A but for the number of mounts with thrusts. (D)

Same as B but for the number of mounts with thrusts. (E) Same as A but for the number of thrusts. (F) Same as B but for the number of thrusts. (G) Same as A but for the number of anogenital investigations. (H) Same as B but for the number of anogenital investigations. (I) Same as A but for the total probing duration before the first thrust. (J) Same as B but for the total probing duration before the first thrust.

4.3 Discussion

To have a deep understanding of animal behaviour is one of the most exciting and challenging aspects of neuroethology. Here, we have conducted a rigorous analysis of mice sexual behaviour, the role of Gal+ cells throughout different stages of the behaviour and how their ablation leads to strong changes in the copulatory sequence.

4.3.1 Gal+ cells are increasingly active with the progression of copulation

Using cFos, an immediate early gene and a proxy for neuronal activity (Krukoff, 1999), we performed a behaviour assay during which we showed that Gal+ cells are strongly activated with ejaculation in male mice. Surprisingly, we also found significantly higher cFos labelling with other components of sexual behaviour, namely when the male was aroused in the presence of a female, or when he performed thrusts but did not reach ejaculation, when compared to the male alone in a cage. Previous studies performed in rats, showed cFos signal in the SEG (equivalent to our Gal+ population) when males were allowed to intromit, and showed a significantly higher number of cFos-positive cells after one ejaculation, being further increased with a second ejaculation (Truitt et al., 2003). This goes in accordance with our findings that Gal+ cells in the mice are active

throughout sexual behaviour. However, to our knowledge, we are the first to describe the activation of the Gal+ population with sexual arousal (simply by the presence of a receptive female). One possible explanation for this is the potential involvement of the Gal+ cells and the BSM in erection (Schmidt & Schmidt, 1993), that may be triggered by arousal before any consummatory behaviour is performed.

4.3.2 Ablation of the lumbar Gal+ cells disrupts male mice sexual behaviour

Using a chemogenetic approach, based on DTR being expressed on Gal+ cells, we ablated these cells and assessed its effect on the copulatory sequence of mice sexual behaviour. Interestingly, and contrary to rat evidence (Truitt & Coolen, 2002), when this population of spinal Gal+ cells was eliminated, not only ejaculation was disrupted but also other components of sexual behaviour. From the 12 DTR animals, 3 were not able to ejaculate during the experiment length, even though they displayed other sexual behaviour components, namely mount attempts and mounts with probing. The remaining 9 animals were able to reach ejaculation but showed striking behavioural differences: the latency to ejaculation was greatly increased and the number and duration of mounts with probing was significantly higher. However, the number and duration of mounts with thrusting and the number of thrusting events was similar across animals. This suggests that the sensory input necessary to reach ejaculation is conserved and is not affected by the Gal+ cell ablation. In rats and humans, it as been described that sensory input caused by urethral distention and consequent urethral pressure increase is sufficient to induce ejaculatory like contractions in the BSM (Shafik & El-Sibai, 2000; Tanahashi et al., 2012). Reports in the rat show the connection between

the sensory pelvic innervation and the BSM-MNs, via the sensory branch of the pudendal nerve, through the dorsal penile nerve (Núñez et al., 1986; Pascual et al., 1992; Ueyama et al., 1987), which might be sufficient to relay the sensory information, without the action of Gal+ cells. Furthermore, denervation of sensory penile information, by severing the dorsal penile nerve, resulted in severe sexual impairments in rats, namely complete abolishment of ejaculation in most animals (Larsson & Sodersten, 1973), reinforcing the role of the sensory feedback in ejaculation. Another possibility for these behavioural differences, is that different subsets of Gal+ cell express distinct neuropeptides, like substance P, cholecystokinin, enkephalin or gastrin releasing peptide (Coolen et al., 2003; Kozyrev et al., 2012; Nicholas et al., 1999), in a partially non-overlapping fashion which may reflect their functional specialisation in terms of sensory processing. Additionally, even though our ablation is quite thorough, a small percentage of Gal+ cells was not affected, which may be sufficient to integrate the pelvic sensory input and drive ejaculation.

Besides the role of sensory relay, the spinal cord may also have redundant circuits to compensate for the loss of the Gal+ cells. Namely, the spinal circuits controlling the pelvic floor muscles and organs, which are responsible for emission and expulsion of sperm, micturition and defecation, may be shared (for instance their MNs are located in the Onuf's nucleus in the dorsomedial part of the ventral lumbar spinal cord, like the BSM-MNs) with common connections between the spinal and brain nuclei (Schellino et al., 2020). Connections between the sacral parasympathetic nuclei, that controls the function of the pelvic organs, and the Onuf's nucleus have been described for cats (Holstege & Tan, 1987; Nadelhaft et al., 1980) and rats (Hancock & Peveto, 1979), which may be a direct way to induce sperm emission without the Gal+ cells presence.

Holstege and Tan (1987), also discussed the possibility of Onuf's nucleus motor neurons being a special class of neurons that are not only somatic but also autonomic neurons, and therefore could be involved in controlling both muscle contractions and sperm emission, since they share properties with both groups (Hancock & Peveto, 1979). However, this has not been tested directly. Therefore, alternative pathways to induce ejaculation without the Gal+ cells presence may be obtained through all this spinal connectivity redundancy. Furthermore, there may be redundant pathways coming directly from the brain to control the BSM-MNs and the autonomic system, that we will discuss in the next Chapter.

4.4 Materials and Methods

4.4.1 Experimental model and subject details

All experimental procedures were carried out in strict accordance with the guidelines of the European Committee Council Directive and were approved by the Animal Care and Users Committee of the Champalimaud Neuroscience Program, the Portuguese National Authority for Animal Health (Direcção Geral de Veterinária; approval number 0421/000/000/2022) and by the local ethic committee of the University of Bordeaux and the French Agriculture and Forestry Ministry for handling animals (approval number 2016012716035720). For the cFos experiment and the DTR ablation, Gal-cre x TdTomato (*Mus musculus domesticus*, B6;129S6-Gt(ROSA)26Sortm9(CAG-tdTomato) Hze/J) male mice aged 3-6 months old were obtained from Jackson Laboratories. As a sexual stimuli, after ovariectomy and hormonal priming, C57BL6 female mice aged 3-6 months were used. All the animals were bred and maintained in our animal facility. All animals were weaned at 21 days and housed in

same-sex groups in stand-alone cages (1284L, Techniplast, 365 × 207 × 140 mm) with access to food and water *ad libitum*. Mice were maintained on an inverse 12:12 light/dark cycle and experiments were performed during the dark phase of the cycle, phase of higher animal activity. After initiation of sexual behaviour training or immediately after surgery, male mice were kept single-housed until the experiment was over.

4.4.2 Spinal cord stereotaxic viral injections and histology

Mice were anaesthetised with 3% isoflurane in oxygen and spinally fixed into a stereotaxic frame using adapted vertebrae clamps (Kopf, Tujunga, CA, USA). During surgery, anaesthesia was maintained using 1.5% isoflurane. Injection sites (lumbar segments 2/3) were targeted by using vertebral landmarks as described in (Harrison et al., 2013). Muscle and fat tissue were gently removed in order to get a better sight onto the spinal cord. The injection pipette was inserted in between the thoracic vertebrae T11 and T12 before having made a small puncture into the dura mater that allowed for better insertion of the injection pipette. Pulled capillaries (length 31/2 inches [9 cm]; inner diameter 0.53, outer diameter 1.14 mm; tip diameter 40 µm; DrummondScientific, Broomall, PA, USA) were used to inject the AAVs at 100 µm medial from the midline, at a depth of 750-850 µm from the spinal cord surface at a rate of 0.1 Hz with 2.3-4.6 nL per pulse. For the pAAV8-FLEX-DTR-GFP (N=12), 150-300 nL were injected either in one or two locations of the spinal cord. Before and after the pressure injection a waiting time of 10 min was kept. Afterwards, the pipette was retracted, eventual bleeding stopped and the skin sutured. Furthermore, as a control for the DTR experiment, sham injections were performed (N=7). Using the same method described above, the animals were anaesthetised and spinal clamped to a stereotaxic frame. After fat

and tissue removal to expose the vertebrae, a glass pipette without virus was lowered to the spinal cord at the Gal+ cells location. The pipette was kept inside the spinal cord for a total of 25 min, after which it was carefully removed and the animal was sutured. Analgesic (buprenorphine 0.1 mg/kg) was administered post surgery at all times. After sufficient time for viral expression (2 weeks) and behavioural experiments, animals were deeply anaesthetised and perfused transcardially with saline, followed by a cold 4% paraformaldehyde solution (PFA) in 0.01 mol/L PBS. Spinal cords were removed from the spine and kept for 1 h in 4% PFA before transferring them for another hour into 0.01 M PBS. Subsequently spinal cords were stored overnight in 30% sucrose in 0.01 M PBS, 0.1% azide in order to cryo-protect the tissue. Spinal cords were embedded in frozen section medium and frozen for half an hour at -80 °C in 2-methylbutane solution before mounting them in the cryostat. Spinal cord sections which did not undergo subsequent immunohistochemical staining were cut and mounted on a poly-lysine-coated glass slide at 50 µm, sections with post-hoc immunohistochemical staining were cut and mounted at 30 µm.

4.4.3 Nissl stain

The slides were washed 2 times in 0.01 M PBS to remove the excess of frozen section medium. After that the sections were rehydrated for 40 min in PBS 0.1 M, pH 7.2 (PBS 10x) and permeabilized for 10 min with 0.1% Triton-X (T9284-100ML, SigmaAldrich) in PBS 10x. The tissue was washed 2 times 5 min with PBS 10x before incubating them for 20 min with a 1:100 Neurotrace staining solution (in PBS 10x; (NeuroTrace™ 500/525 Green Fluorescent Nissl Stain, N21480, ThermoFisher Scientific; or NeuroTrace™ 530/615 Red Fluorescent Nissl Stain, N21482, ThermoFisher Scientific; or NeuroTrace™ 640/660 Deep-Red

Fluorescent Nissl Stain, ThermoFisher Scientific). Subsequently the tissue was washed with 0.1% Triton-X in PBS 10x for 10 min. After washing 2 times 5 min with PBS 10x, the slides were rinsed with distilled water, dried and coverslipped with Mowiol.

4.4.4 Immunohistochemistry

Immunohistochemical staining for the immediate early gene cFos deferred slightly from the procedure described in the previous chapters. Namely, after washing with PBS 0,01 M and PBS 10x, the sections were incubated in a different blocking solution (PBS 10x, 0.3% Triton X-100, 4% normal donkey serum, 1% bovine serum albumin) for 1 h at room temperature. The primary antibody (rabbit anti-cFos, Synaptic Systems, 226 003), diluted 1:500 in blocking solution was added for 2 overnights at 4 ºC. Afterwards, the sections were washed 3 times 5 min in PBS 10x, 0.3% Triton X-100, and the secondary antibody (Alexa Fluor 488 or 647, ThermoFisher Scientific) was added in blocking solution, diluted 1:500, for 2 h at room temperature. Finally, the sections were washed 3 times 5 min in PBS 10x, 0.3% Triton X-100, rinsed with distilled water, dried and coverslipped with Mowiol mounting medium. As described before, slides were also counterstained with Nissl. After the staining procedure, sections were washed 5 times 10 min with PBS 10x, rinsed with distilled water, dried and coverslipped with Mowiol mounting medium.

4.4.5 Behaviour

cFos experiments

Male Gal-cre x TdTomato mice were single-housed and trained in sexual behaviour, with a primed ovariectomised female, until ejaculation was reached in 3 sessions. After one week, the animals underwent a behavioural paradigm and were divided into three different groups: in the first group, animals were allowed to socially interact with a female for 10 min (Aroused, N=7), without performing mounts or intromissions. Note that the mice were prevented from mounting by putting the hand into the experimental arena thereby separating the mice. The second group of male mice performed five mounts with intromissions (5 Mounts, N=5), after which the female was removed and in the third group, the animals were allowed to reach ejaculation (Ejaculation, N=6). In another group of animals (Cage control) male mice were either alone in their home cages, without sexual encounters or female odours present (N=3), or had the same sexual training but were then alone in the clean behaving box for 10 min (N=3), in order to assess the baseline neuronal activity in the spinal cord (no differences in the cFos count was observed in these two control conditions). In the last group, animals (N=5) previously sexually trained, were allowed to interact with another male mouse (5 weeks old) for 10 min or until 10 attack bouts happened. After the behaviour session, the experimental mice were placed back in their home cages for 90 minutes to allow for sufficient cFos expression. Finally, the animals were deeply anaesthetised and perfused transcardially with saline, followed by a cold 4% PFA in 0.01 mol/L PBS. Spinal cords were removed from the spine and kept for 1 h in 4% PFA before transferring them for another hour into 0.01 M PBS. Subsequently spinal cords were stored overnight in 30% sucrose in 0.01 M PBS, 0.1% azide in order to cryo-protect the tissue.

Spinal cords were embedded in frozen section medium for half an hour at -80 °C in 2-methylbutane solution before mounting them in the cryostat. The spinal cords were sectioned at 30 µm for post-hoc immunohistochemical staining as described above.

DTR experiments

Male Gal-cre x TdTomato animals (2-3 months old) were single-housed and trained for sexual behaviour until ejaculation was reached once. After that, the animals were spinally injected with an AA8V-FLEX-DTR-GFP (N = 12) at the location of the Gal+ cells (allowing for the specific expression of the Diphtheria Toxin Receptor) or had a sham surgery (N = 7), as described above, and allowed to recover for 2 weeks. Afterwards, the animals underwent another round of sexual behaviour training to confirm that they were still reliably ejaculating. After this, the animals received an intraperitoneal injection of 50 ng/g (0.1 mL/10 g) of Diphtheria Toxin (DT, Sigma, D0564-1MG). One week after, the animals were transferred to an experimental box, where they had a 10 min habituation, after which a primed ovariectomised female was introduced. The animals were allowed to perform the full repertoire of sexual behaviour and after ejaculation was reached, or 90 min after female introduction passed when sexual behaviours were observed, the animals were returned to their homecage. If the animals did not initiate behaviour, the experiment was stopped after 30 min and the sexual experimental paradigm was repeated for two more weeks. In the final session, or after ejaculation, the animals were returned to their homecage and a 90 min interval was kept before perfusion, for cFos expression to occur. Finally, the animals were deeply anaesthetised, transcardially perfused and the spinal cords collected for histological processing as described above (cFos experiments).

Erection assessment in DTR experiment

To assess the effect of the Gal+ cells ablation on the erection of DTR animals, a set up with a glass at the bottom was used to observe the pelvic area movements on DTR and sham animals. The set up consists of a mirror at a 45 degrees angle below the experimental box and a glass floor, allowing for the recording of the side view and bottom view of the sexual encounter with the same camera. Male mice underwent the DTR experiments behavioural protocol explained above and had an additional experimental week where they were transferred for the glass set up and the pelvic movements were recorded while the animal performed sexual behaviour until ejaculation was reached. Afterwards, the animals were returned to their homecage and a 90 min interval was kept before perfusion, for cFos expression to occur. Finally, the animals were deeply anaesthetised, transcardially perfused and the spinal cords collected for histological processing as described above.

Ovariectomy and hormonal priming

All female mice (N=20) used as sexual stimuli were ovariectomised. Briefly, female mice were anaesthetised using 3% isoflurane in oxygen and placed into a mouth piece allowing for continuous isoflurane anaesthesia. After all reflexes were gone, an incision was made at the centre of the lower back. The skin was separated from the muscle towards both sides of the back. After that, on one side, levelled with the hindlimb, the ovary fat pad was located and a small incision was made in the muscle above this area. The ovary was gently pulled and the connection between the ovary and the uterus was cut using a cauterizer. The same procedure was repeated for the second ovary. Finally, the incision in the back was

sutured and the animal was allowed to fully recover on a heating pad. After two weeks of recovery, the animals underwent hormonal priming during which they received an oestrogen (1 mg/ml, Sigma E815 in sesame oil) injection 2 days prior to the sexual behaviour experiment and a progesterone (5 mg/ml, Sigma P0130 in sesame oil) injection 4h before the experiment was scheduled. Hormonal priming with oestrogen and progesterone was conducted before each experiment.

4.4.6 Quantification and Statistical Analysis

Histological analysis

After immunohistochemical labelling of cFos (as described above), the spinal cord sections were imaged using a Slide Scanner (Zeiss AxioScan.Z1, Zeiss Microscopy). The obtained images were processed using the Zen Software (Zen 2.6, Zeiss Microscopy), and tiff images of each channel (488 for the cFos, cy3 for the Gal-cre TdTomato cells and cy5 for the Nissl staining) were exported. These tiff files were, together with the corresponding image of the spinal segment from the mouse spinal cord atlas (Watson et al., 2009), opened in Photoshop (Adobe Photoshop, Adobe). Once the overlap between the spinal atlas outlines and the immunohistochemical tiff image was adjusted, the cells present in laminae X (around the central canal and the location of the Gal+ cells) of the spinal cord were manually counted by placing dots on each cell. This counting procedure was done for every other slide given the thickness of the slices and thus to prevent double counting. The manual counting procedure was done for both channels, the cFos in green and TdTomato in red. Custom written Matlab code was finally used to count the dots and identify overlaps between the two channels. Counting of cFos and Gal-cre x

TdTomato positive cells was done blindly. The experimenter that performed the counting was blind to the paradigm to prevent eventual bias. Moreover different experimenters were involved in the counting: Ana Rita Mendes counted the animals for the cFos experiment, except for 3 cage alone animals that were counted by Constanze Lenschow; Liliana Ferreira counted the animals for the Diphtheria Toxin experiment. For the cell normalisation, we divided the number of cFos-positive and Gal-cre x TdTomato-positive cells by the total amount of Gal-cre x TdTomato positive cells.

Behavioural Analysis

The DTR and cFos behavioural experiments were carefully recorded using two point grey cameras (Teledyne FLIR), at 60 frames per second. The cameras acquired a top and front video of the cage and were controlled using a bonsai script (Bonsai Visual Reactive Programming). Afterwards, the videos were analysed using Python Video Annotator (developed at the Champalimaud Foundation). A wide range of behaviours was annotated, namely: sniffing of the anogenital area of the female; mount attempts (when the male was not able to perform intromissions) mounts with probing (shallow pelvic movements when the male is trying to intromit but still has not inserted the penis); mounts with intra-vaginal thrustings; intra-vaginal thurstings (when the male successful inserted the penis in the female's vagina); and finally ejaculation (time between the beginning of shivering and the moment the male dismounted the female). The duration, in frames, for each behaviour was then aligned to the camera timestamps, acquired during video recording. Analysis of behavioural timestamp data was performed using a python script in Spyder 3.3.6 (Python).

Statistical Analysis

Statistical analysis was performed with homemade code in Matlab and Python (scipy and statsmodels). All error ranges represent standard error of the mean. For two-sample comparisons of a single variable, Student's t test was used, unless in cases when the underlying distributions were non-Gaussian (Shapiro-Wilk test, $p<0.05$), where a two-tailed Mann-Whitney-U Test was performed. When multiple variables were compared, a Kruskal Wallis test or a Wilcoxon-Signed-Rank test were used since the data did not follow a Gaussian distribution. Probabilities of the null hypothesis $p<0.05$ were judged to be statistically significant. Elements of violin plots: centre line, median; box limits, upper (75) and lower (25) quartiles; and whiskers, 1.5x interquartile range.

To estimate the inter-thrust interval (ITI) versus mount progression, the thrust number was divided by the total number of thrusts in the mount, what we call mount progression. Then data from all the mounts and all the sessions from the different groups was pulled together and a non-parametric kernel regression was performed. The shadow region corresponds to the standard deviation.

4.5 Author Contributions

A.R.M., C.L. and S.Q.L designed the experiments and the analysis. A.R.M. performed the spinal cord injections and the ovariectomies. A.R.M. performed the cFos and DTR behavioural experiments. A.R.M. and L.F. performed immunohistochemistry and histological image acquisition. A.R.M and L.F performed the histological analysis (with the help of C.L for the cFos experiment). A.R.M and B.L performed the behavioural analysis.

5 General Discussion

5.1 Brief summary of main findings

In mammals, pre-copulatory and copulatory actions orchestrated by the brain are thought to bring the male to the “ejaculatory threshold”, such that penile insertion in the female’s vagina triggers ejaculation and sperm ejection, a reflex controlled by spinal cord circuitry. This assumption implies that the brain plays no role in the ejaculatory reflex (other than inhibiting it until the threshold is reached) and that the activity of the spinal network is inconsequential to the orchestration of copulatory behaviour (serving only as a relay of ascending sensory input). However, this division of labour between the brain and the spinal cord has been repeatedly challenged, particularly by the existence of neurological disorders suggesting that spinal neurons are integral to the control system, with central and effector players in continuous information exchange (Giuliano & Clement, 2005; Pfaus, 1999). This thesis provides new evidence supporting the involvement of the spinal cord in controlling male mice’s internal state and copulation, rather than merely relaying penile sensory information and controlling ejaculation.

We began by using the BSM as an entry point into the circuit and traced the MNs controlling this muscle involved in sperm expulsion and the presynaptic partners connected to the BSM-MNs. We described these presynaptic partners as being a group of Gal+ cells located in the lumbar region of the spinal cord, more specifically around the central canal in the L2 and L3 segments. We further described the role of the Gal+ cells in the control of ejaculation and sexual behaviour, namely through their electrical and optogenetic manipulation, by assessing their role in behaving animals and finally by ablating them and studying the differences in male mice sexual behaviour.

Interestingly, our results argue against the current idea that the spinal circuitry is not involved in the control of copulatory sequences, behaving as a bystander until the arousal threshold is reached and ejaculation takes place, triggering the spinal circuits controlling the motor and autonomic systems. Our data supports an alternative model, where the spinal circuit controlling the BSM has a prominent role in the organisation of copulation and in the arousal build up. This model is not only supported by the fact that the genetic ablation of Gal+ cells, that are functionally connected to BSM-MNs and are the recipients of genital input, led to profound disruptions in the copulatory behaviour, but also because BSM activity, induced by the activation of Gal+ neurons in spinalised animals, was dependent on the internal state of the animal.

5.2 Anatomical description of the spinal circuit controlling the BSM and ejaculation

Using the penile muscle involved in sperm expulsion, the BSM, as a point of entry, we have characterised a microcircuit in the lumbar spinal cord of male mice consisting of motor neurons innervating this muscle and a population of Gal+ neurons that is monosynaptically connected to the BSM-MNs. Interestingly, we observed that the BSM-MNs were more widely distributed than previously described, but with similar total number of BSM-MNs and location within the spinal segment, namely the dorsomedial ventral horn (Sengelaub & Forger, 2008; Wagner & Clemens, 1989). Moreover, we provide strong anatomical evidence for a reciprocal connection between the Gal+ neurons and autonomic nuclei, as well as the ischiocavernosus MNs. We believe to be the first ones to show this connection between the Gal+ cells and the autonomic nervous system in mice, and to show this potential reciprocal connection that could

coordinate sperm emission. Also, these anatomical tracings suggest a potential role of the Gal+ population not only in emission but also in erection (El-Sakka & Lue, 2004; Kolbeck & Steers, 1992; Schmidt & Schmidt, 1993). Namely, the output to the ischiocavernosus MNs might be important for the regulation of penile detumescence, which must be finely regulated at the time of ejaculation, as pressure has to momentarily decrease for expulsion to take place (El-Sakka & Lue, 2004).

To functionally prove the monosynaptic connection between the BSM-MNs and the Gal+ cells we performed *in vitro* whole cell patch clamp recordings in BSM-MNs of mice pups (P0-P4) using a Gal-cre line crossed with ChR2. By activating the ChR2-positive terminals of the Gal+ cells we triggered light specific EPSPs in BSM-MNs but not other MNs in the ventral horn pointing once more to the functional monosynaptic connection between Gal+ cells and BSM-MNs. We observed a rather long onset of light induced EPSPs, that can be attributed to the non existence of myelin in the spinal cord of small pups and hence neural transmission is delayed (Susuki, 2010). Moreover, it is worth noting that these experiments were not performed in sexually mature adult animals. Keeping adult principal MNs alive during the preparation of acute spinal cord slices is experimentally challenging due to the slicing of their massive dendritic branching (Burke & Rudomin, 1977). However, a protocol to obtain viable spinal ex vivo preparations has been recently reported and should be the focus of future research (Liu et al., 2023). Taking all of this into account, the main neuronal players that seem to be controlling ejaculation in male mice are the BSM-MNs and the Gal+ cells that control their activity.

The Gal+ cells population described in our study shares a similar molecular profile with the previously identified rat SEG (Coolen et al.,

2003; Kozyrev et al., 2012; Nicholas et al., 1999), despite some differences in the spinal segments where the Gal+ cells are located (L2/L3 segments versus L3/L4 in the rat (Truitt & Coolen, 2002)). Several lines of evidence supported labelling the rat Gal+ population as the SEG. While electrical stimulation at the location of the putative SEG evokes ejaculation in anaesthetised rats (Borgdorff et al., 2008), its ablation results in complete disruption of the ejaculatory reflex without affecting copulatory behaviour (Truitt & Coolen, 2002). Furthermore, the SEG seems to be anatomically connected to the sensory branch of the pudendal nerve, indicating it received genital information (McKenna & Nadelhaft, 1986; Ueyama et al., 1987). However, to the best of our knowledge, the functional connectivity between the rat SEG and BSM-MNs has never been established. Our study, using a dual and genetic-based approach combined with *in vitro* whole-cell patch-clamp recordings of BSM-MNs while specifically activating Gal+ axons, is the first to provide data unequivocally establishing a functional monosynaptic connection between Gal+ cells and BSM-MNs. Despite the molecular similarities between the Gal+ neurons described in this study and the rat SEG, our results indicate that the properties of the mouse spinal network may differ significantly from its rat counterpart.

First, electrically induced ejaculation in anaesthetised rats produces similar motor and physiological activity patterns regardless of an intact connection to the brain (which we reproduced in our study), while penile stimulation can activate ejaculation only in anaesthetised spinalized rats (Pescatori et al., 1993). These findings suggest the presence of descending inhibition that gates sensory input from the penis and that the rat SEG can function independently of the brain once this inhibition is removed. In contrast, in mice, pronounced BSM activity was only triggered when the Gal+ cells were electrically or optogenetically activated in a

spinalized preparation, but not if the connection to the brain was intact. Moreover, penile stimulation did not trigger a full ejaculation in our experiments. Therefore, our results support a model where, at least in mice, the Gal+ population and the incoming sensory input is kept under a substantial inhibition from the brain, likely from the ipsilateral paragigantocellular nucleus (Normandin & Murphy, 2011), until the ejaculatory threshold is reached.

5.3 The functional role of Gal+ cells in mice ejaculation and sexual behaviour

After describing the anatomical aspect of this spinal circuit we wanted to further understand its functional role. Either through penile sensory stimulation or through direct stimulation of Gal+ cells in an anaesthetised preparation, we started to dissect the role of this population in the induction of an ejaculatory process. Even though we could observe robust EMG activity in the BSM with the stimulation of this spinal circuit, we were intrigued by our inability to trigger emission in male mice, despite demonstrating an anatomical connection to autonomic centres, the main players in the emission process (Kolbeck & Steers, 1992), in contrast to what was observed in the rat. While we cannot rule out the possibility that our failure to trigger emission was due to suboptimal stimulation parameters, we propose that these results are biologically plausible and may reflect species differences in the regulation of ejaculation.

Even though we could not induce emission through artificial stimulation of the spinal cord location containing the Gal+ cells or by directly activating Gal+ neurons, our EMG recordings in sexually behaving animals showed that artificially-induced BSM activities closely resembled natural BSM

activity, further supporting that our stimulation parameters elicited activity within physiological ranges and that Gal+ stimulation alone is insufficient to induce emission.

Mouse copulation is characterised by repeated vaginal thrusting leading to a single ejaculation, a copulatory sequence more similar to humans but quite different from rats, which have multiple ejaculations dependent on the execution of multiple individual penile insertions (Dewsbury, 1972). This suggests that the build up to the ejaculatory threshold in rats may differ from mice and humans, as it might be independent or much less influenced by the integration of genital sensory input, while in the mouse, sensory integration of multiple thrusts is crucial. While rat data suggest that descending inhibition operates primarily at the level of the SEG, our data points for the descending inhibition to modulate Gal+ neurons and the incoming sensory input to them in mice.

While anatomically the circuitry seems to be similar between rats and mice, the functional logic may be fundamentally different. The rat spinal circuitry appears to function as a true “spinal reflex arc”, capable of driving ejaculation with a sensory stimulus if disconnected from the brain (Borgdorff et al., 2008). In contrast, the mouse circuit does not qualify as a proper reflex since the sensory input alone cannot drive emission or full BSM activity, supporting a constant dialogue between the brain and the spinal cord, for the build up of sexual excitation and ejaculation. Future comparative experimental efforts are needed to reveal the operational logic of these circuits in species with different copulatory strategies. For example, it remains to be determined if a “true central pattern generator” for ejaculation exists in the mouse and how the Gal+ neurons we have identified connect to such a network. However, the discrepancies outlined

in this study may simply result from different modus operandi, the product of different evolutionary trajectories.

When analysing the role of the Gal+ cells in sexually behaving animals, we observed an unexpected gradual increase in the activity of the Gal+ population during sex and when interacting with another male, suggesting that the activity of these neurons may be related to the arousal level of the individual. This contrasts with previous studies in rats, which showed that Gal+ cells are only active after an ejaculation (Truitt et al., 2003).

Furthermore, and to our surprise, repeated electrical stimulation of the Gal+ cells was accompanied by a marked decrease in BSM activity, which was not due to a deterioration of the preparation. Moreover, if male mice were allowed to have sex and ejaculate just before the electric stimulation experiment, BSM activity was significantly lower and resembled the activity observed after multiple rounds of stimulation. These results indicate that Gal+ cells are recruited not only during ejaculation but also in response to arousal and sexual activity. This supports the notion of a continuous dialogue between the spinal cord and the rest of the body and a possible prominent role of the spinal cord in the control of the refractory period (Turley & Rowland, 2013), contrary to what is currently hypothesised. Interestingly, direct optogenetic activation of the BSM-MNs reliably led to BSM activation, regardless of how many times we would stimulate the MNs. This points to a process mainly dependent on Gal+ cells or the connection between these cells and the BSM-MNs, that may set a mechanism into place to depress the spinal cord and BSM activity, setting the refractory period.

Lastly, chemogenetic ablation of Gal+ cells caused a disruption in male copulatory behaviour. Interestingly, and in contrast to the rat SEG, whose ablation led to a complete abolishment of ejaculation while leaving other

copulatory patterns intact (Truitt & Coolen, 2002), only 3 out of 12 animals in our study failed to ejaculate. However, since the session was artificially interrupted after a certain time limit, it is unknown if they would have eventually ejaculated given more time. Also, and contrary to the rat, we observed altered sexual behaviour in all animals, including increased latency to ejaculate, more mounts with probing, and longer durations of probing, suggesting that immediate sensory penile feedback is partially disrupted when the Gal+ cells are ablated.

These results raise two immediate questions: how can animals still ejaculate if the Gal+ cells that contact the BSM-MNs are ablated, and how and where is the penile sensory feedback processed to reach ejaculation? The first question may be explained by a small percentage of Gal+ cells not being ablated, which could suffice to integrate pelvic sensory input and drive ejaculation. Additionally, redundant spinal circuits may compensate for the loss of Gal+ cells. Namely, circuits controlling pelvic floor muscles and organs, responsible for sexual behaviour, micturition and defecation, share common connections between spinal cord and brain nuclei (Schellino et al., 2020). For instance, connections between the sacral parasympathetic nuclei that control pelvic organ function (i.e. emission), and the BSM-MN nucleus have been described in cats (Holstege & Tan, 1987; Nadelhaft et al., 1980) and rats (Hancock & Peveto, 1979). Holstege and Tan (1987) hypothesised that BSM-MNs are a special class of neurons with both somatic and autonomic functions, capable of controlling both processes (Holstege & Tan, 1987).

Moreover, direct brain spinal projections, namely to the BSM-MNs, may drive sperm expulsion independently of Gal+ cells. Anatomical evidence indicates a direct connection between the hypothalamic PVN and the BSM-MNs in cats (Holstege & Tan, 1987) and rats (Argiolas & Melis, 2005;

de Groat, 2016). This pathway appears to facilitate erection, which in turn regulates rat sexual behaviour in general (Argiolas & Melis, 2004). Additionally, in rats, ejaculation can be facilitated by an oxytocinergic PVN projection onto SEG cells (Oti et al., 2021). Projections from the Barrington's nucleus, also known as the pontine micturition centre, connect to pelvic-related nuclei in the spinal cord (in rats (Nuding & Nadelhaft, 1998), cats (Holstege et al., 1986) and humans (Huynh et al., 2013)), and electrical stimulation of the medial-lateral areas induced emission and expulsion-like responses, respectively (Holstege et al., 1986). The brainstem, namely the paragigantocellular reticular nucleus has been shown in the rat (Marson & McKenna, 1990) and cat (Holstege & Tan, 1987) to send direct projections to the lumbosacral spinal cord, namely to the location of the pelvic motor and parasympathetic neurons. These are thought to be serotonergic inhibitory projections that control ejaculation by direct contact with the pelvic motor neurons of the pudendal nerve, since lesion of this brain nuclei increased the display of sexual behaviours (Marson et al., 1992; Marson & McKenna, 1990). Finally, it is also possible that direct projections to the brain from the dorsal penile nerve are the ones integrating the pelvic stimulation and consequently driving behaviour (Yanagimoto et al., 1996). Therefore, the brain connectivity with the spinal cord and peripheral nervous system may be sufficient to overcome the Gal+ cells and drive ejaculation.

Regarding the sensory relay from the pelvic area to the spinal cord and brain, studies in rats and humans showed that pressure increase in the prostatic urethra caused by the arrival of sperm and seminal fluid at the time of emission is sufficient to induce ejaculatory-like contractions in the BSM (Shafik & El-Sibai, 2000; Tanahashi et al., 2012). Rat dorsal penile nerve to BSM-MNs connectivity has been described (Núñez et al., 1986; Pascual et al., 1992; Ueyama et al., 1987) and might be sufficient to relay

sensory information, without the Gal+ neurons in our experiments. Finally, Qi *et al.* (2024) described Krause corpuscles as relayers of genital sensory information in mice, and their manipulation impacted sexual behaviour, reinforcing the idea that sensory feedback may be necessary to sustain copulation and ejaculation (Qi et al., 2024).

As for the second question, regarding how the penile sensory feedback is processed to reach ejaculation, it remains unclear where arousal is controlled and how sensory input impinges on such circuits. But our results point towards an involvement of the spinal network. In summary, we have identified a cluster of Gal+ cells in the lumbar spinal cord of mice that are directly connected to BSM-MNs and that seem to be involved in the integration of sensory signals during copulation and the male's internal state, thereby taking a more central and intricate involvement in the control of mice copulatory behaviour than a simple reflex arc.

5.4 Concluding Remarks

This thesis is the first to describe the spinal neuronal circuits controlling ejaculation and sexual behaviour in male mice. We believe to have uncovered the main neurons involved in the control of the BSM and consequently ejaculation. We also uncovered that this spinal circuit may be involved in more than just the ejaculatory reflex, as previously believed. We show that the Gal+ cells can integrate external signals (receiving direct sensory input from the pelvic area) and the internal state of the animal. Their activation is dependent on the sexual satiety state and repeated stimulation induces such satiety. Furthermore, Gal+ cells are active throughout the several phases of copulation and their ablation strongly impacts the copulatory sequence.

Therefore, we have unravelled a key circuit controlling sexual behaviour in mice. Despite building upon several years of research of the ejaculatory modulation in rats (Marson & Carson, 1999; Marson & McKenna, 1996; Truitt & Coolen, 2002), we believe that our results in mice represent an important contribution to understanding sexual behaviour and copulation. Not only mice have more genetic and experimental tools available, but they also have a sexual behaviour repertoire closer to humans, which makes them an extremely relevant model to better understand the basic circuitry that controls copulation and ejaculation.

This work already sheds some light on said circuits, but a lot is still to uncover. Namely, the connection between this circuitry and the brain, both how it sends input of when ejaculation should happen, and also how it receives the brain signals to control more complex copulatory sequences. We did not comprehensively address the role of the autonomic nervous system in this circuitry. It is important to understand such a role since it may be the key to uncover the emission step in the ejaculatory process and the timing for its occurrence. Finally, Gal+ cells may also be involved in other behaviours that rely on the pelvic floor, like micturition or defecation, therefore it is important to further understand the role of these cells in a more holistic approach. We believe that this work sets the foundation to study in more depth the spinal control of sexual behaviour and it should be seen as an open gate to further explore the role of the spinal cord in complex animal behaviours.

6 References

Adkins-Regan, E. (1999). Biological Exuberance: Animal Homosexuality and Natural Diversity. *BioScience*, 49(11), 926.

Agmo, A. (1997). Male rat sexual behavior. *Brain Research Protocols*, 1, 203–209. www.diva.nlrnoldusr

Allard, J., & Edmunds, N. J. (2008). Reflex penile erection in anesthetized mice: an exploratory study. *Neuroscience*, 155(1), 283–290. https://doi.org/10.1016/j.neuroscience.2008.05.027

Allard, J., Truitt, W. A., McKenna, K. E., & Coolen, L. M. (2005). Spinal cord control of ejaculation. *World Journal of Urology*, 23(2), 119–126. https://doi.org/10.1007/s00345-004-0494-9

Althof, S. E. (2006). Prevalence, characteristics and implications of premature ejaculation/rapid ejaculation. *In Journal of Urology*, Vol. 175(3), 842–848. https://doi.org/10.1016/S0022-5347(05)00341-1

Argiolas, A., & Melis, M. R. (2004). The role of oxytocin and the paraventricular nucleus in the sexual behaviour of male mammals. *Physiology and Behavior*, 83(2), 309–317. https://doi.org/10.1016/j.physbeh.2004.08.019

Argiolas, A., & Melis, M. R. (2005). Central control of penile erection: Role of the paraventricular nucleus of the hypothalamus. *Progress in Neurobiology*, 76(1), 1–21. https://doi.org/10.1016/j.pneurobio.2005.06.002

Asaba, A., Osakada, T., Touhara, K., Kato, M., Mogi, K., & Kikusui, T. (2017). Male mice ultrasonic vocalizations enhance female

sexual approach and hypothalamic kisspeptin neuron activity. *Hormones and Behavior*, 94, 53–60. https://doi.org/10.1016/j.yhbeh.2017.06.006

Azim, E., Jiang, J., Alstermark, B., & Jessell, T. M. (2014). Skilled reaching relies on a V2a propriospinal internal copy circuit. *Nature*, 508, 357–363. https://doi.org/10.1038/nature13021

Balcombe, J. (2009). Animal pleasure and its moral significance. *Applied Animal Behaviour Science*, 118(3–4), 208–216. https://doi.org/10.1016/j.applanim.2009.02.012

Baron, R., & Janig, W. (1991). Afferent and sympathetic neurons projecting into lumbar visceral nerves of the male rat. *Journal of Comparative Neurology*, 314(3), 429–436. https://doi.org/10.1002/cne.903140302

Bermant, G. (1964). Effects of single and multiple enforced intercopulatory intervals on the sexual behavior of male rats. *Journal of Comparative and Physiological Psychology*, 57(3), 398–403.

Blumenthal, S. A., & Young, L. J. (2023). The neurobiology of love and pair bonding from human and animal perspectives. *Biology*, 12(844), 1–23. https://doi.org/10.3390/biology12060844

Boldogkői, Z., Balint, K., Awatramani, G. B., Balya, D., Busskamp, V., Viney, T. J., Lagali, P. S., Duebel, J., Pásti, E., Tombácz, D., Tóth, J. S., Takács, I. F., Scherf, B. G., & Roska, B. (2009). Genetically timed, activity-sensor and rainbow transsynaptic viral

tools. *Nature Methods*, 6(2), 127–130. https://doi.org/10.1038/nmeth.1292

Borgdorff, A. J., Bernabé, J., Denys, P., Alexandre, L., & Giuliano, F. (2008). Ejaculation elicited by microstimulation of lumbar spinothalamic neurons. *European Urology*, 54(2), 449–456. https://doi.org/10.1016/j.eururo.2008.03.043

Borgdorff, A. J., Rössler, A. S., Clément, P., Bernabé, J., Alexandre, L., & Giuliano, F. (2009). Differences in the spinal command of ejaculation in rapid ejaculating rats. *Journal of Sexual Medicine*, 6(8), 2197–2205. https://doi.org/10.1111/j.1743-6109.2009.01308.x

Boyden, E. S., Zhang, F., Bamberg, E., Nagel, G., & Deisseroth, K. (2005). Millisecond-timescale, genetically targeted optical control of neural activity. *Nature Neuroscience*, 8(9), 1263–1268. https://doi.org/10.1038/nn1525

Brackett, N. L., Iuvone, P. M., & Edwards, D. A. (1986). Midbrain lesions, dopamine and male sexual behavior. *Behavioural Brain Research*, 20, 231–240.

Burke, R., & Rudomin, P. (1977). Spinal neurons and synapses. In *Handbook of physiology*: Vol. I (pp. 877–944). American Physiology Society.

Carro-Juárez, M., & Rodríguez-Manzo, G. (2000). Sensory and motor aspects of the coital reflex in the spinal male rat. *Behavioural Brain Research*, 108, 97–103. www.elsevier.com/locate/bbr

Carro-Juárez, M., & Rodríguez-Manzo, G. (2005). Role of genital sensory information in the control of the functioning of the spinal generator for ejaculation. *International Journal of Impotence Research*, 17(2), 114–120. https://doi.org/10.1038/sj.ijir.3901277

Carro-Juárez, M., & Rodríguez-Manzo, G. (2008). The spinal pattern generator for ejaculation. *Brain Research Reviews*, 58(1), 106–120. https://doi.org/10.1016/j.brainresrev.2007.12.002

Carson, C., & Gunn, K. (2006). Premature ejaculation: definition and prevalence. *International Journal of Impotence Research*, 18, S5–S13. https://doi.org/10.1038/sj.ijir.3901507

Chen, P., & Hong, W. (2018). Neural circuit mechanisms of social behavior. *Neuron*, 98(1), 16–30. https://doi.org/10.1016/j.neuron.2018.02.026

Chung, B., Zia, M., Thomas, K. A., Michaels, J. A., Jacob, A., Pack, A., Williams, M. J., Nagapudi, K., Teng, L. H., Arrambide, E., Ouellette, L., Oey, N., Gibbs, R., Anschutz, P., Lu, J., Wu, Y., Kashefi, M., Oya, T., Ke, R., … Sober, S. J. (2023). Myomatrix arrays for high-definition muscle recording. *ELife*, 1–41. https://doi.org/https://doi.org/10.7554/eLife.88551.2

Chéhensse, C., Facchinetti, P., Bahrami, S., Andrey, P., Soler, J.-M., Chrétien, F., Bernabé, J., Clément, P., Denys, P., & Giuliano, F. (2017). Human spinal ejaculation generator. *Annals of Neurology*, 81(1), 35–45. https://doi.org/10.1002/ana.24819

Clarac, F., Pearlstein, E., Pflieger, J. F., & Vinay, L. (2004). The in vitro neonatal rat spinal cord preparation: a new insight into mammalian locomotor mechanisms. *Journal of Comparative Physiology*, 190(5), 343–357. https://doi.org/10.1007/s00359-004-0499-2

Clement, P., & Giuliano, F. (2016). Physiology and pharmacology of ejaculation. *Basic & Clinical Pharmacology & Toxicology*, 119, 18–25. https://doi.org/10.1111/bcpt.12546

Coolen, L. M., Allard, J., Truitt, W. A., & McKenna, K. E. (2004). Central regulation of ejaculation. *Physiology & Behavior*, 83(2), 203–215. https://doi.org/10.1016/j.physbeh.2004.08.023

Coolen, L. M., Veening, J. G., Petersen, D. W., & Shipley, M. T. (2003). Parvocellular subparafascicular thalamic nucleus in the rat: anatomical and functional compartmentalization. *Journal of Comparative Neurology*, 463(2), 117–131. https://doi.org/10.1002/cne.10740

Coolen, L. M., Veening, J. G., Wells, A. B., & Shipley, M. T. (2003). Afferent connections of the parvocellular subparafascicular thalamic nucleus in the rat: evidence for functional subdivisions. *Journal of Comparative Neurology*, 463(2), 132–156. https://doi.org/10.1002/cne.10739

Corona, G., Jannini, E. A., Vignozzi, L., Rastrelli, G., & Maggi, M. (2012). The hormonal control of ejaculation. *Nature Reviews Urology*, 9(9), 508–519. https://doi.org/10.1038/nrurol.2012.147

de Groat, W. C. (2016). Autonomic nervous system: central urogenital control. In *Reference Collection in Neuroscience and Biobehavioral Psychology*. Elsevier. https://doi.org/10.1016/B978-0-12-809324-5.01816-2

Dewsbury, D. A. (1969). Copulatory behaviour of rats (Rattus Norvegicus) as a function of prior copulatory experience. *Animal Behaviour*, 17, 217–223.

Dewsbury, D. A. (1972). Patterns of copulatory behavior in male mammals. *The Quarterly Review of Biology*, 47(1), 1–33. http://www.journals.uchicago.edu/t-and-c

Dewsbury, D. A. (1975). Diversity and adaptation in rodent copulatory behavior. *Science*, 190(4218), 947–954. https://doi.org/10.1126/science.1188377

Dobberfuhl, A. D., Oti, T., Sakamoto, H., & Marson, L. (2014). Identification of CNS neurons innervating the levator ani and ventral bulbospongiosus muscles in male rats. *Journal of Sexual Medicine*, 11(3), 664–677. https://doi.org/10.1111/jsm.12418

Dulac, C., & Wagner, S. (2006). Genetic analysis of brain circuits underlying pheromone signaling. *Annual Review of Genetics*, 40, 449–467.
https://doi.org/10.1146/annurev.genet.39.073003.093937

Dulac, C., & Wagner, S. (2006). Genetic analysis of brain circuits underlying pheromone signaling. *In Annual Review of Genetics*, 40, 449–467.

https://doi.org/10.1146/annurev.genet.39.073003.093937

El-Sakka, A. I., & Lue, T. F. (2004). Physiology of penile erection. *The Scientific World Journal*, 4, 128–134. https://doi.org/10.1100/tsw.2004.58

Elmore, L. A., & Sachs, B. D. (1988). Role of the bulbospongiosus muscles in sexual behavior and fertility in the house mouse. *Physiology & Behavior*, 44(1), 125–129. https://doi.org/10.1016/0031-9384(88)90355-1

Facchinetti, P., Giuliano, F., Laurin, M., Bernabé, J., & Clément, P. (2014). Direct brain projections onto the spinal generator of ejaculation in the rat. *Neuroscience*, 272, 207–216. https://doi.org/10.1016/j.neuroscience.2014.04.064

Falgairolle, M., & O'Donovan, M. J. (2019). Feedback regulation of locomotion by motoneurons in the vertebrate spinal cord. *Current Opinion in Physiology*, 8, 50–55. https://doi.org/10.1016/j.cophys.2018.12.009

Friese, A., Kaltschmidt, J. A., Ladle, D. R., Sigrist, M., Jessell, T. M., & Arber, S. (2009). Gamma and alpha motor neurons distinguished by expression of transcription factor Err3. *PNAS*, 106(32), 13588–13593.

Georgiadis, J. R., Kringelbach, M. L., & Pfaus, J. G. (2012). Sex for fun: a synthesis of human and animal neurobiology. *Nature Reviews Urology*, 9(9), 486–498. https://doi.org/10.1038/nrurol.2012.151

Gerendai, I., Tóth, I. E., Boldogkoi, Z., Medveczky, I., & Halász, B. (2000). Central nervous system structures labelled from the testis using the transsynaptic viral tracing technique. *Journal of Neuroendocrinology*, 12(11), 1087–1095. https://doi.org/10.1046/j.1365-2826.2000.00560.x

Gerendai, I., Wiesel, O., Tóth, I. E., Boldogkõi, Z., Rusvai, M., & Halász, B. (2003). Identification of neurons of the brain and spinal cord involved in the innervation of the ductus deferens using the viral tracing method. *International Journal of Andrology*, 26(2), 91–100. https://doi.org/10.1046/j.1365-2605.2003.00392.x

Giuliano, F., & Clement, P. (2005). Neuroanatomy and physiology of ejaculation. *Annual Review of Sex Research*, 16(1), 190–216. http://www.ncbi.nlm.nih.gov/pubmed/16913292

Giuliano, F., Bernabé, J., Brown, K., Droupy, S., Benoit, G., & Rampin, O. (1997). Erectile response to hypothalamic stimulation in rats: role of peripheral nerves. *American Journal of Physiology - Regulatory Integrative and Comparative Physiology*, 273, 1990–1997. https://doi.org/10.1152/ajpregu.1997.273.6.r1990

Gong, S., Doughty, M., Harbaugh, C. R., Cummins, A., Hatten, M. E., Heintz, N., & Gerfen, C. R. (2007). Targeting Cre recombinase to specific neuron populations with bacterial artificial chromosome constructs. *Journal of Neuroscience*, 27(37), 9817–9823. https://doi.org/10.1523/JNEUROSCI.2707-07.2007

Gong, S., Zheng, C., Doughty, M. L., Losos, K., Didkovsky, N., Schambra, U. B., Nowak, N. J., Joyner, A., Leblanc, G., Hatten, M.

E., & Heintz, N. (2003). A gene expression atlas of the central nervous system based on bacterial artificial chromosomes. *Nature*, 425(6961), 917–925. https://doi.org/10.1038/nature02033

Gréco, B., Edwards, D. A., Michael, R. P., & Clancy, A. N. (1996). Androgen receptor immunoreactivity and mating-induced Fos expression in forebrain and midbrain structures in the male rat. *Neuroscience*, 75(1), 161–171.

Hancock, M. B., & Peveto, C. A. (1979). A preganglionic autonomic nucleus in the dorsal gray commissure of the lumbar spinal cord of the rat. *Journal of Comparative Neurology*, 183(1), 65–72. https://doi.org/10.1002/cne.901830106

Hancock, M. B., & Peveto, C. A. (1979). Preganglionic neurons in the sacral spinal cord of the rat: an HRP study. *Neuroscience Letters*, 11(1), 1–5. https://doi.org/10.1016/0304-3940(79)90046-6

Harrison, M., O'Brien, A., Adams, L., Cowin, G., Ruitenberg, M. J., Sengul, G., & Watson, C. (2013). Vertebral landmarks for the identification of spinal cord segments in the mouse. *NeuroImage*, 68, 22–29. https://doi.org/10.1016/j.neuroimage.2012.11.048

Hashikawa, K., Hashikawa, Y., Falkner, A., & Lin, D. (2016). The neural circuits of mating and fighting in male mice. *Current Opinion in Neurobiology*, 38, 27–37. https://doi.org/10.1016/j.conb.2016.01.006

Holmes, G. M., & Sachs, B. D. (1991). The ejaculatory reflex in copulating rats: normal bulbospongiosus activity without apparent urethral stimulation. *Neuroscience Letters*, 125, 195–197.

Holmes, G. M., Chapple, W. D., Leipheimert, R. E., & Sachs, B. D. (1991). Electromyographic analysis of male rat perineal muscles during copulation and reflexive erections. *Physiology & Behavior*, 49, 1235–1246.

Holstege, G., & Tan, J. (1987). Supraspinal control of motoneurons innervating the striated muscles of the pelvic floor including urethral and anal sphincters in the cat. *Brain*, 110(5), 1323–1344. https://doi.org/10.1093/brain/110.5.1323

Holstege, G., Griffiths, D., De Wall, H., & Dalm, E. (1986). Anatomical and physiological observations on supraspinal control of bladder and urethral sphincter muscles in the cat. *Journal of Comparative Neurology*, 250(4), 449–461. https://doi.org/10.1002/cne.902500404

Huang, Y., Li, X., Sun, X., Yao, J., Gao, F., Wang, Z., Hu, J., Wang, Z., Ouyang, B., Tu, X., Zou, X., Liu, W., Lu, M., Deng, C., Yang, Q., & Xie, Y. (2022). Anatomical transcriptome atlas of the male mouse reproductive system during aging. *Frontiers in Cell and Developmental Biology*, 9, 1–17. https://doi.org/10.3389/fcell.2021.782824

Huijgens, P. T., Guarraci, F. A., Olivier, J. D. A., & Snoeren, E. M. S. (2021). Male rat sexual behavior: insights from inter-copulatory

intervals. *Behavioural Processes*, 190(104458), 1–10. https://doi.org/10.1016/j.beproc.2021.104458

Hull, E. M., & Dominguez, J. M. (2007). Sexual behavior in male rodents. *Hormones and Behavior*, 52(1), 45–55. https://doi.org/10.1016/j.yhbeh.2007.03.030

Hull, E. M., Wood, R. I., & McKenna, K. E. (2006). Neurobiology of male sexual behavior. In J. D. Neill (Ed.), Knobil and Neill's *Physiology of Reproduction* (Third Edit, pp. 1729–1824). Elsevier. https://doi.org/10.1016/B978-012515400-0/50038-5

Hurst, J. L. (2009). Female recognition and assessment of males through scent. *Behavioural Brain Research*, 200(2), 295–303. https://doi.org/10.1016/j.bbr.2008.12.020

Huynh, H. K., Willemsen, A. T. M., Lovick, T. A., & Holstege, G. (2013). Pontine control of ejaculation and female orgasm. *Journal of Sexual Medicine*, 10(12), 3038–3048. https://doi.org/10.1111/jsm.12300

Ishiyama, S., Kaufmann, L. V., & Brecht, M. (2019). Behavioral and cortical correlates of self-suppression, anticipation, and ambivalence in rat tickling. *Current Biology*, 29(19), 3153-3164.e3. https://doi.org/10.1016/j.cub.2019.07.085

Jean, A., Bonnet, P., Liere, P., Mhaouty-Kodja, S., & Hardin-Pouzet, H. (2017). Revisiting medial preoptic area plasticity induced in male mice by sexual experience. *Scientific Reports*, 7(17846), 1–13. https://doi.org/10.1038/s41598-017-18248-3

Juárez, R., & Cruz, Y. (2014). Urinary and ejaculatory dysfunction induced by denervation of specific striated muscles anatomically related to the urethra in male rats. *Neurourology and Urodynamics*, 33(4), 437–442. https://doi.org/10.1002/nau.22432

Karen, L. M., & Barfield, R. J. (1975). Differential rates of exhaustion and recovery of several parameters of male rat sexual behaviour. *Journal of Comparative and Physiological Psychology*, 88(2), 693–703.

Knoblaugh, S., & True, L. (2012). Male reproductive system. *In Comparative Anatomy and Histology* (pp. 285–308). Elsevier. https://doi.org/10.1016/B978-0-12-381361-9.00018-4

Kolbeck, S. C., & Steers, W. D. (1992). Neural regulation of the vas deferens in the rat: an electrophysiological analysis. *American Journal of Physiology - Regulatory Integrative and Comparative Physiology*, 263, 331–338. https://doi.org/10.1152/ajpregu.1992.263.2.r331

Kozyrev, N., Lehman, M. N., & Coolen, L. M. (2012). Activation of gastrin-releasing peptide receptors in the lumbosacral spinal cord is required for ejaculation in male rats. *The Journal of Sexual Medicine*, 9(5), 1303–1318. https://doi.org/10.1111/j.1743-6109.2012.02688.x

Krukoff, T. L. (1999). c-fos expression as a marker of functional activity in the brain. *Springer Protocols*, 213–230. https://doi.org/10.1385/0-89603-510-7:213

Köbbert, C., Apps, R., Bechmann, I., Lanciego, J. L., Mey, J., & Thanos, S. (2000). Current concepts in neuroanatomical tracing. *Progress in Neurobiology*, 62(4), 327–351. https://doi.org/10.1016/S0301-0082(00)00019-8

Larsson, K., & Sodersten, P. (1973). Mating in male rats after section of the dorsal penile nerve. *Physiology and Behavior*, 10(3), 567–571. https://doi.org/10.1016/0031-9384(73)90223-0

Lee, H., Kim, D. W., Remedios, R., Anthony, T. E., Chang, A., Madisen, L., Zeng, H., & Anderson, D. J. (2014). Scalable control of mounting and attack by Esr1+ neurons in the ventromedial hypothalamus. *Nature*, 509(7502), 627–632. https://doi.org/10.1038/nature13169

Leitzmann, M. F., Platz, E. A., Stampfer, M. J., Willett, W. C., & Giovannucci, E. (2004). Ejaculation frequency and subsequent risk of prostate cancer. *JAMA*, 291(13), 1578–1586. http://jama.jamanetwork.com/

Lenschow, C., & Brecht, M. (2015). Barrel cortex membrane potential dynamics in social touch. *Neuron*, 85(4), 718–725. https://doi.org/10.1016/j.neuron.2014.12.059

Lenschow, C., & Lima, S. Q. (2020). In the mood for sex: neural circuits for reproduction. In *Current Opinion in Neurobiology*, 60, 155–168. Elsevier Ltd. https://doi.org/10.1016/j.conb.2019.12.001

Lenschow, C., Copley, S., Gardiner, J. M., Talbot, Z. N., Vitenzon, A., & Brecht, M. (2016). Sexually monomorphic maps and dimorphic

responses in rat genital cortex. *Current Biology*, 26(1), 106–113. https://doi.org/10.1016/j.cub.2015.11.041

Lima, S. Q., Hromádka, T., Znamenskiy, P., & Zador, A. M. (2009). PINP: a new method of tagging neuronal populations for identification during in vivo electrophysiological recording. *PLoS ONE*, 4(7), 1–10. https://doi.org/10.1371/journal.pone.0006099

Liu, J., Yao, Q., Luo, X., & Li, L. (2023). The Ex vivo Preparation of Spinal Cord Slice for the Whole-Cell Patch-Clamp Recording in Motor Neurons During Spinal Cord Stimulation. *JoVE*, 199, e65385. https://doi.org/doi:10.3791/65385

Liu, Y. C., Salamone, J. D., & Sachs, B. D. (1997). Impaired sexual response after lesions of the paraventricular nucleus of the hypothalamus in male rats. *Behavioral Neuroscience*, 111(6), 1361–1367. https://doi.org/10.1037/0735-7044.111.6.1361

Láng, T., Dimén, D., Oláh, S., Puska, G., & Dobolyi, A. (2024). Medial preoptic circuits governing instinctive social behaviors. In *iScience*, 27(7). Elsevier Inc. https://doi.org/10.1016/j.isci.2024.110296

Madisen, L., Mao, T., Koch, H., Zhuo, J. M., Berenyi, A., Fujisawa, S., Hsu, Y. W. A., Garcia, A. J., Gu, X., Zanella, S., Kidney, J., Gu, H., Mao, Y., Hooks, B. M., Boyden, E. S., Buzsáki, G., Ramirez, J. M., Jones, A. R., Svoboda, K., … Zeng, H. (2012). A toolbox of Cre-dependent optogenetic transgenic mice for light-induced activation and silencing. *Nature Neuroscience*, 15(5), 793–802. https://doi.org/10.1038/nn.3078

Madisen, L., Zwingman, T. A., Sunkin, S. M., Oh, S. W., Zariwala, H. A., Gu, H., Ng, L. L., Palmiter, R. D., Hawrylycz, M. J., Jones, A. R., Lein, E. S., & Zeng, H. (2010). A robust and high-throughput Cre reporting and characterization system for the whole mouse brain. *Nature Neuroscience*, 13(1), 133–140. https://doi.org/10.1038/nn.2467

Mao, T., Kusefoglu, D., Hooks, B. M., Huber, D., Petreanu, L., & Svoboda, K. (2011). Long-range neuronal circuits underlying the interaction between sensory and motor cortex. *Neuron*, 72(1), 111–123. https://doi.org/10.1016/j.neuron.2011.07.029

Marder, E., & Bucher, D. (2001). Central pattern generators and the control of rhythmic movements. In *Current Biology* (Vol. 11).

Marini, G., Pianca, L., & Tredici, G. (1999). Descending projections arising from the parafascicular nucleus in rats: trajectory of fibers, projection pattern and mapping of terminations. *Somatosensory & Motor Research*, 16(3), 207–222.

Marson, L., & Carson, C. (1999). Central nervous system innervation of the penis, prostate, and perineal muscles: a transneuronal tracing study. *Molecular Urology*, 3(2), 43–50.

Marson, L., & McKenna, K. E. (1990). The identification of a brainstem site controlling spinal sexual reflexes in male rats. *Brain Research*, 515, 303–308.

Marson, L., & McKenna, K. E. (1992). A role for 5-hydroxytryptamine in descending inhibition of spinal sexual

reflexes. Experimental Brain Research, 88(2), 313–320. https://doi.org/10.1007/BF02259106

Marson, L., & McKenna, K. E. (1996). CNS cell groups involved in the control of the ischiocavernosus and bulbospongiosus muscles: a transneuronal tracing study using pseudorabies virus. *The Journal of Comparative Neurology*, 374(2), 161–179. http://www.ncbi.nlm.nih.gov/pubmed/8906491

Marson, L., List, M. S., & McKenna, K. E. (1992). Lesions of the nucleus paragigantocellularis alter ex copula penile reflexes. *Brain Research*, 592, 187–192.

Marson, L., Platt, K. B., & McKenna, K. E. (1993). Central nervous system innervation of the penis as revealed by the transneuronal transport of pseudorabies virus. *Neuroscience*, 55(1), 263–280. https://doi.org/10.1016/0306-4522(93)90471-Q

Matsuo, T., Hattori, T., Asaba, A., Inoue, N., Kanomata, N., Kikusui, T., Kobayakaw, R., & Kobayakaw, K. (2015). Genetic dissection of pheromone processing reveals main olfactory system-mediated social behaviors in mice. *PNAS*, 112(3), E311–E320. https://doi.org/10.1073/pnas.1416723112

Maunder, L., Schoemaker, D., & Pruessner, J. C. (2017). Frequency of penile–vaginal intercourse is associated with verbal recognition performance in adult women. *Archives of Sexual Behavior*, 46(2), 441–453. https://doi.org/10.1007/s10508-016-0890-4

McGill, T. E. (1962). Sexual behavior in three inbred strains of mice. *Behavior*, 19(4), 341–350.

McGill, T. E., & Coughlin, R. C. (1970). Ejaculatory reflex and luteal activity induction in Mus musculus. *Journal of Reproduction and Fertility*, 21, 215–220.

McKenna, K. E., & Nadelhaft, I. (1986). The organization of the pudendal nerve in the male and female rat. *The Journal of Comparative Neurology*, 248, 532–549. https://doi.org/10.1002/cne.902480406

Misawa, H., Hara, M., Tanabe, S., Niikura, M., Moriwaki, Y., & Okuda, T. (2012). Osteopontin is an alpha motor neuron marker in the mouse spinal cord. *Journal of Neuroscience Research*, 90, 732–742. https://doi.org/10.1002/jnr.22813

Nadelhaft, I., & McKenna, K. E. (1987). Sexual dimorphism in sympathetic preganglionic neurons of the rat hypogastric nerve. *Journal of Comparative Neurology*, 256, 308–315.

Nadelhaft, I., deGroat, W. C., & Morgan, C. (1980). Location and morphology of parasympathetic preganglionic neurons in the sacral spinal cord of the cat revealed by retrograde axonal transport of horseradish peroxidase. *Journal of Comparative Neurology*, 193, 265–281.

Neunuebel, J. P., Taylor, A. L., Arthur, B. J., & Egnor, S. R. (2015). Female mice ultrasonically interact with males during courtship

displays. *ELife*, 4(e06203), 1–24. https://doi.org/10.7554/eLife.06203.001

Newman, H. F., Reiss, H., & Northup, J. D. (1982). Physical basis of emission, ejaculation, and orgasm in the male. *Urology*, XIX(4), 341–350.

Newman, S. W. (1999). The medial extended amygdala in male reproductive behavior: a node in the mammalian social behavior network. *Annals New York Academy of Sciences*, 877, 242–257.

Nicholas, A. P., Zhang, X., & Hokfelt, T. (1999). An immunohistochemical investigation of the opioid cell column in lamina X of the male rat lumbosacral spinal cord. *Neuroscience Letters*, 270, 9–12.

Normandin, J. J., & Murphy, A. Z. (2011). Serotonergic lesions of the periaqueductal gray, a primary source of serotonin to the nucleus paragigantocellularis, facilitate sexual behavior in male rats. *Pharmacology, Biochemistry and Behavior*, 98(3), 369–375. https://doi.org/10.1016/j.pbb.2011.01.024.Serotonergic

Nuding, S. C., & Nadelhaft, I. (1998). Bilateral projections of the pontine micturition center to the sacral parasympathetic nucleus in the rat. *Brain Research*, 785, 185–194.

Núñez, R., Gross, G. H., & Sachs, B. D. (1986). Origin and central projections of rat dorsal penile nerve: possible direct projection to autonomic and somatic neurons by primary afferents of non muscle

origin. *Journal of Comparative Neurology*, 247(4), 417–429. https://doi.org/10.1002/cne.902470402

Orr, R., & Marson, L. (1998). Identification of CNS neurons innervating the rat prostate: a transneuronal tracing study using pseudorabies virus. *Journal of the Autonomic Nervous System*, 72, 4–15.

Oti, T., Satoh, K., Uta, D., Nagafuchi, J., Tateishi, S., Ueda, R., Takanami, K., Young, L. J., Galione, A., Morris, J. F., Sakamoto, T., & Sakamoto, H. (2021). Oxytocin influences male sexual activity via non-synaptic axonal release in the spinal cord. *Current Biology*, 31(1), 103–114. https://doi.org/10.1016/j.cub.2020.09.089

Pascual, J. I., Insausti, R., & Gonzalo, L. M. (1992). Pudendal nerve topography in the rat spinal cord projections studied with the axonal tracer wheat germ agglutimnin conjugated-horseradish peroxidase. *The Journal of Urology*, 147(3), 718–722. https://doi.org/10.1016/S0022-5347(17)37365-2

Peikert, K., Platzek, I., Bessède, T., & May, C. A. (2015). The male bulbospongiosus muscle and its relation to the external anal sphincter. *The Journal of Urology*, 193(4), 1433–1440. https://doi.org/10.1016/j.juro.2014.10.050

Pescatori, E. S., Calabro, A., Artibani, W., Pagano, F., Triban, C., & Italino, G. (1993). Electrical stimulation of the dorsal nerve of the penis evokes reflex tonic erections of the penile body and reflex ejaculatory responses in the spinal rat. *The Journal of Urology*, 149(3), 627–632. https://doi.org/10.1016/S0022-5347(17)36168-2

Pfaus, J. G. (1999). Neurobiology of sexual behavior. *Current Opinion in Neurobiology*, 9(6), 751–758. https://doi.org/10.1016/S0959-4388(99)00034-3

Qi, L., Iskols, M., Greenberg, R. S., Xiao, J. Y., Handler, A., Liberles, S. D., & Ginty, D. D. (2024). Krause corpuscles are genital vibrotactile sensors for sexual behaviours. *Nature*, 630(8018), 926–934. https://doi.org/10.1038/s41586-024-07528-4

Qi, L., Iskols, M., Greenberg, R. S., Xiao, J. Y., Handler, A., Liberles, S. D., & Ginty, D. D. (2024). Krause corpuscles of the genitalia are vibrotactile sensors required for normal sexual behavior. *Nature*, 630, 926–934.

Reinhold, A. S., Sanguinetti-Scheck, J. I., Hartmann, K., & Brecht, M. (2019). Behavioral and neural correlates of hide-and-seek in rats. *Science*, 365(6458), 1180–1183. https://doi.org/10.1126/science.aax4705

Sachs, B. D. (1982). Role of striated penile muscles in penile reflexes, copulation, and induction of pregnancy in the rat. *Journal of Reproduction and Fertility*, 66, 433–443.

Sachs, B. D., & Barfield, R. J. (1970). Temporal patterning of sexual behaviour in the male rat. *Journal of Comparative and Physiological Psychology*, 73(3), 359–364.

Saleeba, C., Dempsey, B., Le, S., Goodchild, A., & McMullan, S. (2019). A student's guide to neural circuit tracing. *Frontiers in*

Neuroscience, 13(897), 1–20. https://doi.org/10.3389/fnins.2019.00897

Schellino, R., Boido, M., & Vercelli, A. (2020). The dual nature of Onuf's nucleus: neuroanatomical features and peculiarities, in health and disease. *Frontiers in Neuroanatomy*, 14(572013), 1–13. https://doi.org/10.3389/fnana.2020.572013

Schmidt, M. H., & Schmidt, H. S. (1993). The ischiocavernosus and bulbospongiosus muscles in mammalian penile rigidity. *Sleep*, 16(2), 171–183.

Sengelaub, D. R., & Forger, N. G. (2008). The spinal nucleus of the bulbocavernosus: firsts in androgen-dependent neural sex differences. *Hormones and Behavior*, 53(5), 596–612.

Shafik, A., & El-Sibai, O. (2000). Mechanism of ejection during ejaculation: identification of a urethrocavernosus reflex. *Archives of Andrology*, 44, 77–83.

Shen, P., Arnold, A., & Micevych, P. (1990). Supraspinal projections to the ventromedial lumbar spinal cord in adult male rats. *Journal of Comparative Biology*, 272, 263–272.

Sheu, G., Revenig, L. M., & Hsiao, W. (2014). Physiology of ejaculation. In J. P. Mulhall & W. Hsiao (Eds.), *Men's Sexual Health and Fertility* (pp. 173–182). Springer New York. https://doi.org/10.1007/978-1-4939-0425-9

Sigl-Glöckner, J., Maier, E., Takahashi, N., Sachdev, R., Larkum, M., & Brecht, M. (2019). Effects of sexual experience and puberty

on mouse genital cortex revealed by chronic imaging. *Current Biology*, 29(21), 3588–3599. https://doi.org/10.1016/j.cub.2019.08.062

Simerly, R. B., & Swanson, L. W. (1986). The organization of neural inputs to the medial preoptic nucleus of the rat. *The Journal of Comparative Biology*, 246, 312–342.

Simerly, R. B., & Swanson, L. W. (1988). Projections of the medial preoptic nucleus: a Phaseolus vulgaris leucoagglutinin anterograde tract-tracing study in the rat. *The Journal of Comparative Biology*, 270, 209–242.

Soukhova-O'Hare, G. K., Schmidt, M. H., Nozdrachev, A. D., & Gozal, D. (2007). A novel mouse model for assessment of male sexual function. *Physiology and Behavior*, 91(5), 535–543. https://doi.org/10.1016/j.physbeh.2007.04.016

Stepien, A. E., Tripodi, M., & Arber, S. (2010). Monosynaptic rabies virus reveals premotor network organization and synaptic specificity of cholinergic partition cells. *Neuron*, 68(3), 456–472. https://doi.org/10.1016/j.neuron.2010.10.019

Strack, A. M., & Loewy, A. D. (1990). Pseudorabies virus: a highly specific transneuronal cell body marker in the sympathetic nervous system. *The Journal of Neuroscience*, 10(7), 2139–2147.

Struthers, W. M. (2001). Sex-induced fos in the medial preoptic area: projections to the midbrain. *NeuroReport*, 12(14), 3065–3068. www.scioncorp.com

Susuki, K. (2010). Myelin: a specialized membrane for cell communication. *Nature Education*, 3(9), 59.

Sutter, A., & Lindholm, A. K. (2016). The copulatory plug delays ejaculation by rival males and affects sperm competition outcome in house mice. *Journal of Evolutionary Biology*, 29(8), 1617–1630. https://doi.org/10.1111/jeb.12898

Sürmeli, G., Marcu, D. C., McClure, C., Garden, D. L. F., Pastoll, H., & Nolan, M. F. (2015). Molecularly defined circuitry reveals input-output segregation in deep layers of the medial entorhinal cortex. *Neuron*, 88(5), 1040–1053. https://doi.org/10.1016/j.neuron.2015.10.041

Taccola, G., Marchetti, C., & Nistri, A. (2004). Modulation of rhythmic patterns and cumulative depolarization by group I metabotropic glutamate receptors in the neonatal rat spinal cord in vitro. *European Journal of Neuroscience*, 19, 533–541. https://doi.org/10.1111/j.1460-9568.2003.03148.x

Tanahashi, M., Karicheti, V., Thor, K. B., & Marson, L. (2012). Characterization of bulbospongiosus muscle reflexes activated by urethral distension in male rats. *American Journal of Physiology - Regulatory Integrative and Comparative Physiology*, 303, 737–747. https://doi.org/10.1152/ajpregu.00004.2012

Tang, Y., Rampin, O., Giuliano, F., & Ugolini, G. (1999). Spinal and brain circuits to motoneurons of the bulbospongiosus muscle: retrograde transneuronal tracing with rabies virus. *The Journal of Comparative Neurology*, 414(2), 167–192.

https://doi.org/10.1002/(SICI)1096-9861(19991115)414:2<167::AID-CNE3>3.0.CO;2-P

Truitt, W. A., & Coolen, L. M. (2002). Identification of a potential ejaculation generator in the spinal cord. *Science*, 297(5586), 1566–1569. https://doi.org/10.1126/science.1073885

Truitt, W. A., Shipley, M. T., Veening, J. G., & Coolen, L. M. (2003). Activation of a subset of lumbar spinothalamic neurons after copulatory behavior in male but not female rats. *The Journal of Neuroscience*, 23(1), 325–331. http://www.ncbi.nlm.nih.gov/pubmed/12514231

Turley, K. R., & Rowland, D. L. (2013). Evolving ideas about the male refractory period. *BJU International*, 112, 442–452. https://doi.org/10.1111/bju.12011

Ueyama, T., Arakawa, H., & Mizuno, N. (1987). Central distribution of efferent and afferent components of the pudendal nerve in rat. *Anatomy and Embryology*, 177, 37–49.

Valente, S., Marques, T., & Lima, S. Q. (2021). No evidence for prolactin's involvement in the post-ejaculatory refractory period. *Communications Biology*, 4(10), 1–10. https://doi.org/10.1038/s42003-020-01570-4

Veening, J. G., & Coolen, L. M. (2014). Neural mechanisms of sexual behavior in the male rat: emphasis on ejaculation-related circuits. *Pharmacology, Biochemistry, and Behavior*, 121, 170–183. https://doi.org/10.1016/j.pbb.2013.12.017

Vizzard, M. A., Erickson, V. L., Card, J. P., Roppolo, J. R., & de Groat, W. C. (1995). Transneuronal labeling of neurons in the adult rat brainstem and spinal cord after injection of pseudorabies virus into the urethra. *The Journal of Comparative Neurology*, 355(4), 629–640. https://doi.org/10.1002/cne.903550411

Wagner, C. K., & Clemens, L. G. (1989). Anatomical organization of the sexually dimorphic perineal neuromuscular system in the house mouse. *Brain Research*, 499, 93–100.

Wagner, C. K., & Clemens, L. G. (1991). Projections of the paraventricular nucleus of the hypothalamus to the sexually dimorphic lumbosacral region of the spinal cord. *Brain Research*, 539(2), 254–262. https://doi.org/10.1016/0006-8993(91)91629-F

Watson, C., Paxinos, G., Kayalioglu, G., & Heise, C. (2009). Atlas of the mouse spinal cord. In C. Watson, G. Paxinos, & G. B. T.-T. S. C. Kayalioglu (Eds.), *The spinal cord* (pp. 308–379). Academic Press. https://doi.org/https://doi.org/10.1016/B978-0-12-374247-6.50020-1

Wei, Y.-C., Wang, S.-R., Jiao, Z.-L., Zhang, W., Lin, J.-K., Li, X.-Y., Li, S.-S., Zhang, X., & Xu, X.-H. (2018). Medial preoptic area in mice is capable of mediating sexually dimorphic behaviors regardless of gender. *Nature Communications*, 9(279), 1–15. https://doi.org/10.1038/s41467-017-02648-0

Xia, J. D., Chen, J., Sun, H. J., Zhou, L. H., Zhu, G. Q., Chen, Y., & Dai, Y. T. (2017). Centrally mediated ejaculatory response via sympathetic outflow in rats: role of N-methyl-D-aspartic acid

receptors in paraventricular nucleus. *Andrology*, 5(1), 153–159. https://doi.org/10.1111/andr.12274

Xu, C., Giuliano, F., Yaici, E. D., Conrath, M., Trassard, O., Benoit, G., & Vergé, D. (2006). Identification of lumbar spinal neurons controlling simultaneously the prostate and the bulbospongiosus muscles in the rat. *Neuroscience*, 138(2), 561–573. https://doi.org/10.1016/j.neuroscience.2005.11.016

Xu, C., Yaici, E. D., Conrath, M., Blanchard, P., Leclerc, P., Benoît, G., Vergé, D., & Giuliano, F. (2005). Galanin and neurokinin-1 receptor immunoreactive spinal neurons controlling the prostate and the bulbospongiosus muscle identified by transsynaptic labeling in the rat. *Neuroscience*, 134(4), 1325–1341. https://doi.org/10.1016/j.neuroscience.2005.06.002

Yanagimoto, M., Honda, K., Goto, Y., & Negoro, H. (1996). Afferents originating from the dorsal penile nerve excite oxytocin cells in the hypothalamic paraventricular nucleus of the rat. *Brain Research*, 733, 292–296.

Yang, C. F., Chiang, M. C., Gray, D. C., Prabhakaran, M., Alvarado, M., Juntti, S. A., Unger, E. K., Wells, J. A., & Shah, N. M. (2013). Sexually dimorphic neurons in the ventromedial hypothalamus govern mating in both sexes and aggression in males. *Cell*, 153(4), 896–909. https://doi.org/10.1016/j.cell.2013.04.017

Zhong, G., Shevtsova, N. A., Rybak, I. A., & Harris-Warrick, R. M. (2012). Neuronal activity in the isolated mouse spinal cord during spontaneous deletions in fictive locomotion: insights into locomotor

central pattern generator organization. *The Journal of Physiology*, 590(19), 4735–4759. https://doi.org/10.1113/jphysiol.2012.240895

ITQB NOVA, Avenida da República, 2780-157 Oeiras, Portugal | Tel +351 214 469 100 | itqb.unl.pt